# Molecular insights into inhibitory synapses:
## Immunohistological and transcriptomic analysis in the auditory brainstem of
## miR-183/96 double knockout mice

Von der Fakultät VI - Medizin und Gesundheitswissenschaften
der Carl von Ossietzky Universität Oldenburg zur Erlangung des
Grades und Titels einer

Doktorin der Naturwissenschaften
(Dr. rer. nat.)

angenommene Dissertation

von Frau Faiza Altaf

geboren am 24.08.1988 in Pakistan

# Table of Contents

## List of Figures

## List of Tables

# 1 Introduction

Hearing is an essential component of our lives and is intricately interwoven with our relationships, experiences, and overall quality of life. It serves as a bridge connecting us with friends and family, allowing us to cherish the voices and laughter of loved ones. Hearing enables us to participate in community activities, work as a team, and enjoy life events. However, loss of this sense can cast a shadow over these cherished moments, leading to social isolation, depression, and chronic health issues. Hearing loss is the most prevalent sensory deficit (Morton & Nance, 2006; Quaranta et al., 2014) , affecting 1.5 billion people globally (Collaborators, 2021). Hearing loss etiologies include age, genetics, and various environmental factors (Van Eyken et al., 2007), however 50% of hearing loss cases are attributed to genetics (Nance, 2003). Recent research has identified more than 250 genes associated with hearing problems [(https://hereditaryhearingloss.org),](https://hereditaryhearingloss.org) emphasizing the intricate nature of the hearing system. Intriguingly, some of these deafness genes serve a dual purpose, playing a critical role not only in the development and function of the inner ear but also in the central auditory system located in the brain (Michalski & Petit, 2019). Comprehensive knowledge regarding how genetic elements can disrupt the normal processes of development and thereby function, which play a pivotal role in most hearing disorders must be acquired. This could greatly advance our capacity to devise effective therapies for individuals affected by hearing loss. My thesis focuses on analysing one of a key regulatory elements, known as microRNAs in the auditory brainstem of mice. Since the use of human tissue samples for scientific research purposes pose various challenges such as ethical issues, and limited post-mortem availability, we need an organism closely resembling the human's auditory system. Mice provide a valuable model for investigating various diseases in humans. Both the peripheral and central auditory systems of mice closely resemble anatomically and functionally their human counterparts. For example, the mouse cochlea operates on the same fundamental principles as other mammals, sharing genes and proteins and resulting in a significant overlap in deafness-related genes between mice and humans. Additionally, their high reproduction rates, cost-effectiveness, short lifespan, and genetic standardization makes them an excellent choice for hearing research (Ohlemiller, 2019). This has made the mouse

the preferred animal model in hearing research, including my own PhD. The detailed description below of the mammalian auditory system is therefore based on that of the mouse.

## 1.1 The mammalian auditory system

The mammalian auditory system is a highly specialized sensory system responsible for processing and interpreting sounds. It can be divided into the peripheral auditory system comprising of outer, middle, inner ear, and the central auditory system pathways. The sound processing starts in outer ear, termed pinna which first collects sound waves and passes them to tympanic membrane via the auditory canal. The tympanic membrane which forms the border between the outer and the middle ear starts to vibrate due to pressure by soundwaves. These vibrations are transmitted to the middle ear ossicles named malleus, incus, and stapes which in turn amplify the signal and transmit it via the oval window to the inner ear, specifically to the cochlea. Vibrations transmitted by auditory ossicles causes undulation of the basilar membrane in the fluid-filled coiled cochlea. This, in turn causes the deflection of the stereocilia of hair cells located in the organ of Corti. These hair cells are divided into two types; three rows of outer hair cells (OHCs) amplify the undulation of the basilar membrane, while one row of inner hair cells (IHCs) is responsible for the proper mechanotransduction. This spatial arrangement of hair cells is according to the frequency they are most sensitive to, referred to as tonotopy. From inner hair cells, the sound information is then passed on to the axons of spiral ganglion neurons which form the auditory nerve and transmit the information to the central auditory system (Pickles, 2015; Yost & Nielsen, 2000). The pathways in the central auditory system perform several tasks to process auditory input from both cochlea such as directional hearing (Grothe et al., 2010), gap detection (Kopp-Scheinpflug et al., 2011), and echo suppression (Pecka et al., 2007). Since the thesis focuses on auditory brainstem nuclei, mainly responsible for sound localization, it will be discussed in detail in the next section.

## 1.2 Auditory Brainstem: anatomy and function

The auditory brainstem harbors specialized nuclei that are grouped into two larger complexes, the cochlear nucleus complex (CNC) and the superior olivary complex (SOC) (Fig 1.1). The CNC is the first relay centre processing input from auditory nerve which upon

entering the CNC, bifurcates into the ascending branch terminating in the anteroventral cochlear nucleus (AVCN), and the descending branch terminating in the posteroventral (PVCN) and dorsal cochlear nucleus (DCN) (Cant, 1992). The DCN and the PVCN project mainly to the contralateral lateral lemniscus (LL) and inferior colliculus (IC) while the AVCN innervates the ipsi-and contralateral SOC (Moore, 1991). Apart from the relay function, the DCN likely plays an important role in vertical sound localization while the VCN is involved in spectral and temporal sound processing (Middlebrooks, 2015).

The SOC is a hub of several interrelated nuclear groups located symmetrically on either side of the brainstem (Moore, 1991; Schofield, 2002). The SOC nuclei studied in most mammals are the lateral and medial superior olive (LSO and MSO), the lateral, medial and ventral nuclei of the trapezoid body (LNTB, MNTB and VNTB), and finally the superior periolivary nuclei (SPN)(Moore, 1991). The SOC is the first convergence site in the brainstem for binaural processing which is essential for accurate sound localization (Grothe et al., 2010). The MSO and LSO are the primary binaural nuclei which encode interaural time (ITD) and sound level differences (ILD), which are both important for sound localization in the horizontal dimension. MSO neurons compare the timing of excitatory inputs from the ipsi- and contralateral ear, thereby detecting interaural time differences (ITD). This mechanism is especially used at low frequencies. On the other hand , at higher frequencies, the detection of interaural level differences (ILD) in the LSO is employed. LSO neurons receive excitatory input only from the ipsilateral ear via AVCN while the contralateral pathway is indirect. It involves an excitatory projection from globular bushy cells in the contralateral AVCN to the ipsilateral MNTB, then an inhibitory projection from the ipsilateral MNTB to the LSO. This convergent binaural input leads to detecting differences in sound levels at the two ears (ILD) (Grothe et al., 2010). Figure 1.1 shows the general auditory brainstem nuclei layout with ILD connectivity in mammalian auditory circuit.

The MNTB is a critical player in both ILD and ITD and its primary task is to convert excitation reliably and rapidly from the contralateral VCN into precisely timed inhibition that is distributed to the other three SOC nuclei (LSO,MSO & SPN) (Altieri et al., 2014; Grothe et al., 2010). This feat is achieved due to a remarkable structure known as the calyx of Held; a giant axosomatic glutamatergic synapse which originates in the globular bushy cells of the AVCN and innervates the contralateral principal neurons of the MNTB (Schneggenburger & Forsythe, 2006). This synapse harbors several hundred presynaptic active zones (AZs), which

are equipped with a readily releasable pool (RRP) of thousands of synaptic vesicles (SVs), specialized for high fidelity neurotransmission (Satzler et al., 2002; Taschenberger et al., 2002).
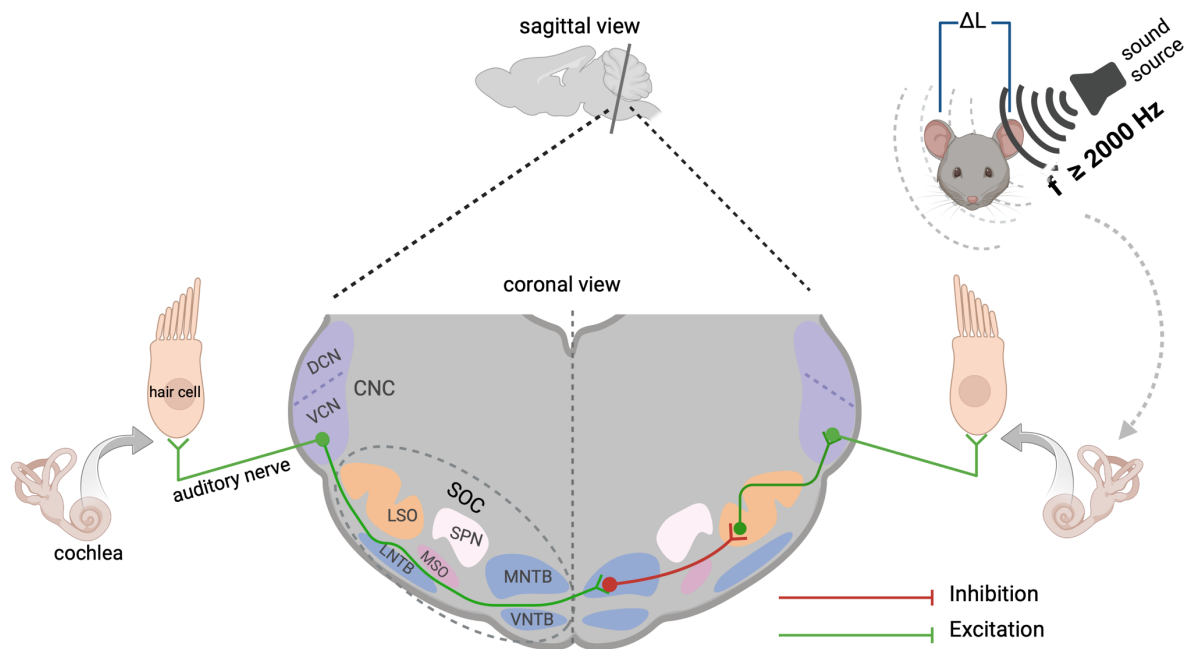


**Figure 1.1 Schematic layout of auditory brainstem nuclei with interaural level difference (ILD) circuitry**

*Schematic drawing of a coronal section through the auditory brainstem region of the mouse brain while the sagittal view shows the localization of the mouse auditory brainstem within the brain with the section plane indicated in a caudal position. The SOC is assembled by the MNTB, VNTB, LNTB, SPN, MSO, and LSO while CNC is comprised of DCN and VCN. At a sound frequency above 2000 Hz, the distances between sound waves are smaller. The sound arrives directly and unchanged at the ear facing to the sound source. The acoustic head shadow produces location specific ILDs between the ears. Cochlear hair cells convert acoustic signals into electrical signals and transmit them via the auditory nerve to neurons of the VCN. These monoaural excitation inputs (green) are projected to the ipsi- and contralateral SOC. ILDs are first detected by LSO neurons by comparing ipsilateral excitatory input from the VCN and contralateral inhibitory (red) input from the MNTB . Figure created with BioRender.com*

## 1.3 Lateral superior olive: model system to address inhibitory synapse studies

In this thesis, the analysis focuses on the role of microRNAs in inhibitory neurotransmission in the auditory brainstem of mice. For this purpose, the LSO, a model structure in auditory hindbrain to address inhibitory synapses, was selected. The murine LSO can be easily recognized in coronal brainstem sections by its distinctive convoluted S-shape (Harrison & Irving, 1966). In mice the volume of the LSO is approx. 0.8% in relation to their whole brain

size (Glendenning & Masterton, 1998) and comprises about 1,500–1,600 neurons (Ebbers et al., 2015; Hirtz et al., 2011; Satheesh et al., 2012). Overall up to seven different neuronal cell types are described in mammals (Rietzel & Friauf, 1998), of which principal neurons make up 75% (Helfert & Schwartz, 1987). These principal cells are equipped with fast gating receptors and receive both glycinergic and glutamatergic inputs that make them suitable for precise timing preservation. The MNTB axon terminals make large and multi-active-zone boutons by contacting the soma of a single principal LSO neuron providing the ultrastructural basis for strong inhibition caused by the MNTB-LSO synapses (Friauf et al., 2018). Other important neuronal cell types are multipolar and marginal cells which make 11% and 4% of the population respectively (Majorossy & Kiss, 1990). Multipolar cells have 3–6 primary dendrites that can originate from all parts of the round soma and branch extensively giving rise to 3-dimensional stellate dendritic trees (Rietzel & Friauf, 1998). Marginal cells are primarily located along the LSO border and contain both glycine and γ-amino butyric acid (GABA) as neurotransmitters, pointing to an inhibitory role of these cells (Korada & Schwartz, 1999; Ollo & Schwartz, 1979).

One of the most important functions of LSO is computing ILD. The acoustic shadow created by an animal's head results in sound reaching the far ear with lower intensity than the signal at the near ear. The LSO neurons extract and encode these differences in sound intensity. In the high frequency hearing mouse (Fig 1.1), the mechanism operates between 2 and 80 kHz (Grothe & Pecka, 2014; Grothe et al., 2010), therefore, most of the directional hearing in mouse is based on ILDs (Heffner & Heffner, 2007). In summary, LSO neurons detect ILDs by making use of a coincidence detector mechanism of ipsilateral excitation and contralateral inhibition. The inhibitory pathway of the MNTB-LSO in particular has evolved both anatomically and physiologically for the temporal precision and robustness (Grothe & Pecka, 2014). These MNTB neurons which project inhibitory inputs onto LSO are way more easily accessible for experimental manipulations than local inhibitory interneurons, therefore this MNTB-LSO projection is suitable for investigating inhibitory synapses. Moreover, the fact that the projection is maintained in transverse LSO brainstem slices makes it suitable for in vitro experiments.

## 1.4  Gene regulatory system: key Influencing elements

All living organisms have a wide variety of specialized cell types with distinct location and roles governed by their genomes. This diversity is achieved by regulating spatiotemporal expression pattern of genes through a variety of gene regulatory elements which work by interacting with each other. There are several types of gene regulatory elements like cis-acting enhancers and silencers and trans-acting regulatory elements like transcription factors (TFs), signal molecules, and non-coding RNAs. These elements are functionally connected in complex gene regulatory networks (GRNs) where every regulatory gene is comparable with a node in a network, every node has a distinctive role, contributing to the overall regulatory state while driving expression of their target genes set (Chatterjee & Ahituv, 2017; Davidson & Erwin, 2006). An example is the shared GRN between peripheral and auditory hindbrain (Bordeynik-Cohen et al., 2023; Willaredt et al., 2015). Both the inner ear and the auditory nerve derive at the same developmental age from the otic placode (Whitfield, 2015; Zine & Fritzsch, 2023). A comparative transcriptomic analysis revealed main components of GRNs that govern the development of both the cochlea and the SOC, identified new miRNAs as key regulators of developmental programs, and uncovered potential regulatory interactions between miRNAs and their gene target genes in both systems (Bordeynik-Cohen et al., 2023). These data corroborated a previous analysis of the SOC transcriptome, which showed an enrichment of deafness-associated genes (Ehmann et al., 2013).

An important shared regulatory element that popped up in these studies was the deafness gene *Mir96*, a microRNA (miRNA or miR) gene coding for miR-96. Mutations of miR-96 causes defects in the peripheral auditory system of both humans and mice (Lewis et al., 2009; Mencia et al., 2009), and in the central auditory system of mice (Schluter et al., 2018). The identification and functional characterization of the gene regulatory elements and their networks is not only important for their association with diseases but also for other biological processes such as development and evolution.

## 1.5  MicroRNAs: post-transcriptional regulators of gene expression

MicroRNAs are endogenous, ~22 nt long non-coding RNAs, which play important regulatory roles in multicellular organisms. They function by binding to the 3' untranslated regions (3' UTRs) of their target of messenger RNAs (mRNAs), thereby inhibiting their translation into

functional proteins (Bartel & Chen, 2004). Despite their relatively recent discovery, miRNAs represent a highly abundant class of regulatory elements within eukaryotes and are believed to impact around 60% of all protein-coding genes (Friedman et al., 2009b). This implies their importance in nearly all cellular processes, including development and pathogenesis.

## 1.5.1  MicroRNA biogenesis and mode of action

Most miRNAs are intragenic and predominantly processed from introns. The remaining miRNAs fall into the intergenic category and are transcribed independently of any host gene and regulated by their own distinct promoter regions (De Rie et al., 2017; Kim & Kim, 2007). The process of miRNA biogenesis begins with their transcription and proceeds through a series of successive maturation steps to yield the final functional regulators (Bartel, 2018). Within miRNA biogenesis, two distinct categories of enzymes play vital roles: processors, comprising RNA endonucleases like Drosha and effectors, which encompasses the Argonaute family (AGO)  and a multitude of proteins responsible for exerting post-transcriptional regulatory effects on mRNA targets through the formation of the the RNA-induced silencing complex (RISC) complex (Costa et al., 2012) (Fig 1.2) .
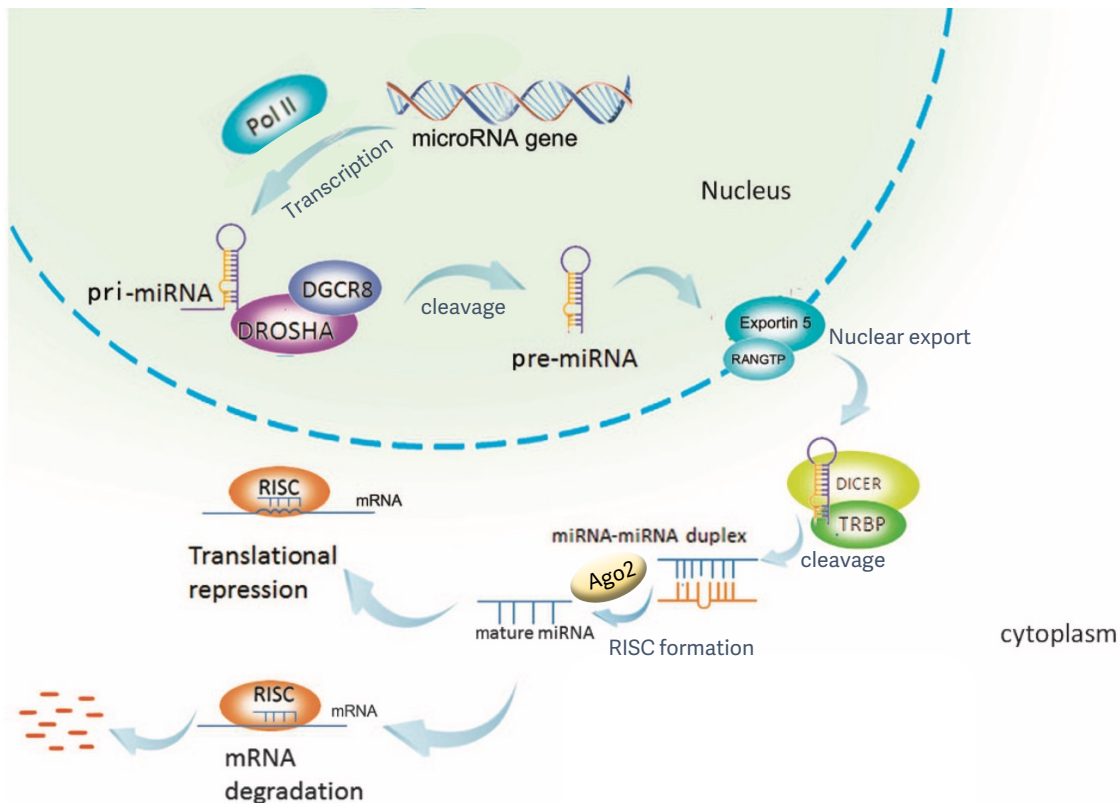
***Figure 1.2 miRNA biogenesis and mode of action***
*Pri-miR is transcribed by RNA Polymerase II and cleaved by the Drosha microprocessor complex to pre-miR*

*hairpin structure. Nuclear export of pre-miR to the cytoplasm is mediated via Exportin5/RANGTP complex.*

*In the cytoplasm, the pre-miR is cleaved by Dicer to become the miRNA-duplex. The guide strand is loaded*

*into Ago2 forming the RISC complex which afterwards target mRNAs. Imperfect binding between microRNA*

*and their target mRNA results in translational repression whereas perfect complementary binding of miR*

*and mRNA leads to target mRNA degradation. Modified after (Peng et al., 2017)*

The dominant pathway through which most microRNAs are processed is known as the
canonical biogenesis pathway. It begins with the transcription of primary miRNAs (pri-miR)
from their respective genes by RNA polymerase II. Pri-miRNAs are subsequently processed
into approximately 70 nt long precursor miRNAs (pre-miRNAs) via the microprocessor
complex, comprised of RNA binding protein DiGeorge Syndrome Critical Region 8 (DGCR8)
and ribonuclease III enzyme Drosha (Denli et al., 2004). DGCR8 recognizes specific motifs
within the pri-miRNA, and Drosha cleaves it at the base of the characteristic hairpin structure,
generating pre-miRNAs characterized by a 2-nucleotide 3' overhang (Alarcon et al., 2015; Han
et al., 2004). These pre-miRNAs undergo nuclear export facilitated by the
exportin5(XPO5)/RanGTP complex (Denli et al., 2004; Okada et al., 2009). Apart from this

canonical biogenesis of pre-miRNAs, there are noncanonical pathways that generate miRNAs independent of the Drosha/DGCR8 microprocessor complex (Babiarz et al., 2008; Ruby et al., 2007). In the cytoplasm, these pre-miRNAs encounter the RNase III endonuclease Dicer, which trims off the terminal loop to yield a mature miRNA duplex (Zhang et al., 2004). The nomenclature of the mature miRNA strand is determined by its origin within the pre-miRNA hairpin: the 5p strand originates from the 5' end, and the 3p strand originates from the 3' end. Both strands of the mature miRNA duplex can be loaded into the AGO protein family in an ATP-dependent manner (Yoda et al., 2010). The selection process depends upon variable factors such as cellular state and environmental factors and is partially governed by thermodynamic conditions at the 5' ends of the miRNA duplex and the presence of a 5' uracil at nucleotide position 1. Typically, the strand with lower 5' stability or the presence of a 5' uracil is favoured for AGO loading and is designated as the guide strand. This structure now consisting of the mature miRNA and the AGO protein is known as the RISC complex (Meijer et al., 2014). The unloaded strand, known as the passenger strand, is eliminated via AGO2-mediated cleavage (Ha & Kim, 2014).

After being processed to mature miRs and loaded into the RISC, miRs are now ready to execute their function. The predominant mechanism of action of microRNAs in *Bilateria* relies on complementary base pairing between the "seed" region of a miRNA (nucleotides 2–8) to the target sequences in the 3' UTR of mRNAs via RISC mediated recognition (Bartel, 2009). This could lead to mRNA cleavage resulting in translation inhibition. In case of complete complementarity between seed region and target mRNA, AGO-2 slices the mRNA causing destabilization of AGO2-miRNA interaction that ultimately results in miRNA degradation (Jo et al., 2015; O'Brien et al., 2018). On the other hand, incomplete complementarity prevents AGO-2 endonuclease activity but initiates the recruitment of other protein complexes leading to mRNA decay (Fukao et al., 2014; Gebert & MacRae, 2019). These mechanisms enable miRNAs to regulate hundreds of target mRNAs, whereas a single mRNA can also be targeted by several microRNAs, thereby forming a complex regulatory network (Friedman et al., 2009b). The importance of microRNAs mediated regulation becomes evident when microRNAs are genetically removed from animal models to investigate their functional impact. For instance, in mouse models with complete knockout of functional miRNAs, a large variety of defects have been observed, including embryonic lethality, neurological and skeletal defects, and sensory disorders such as blindness or deafness (Bartel, 2018). The most

striking example is demonstrated through studies of mouse models with lack of the microRNA processing enzyme Dicer. It's crucial for processing microRNA into a functional state and hence, no mature microRNA is produced in its absence, leading to developmental arrest of the early mouse embryo (Bernstein et al., 2003).

In the following, I will focus on the functional importance of miRs in the auditory system. In the inner ear, the knockout of Dicer resulted in a non-coiled and smaller cochlea at embryonic day 17.5 (Soukup et al., 2009), and hair cells lacked stereocilia (Friedman et al., 2009a), resulting in deafness. In the auditory brainstem, the ablation of Dicer during early embryonic stages caused a severely disrupted SOC missing essential auditory nuclei like LSO and MSO (Rosengauer et al., 2012). Apart from Dicer, *MiR96* was identified as a deafness gene that influences both peripheral and central auditory system, presenting an excellent opportunity for investigating its involvement in the gene regulatory networks responsible for auditory system development and function (Michalski & Petit, 2019).

## 1.6 The miR-183 cluster

The microRNA (miR) 183 cluster, comprising miRs-183, -96 and -182, is transcribed as a single polycistronic transcript, with miR-96 in between miR-183 and miR-182 (Xu et al., 2007) (Fig 1.3A) and has high sequence homology (Dambal et al., 2015) (Fig 1.3B). Despite having a high similarity between the sequences of these miRs, minute differences in their seed sequences result in both overlapping and unique mRNA targets, which are often within the same pathway (Fig 1.3C). This cluster was shown to be highly conserved throughout bilaterian organisms and could be evolutionary traced back 600 million years ago to protostomes and deuterostomes by next generation deep sequencing (Benson et al., 2009; Pierce et al., 2008; Prochnik et al., 2007).
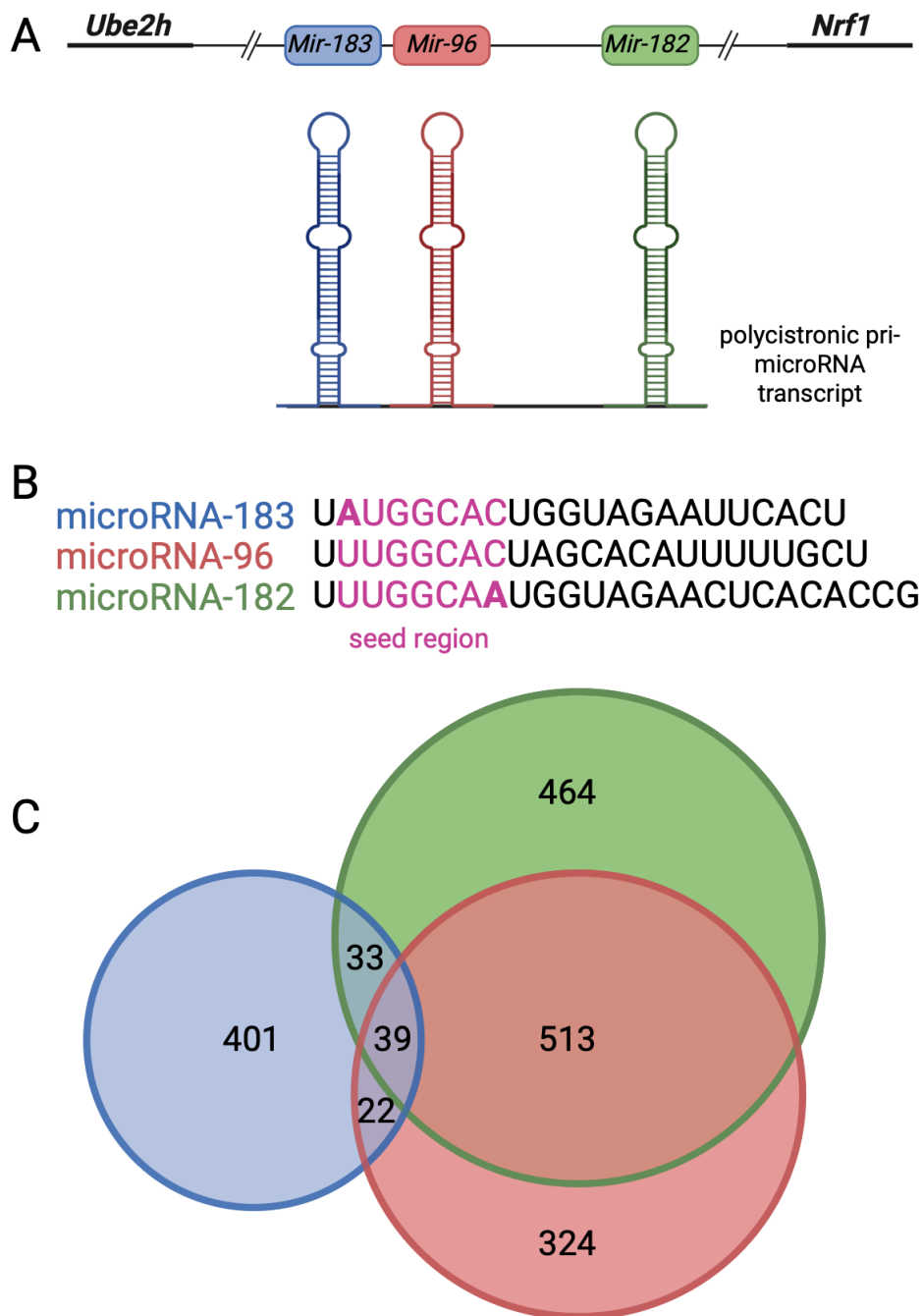
**Figure 1.3 The miR-183 cluster**
*(A) Genomic organization of the murine miR-183, −96 and 182. They are located between the two protein*

*coding genes Ube2h and Nrf1 on chromosome 6 and are jointly transcribed as one polycistronic transcript.*

*(B) MicroRNAs- 183, −96 and 182 show high sequence homology with a single nucleotide difference in their*

*seed regions (pink & bold). (C) The Venn diagram illustrates the predicted mRNA targets attributed to each*

*member of the miR-183 cluster: microRNA-183 (blue), microRNA-96 (red), and microRNA-182 (shown in*

*green) in mice, provided by miRDB, a database for microRNA target predictions. Additionally, it displays*

*areas of overlap, indicating the number of shared targets between microRNAs (Chen & Wang, 2020). Figure*

*modified from (Ebbers et al., 2022).*

## 1.6.1 Role of the miR-183 cluster in sensory systems

All three miRs -183, -96 and -182 have a tightly synchronized expression during development and are essential for maturation and function of sensory systems such as vision, olfaction nociception, and hearing (Dambal et al., 2015; Hilgers et al., 2010; Lagos-Quintana et al., 2003; Pierce et al., 2008; Wienholds et al., 2005). In the retina, disruption of the miR-183 cluster members results in failed maturation of cone photoreceptors (Fan et al., 2017) and investigation of single, double or triple knockout mouse models of this cluster led to attenuated electroretinogram responses indicating their importance in retinal homeostasis (Wu et al., 2019; Xiang et al., 2017; Xu et al., 2007; Zhang et al., 2020). All three members of miR-183 cluster were found to be highly expressed in the mouse olfactory bulbs and their deletion results in reduced numbers of mature sensory olfactory neurons (Bak et al., 2008; Fan et al., 2017). Nociception is an important phenomenon where nociceptors (pain receptors) detect tissue damage making the body aware of potential danger. The dysfunctionality of these pain receptors can lead to a state of chronic pain. Members of miR-183 cluster were found to control both basal mechanical and neuropathic pain while regulating more than 80% of neuropathic pain-related genes. A single knockout of miR-96 or a knockout of the entire miR-183 cluster leads to abnormal pain perceptions (Peng et al., 2017; Sun et al., 2021).

## 1.6.2 The miR-183 cluster: key players in the auditory system

Another sensory system tightly associated with the miR-183 cluster is the auditory system. The research on inner ear in a zebrafish model was the first study to identify three co-expressed microRNAs (miR-182, miR-96, and miR-183) important for inner ear development (Wienholds et al., 2005). Later this microRNA triad was also found to be expressed in the murine inner ear (Weston et al., 2006) and their expression levels correlated with its functional maturation (Sacheli et al., 2009). Expression of all three members was detected in the otic vesicle, cochlear-vestibule ganglion, and cochlear hair cells throughout embryonic (E) development (embryonic day (E)9.5, E11.5, and E17.5) to at least postnatal day (P) 30) (Rudnicki & Avraham, 2012). Among the members of this family, miR-96 is expressed as a sensory organ-specific miRNA in the mammalian cochlea during development (Kuhn et al., 2011). Notably, miR-96 expression extends to the central auditory system. Studies in the

mouse auditory brainstem revealed the expression of miR-96 at different timepoints (E18, P0 and P25) by quantitative PCR (Rosengauer et al., 2012). Additionally, the expression of miR-96 was also detected in the mouse CNC and SOC at P4 and P25 as well as in chicken central auditory structures using *in-situ* hybridization (Pawlik et al., 2016). All these findings hint at the importance of this cluster for proper development and function of both the peripheral and central auditory systems across vertebrates. Indeed, research carried out in auditory structures of mutant mouse models related to miR-183 cluster confirmed the functional impact of all its members. In mouse inner ear, overexpression of the cluster leads to an increased number of inner hair cells at P18. The outer hair cells underwent histological changes and auditory brainstem response (ABR) measurements showed progressive sensorineural hearing loss from P18 to P90 with both inner and outer hair cells completely lost at P115 (Weston et al., 2018).

Out of all three members of this cluster, miR-96 remarkably stands out in both auditory systems. MiR-96 was the first microRNA to be associated with a Mendelian disease (deafness) when point mutations in its seed region were identified as the causal genetic mechanism in an inherited autosomal dominant, progressive hearing loss in humans (Mencia et al., 2009; Solda et al., 2012). A  mouse model known as *Diminuendo (Dmdo)* harbouring a similar point mutation in the seed region of miR-96 (A>T substitution) exhibited peripheral hearing loss, development arrest of inner and outer hair cells, immature stereocilia bundle as well as degeneration of auditory hair cells (Kuhn et al., 2011; Lewis et al., 2009). Additional transcriptomic analysis revealed misregulation of various genes important for inner ear maintenance and function and suggested that the mutation in miR-96 results in both loss-of-function and gain-of-function. Genetic mutations can lead to alterations in protein functions, causing a protein to undergo loss-of-function where it loses its native function or gain-of-function where it acquires a new function. To address the loss of function scenario, knockout (ko) mouse models of miR-96 family members were analysed. Complete ko of all miRs lead to severe defects in stereocilia bundle formation, cochlear hair cells morphogenesis and function; resulting in profound congenital hearing loss as determined by ABRs (Geng et al., 2018). To dissect the individual contribution of each member in the auditory system, a single ko mouse model of each miR has to be analysed. Karen Steel`s group therefore analysed two ko mouse models in the peripheral auditory system: *Mir-183/96^{dko}*, a double ko of both miR-96 and miR-183 (their close proximity renders single ko models challenging) (Prosser et al.,

2011), and a single ko of miR-182. *Mir-183/96^dko* mice were completely deaf while miR-182 ko exhibited progressive hearing loss. Compared to *Dmdo* mice where all hair cells were gone, *Mir-183/96^dko* mice showed a less severe phenotype with reduced numbers of inner hair cell synapses and abnormal hair cell stereocilia bundles. Similar to the structural phenotype, transcriptome analysis in the organ of Corti also resulted in fewer genes with altered expression in *Mir-183/96^dko* compared to *Dmdo* mice pointing to a milder effect of double ko compared to point mutation (Lewis et al., 2020). This implied that the gain of novel targets plays an important role in the phenotype caused by mutations in miR-96.

Both *Dmdo* and *Mir-183/96^dko* mouse lines were subsequently functionally analysed in the central auditory system to assess the impact of the miR-183 cluster beyond the cochlea. Schlüter et al. (2018) showed that mutations in miR-96 effected the development of circuits in the auditory hindbrain. The volume of auditory hindbrain nuclei was significantly reduced due to an arrest of cell growth whereas these changes were not observed in non-auditory structures. Detailed analysis of MNTB revealed a morphologically immature calyx of Held with less fenestration as shown by synaptic vesicle glycoprotein 2 (SV2) immunoreactive signals. This developmental arrest was extended on the functional level as MNTB neurons at P25 displayed an immature state, firing mainly multiple action potentials upon depolarization, in contrast to the predominant single firing pattern exhibited in wild type (wt) mice. On the molecular level, *Kcna6* and *Kcnmb2* coding for the potassium channel subunits Kv1.6 and BKβ2, respectively, were predicted to be new targets of the miR-96 *Dmdo* variant due to the mutation in the seed region using bioinformatic tools. Immunohistochemical analysis in the LSO and MNTB revealed decreased expression of these potassium channels possibly contributing to the immature electrophysiological state of MNTB neurons in *Dmdo* mice. Of notable importance, none of these changes were observed in *Claudin14 (Cldn14)* ko mice (a mouse model of peripheral deafness), strongly suggesting an on-site effect of the miR-96 mutation in the central auditory pathway. Next, *Mir-183/96^dko* mouse model was functionally analysed on the morphological, electrophysiological and molecular level to complement these studies. Krohs et al. (2021) observed a significant reduction in auditory hindbrain nuclei, similar to the findings in *Dmdo* mice. Detailed analysis of the calyx of Held synapse, however, exhibited several striking differences between the two mouse lines. The overall morphology of the calyx of Held remain unchanged in *Mir-183/96^dko*, yet presynaptically, these calyces exhibited an increase in release-ready synaptic vesicles (SVs), quantal content, and the

presence of the proteins Bassoon and Piccolo. Postsynaptically, increased excitatory postsynaptic currents were present accompanied by larger number and size of GluA1 (Glutamate receptor subunit 1) puncta. Overall, the analysis of the *Dmdo* and *Mir-183/96$^{dko}$* mice revealed a critical contribution of this cluster in development and function of key structures in the peripheral and central auditory system.

### 1.6.3  miR-96 targets gene involved in inhibitory neurotransmission

Krohs et al. (2021) demonstrated an essential role of miR-96/183 in excitatory neurotransmission at the calyx of Held synapse in the MNTB. However, the impact of these microRNAs on inhibitory neurotransmission in the auditory brainstem was not addressed in this study. MicroRNA target prediction data bases indeed identified several inhibitory synapse-related genes. *Gad2* encodes Gad65; an enzyme involved in GABA metabolism, the main inhibitory neurotransmitter in mammalian brain. It is associated with the membrane of GABA vesicles and creates GABA for quick synaptic release in response to neural activation and affects GABA levels throughout postnatal maturity (Kaufman et al., 1991). Neurolignin2 (*Nlgn2*) and gephyrin (*Gphn*) were also identified as miR-96 targets; Nlgn2 specifically localizes to inhibitory synapses and regulates transsynaptic signalling (Varoqueaux et al., 2004) whereas Gphn is the most comprehensively studied scaffold protein responsible for organizing the inhibitory postsynaptic density. It forms sub-membranous cytoplasmic lattices at the post-synaptic complex of GABAergic and glycinergic synapses essential for inhibitory synaptic transmission (Choii & Ko, 2015). These features make them an ideal marker for inhibitory postsynaptic structures. Another miR-96 target is *Slc12a5 (*Solute carrier family 12 member 5*)* coding for the potassium chloride co-transporter Kcc2. It is developmentally upregulated which is important for an intracellularly directed Cl$^-$ gradient and hence for maturation of postsynaptic GABAergic inhibitory neurons (Blaesse et al., 2006; Rivera et al., 1999). From these predicted inhibitory synapse-markers, Gad2, Gphn, and Slc12a5/Kcc2 were validated as miR-96 targets in HEK cells while Gphn was specifically validated using western blot analysis on protein level (Jensen & Covault, 2011).

A recent study performed integrated RNA-seq analysis of the inner ear sensory epithelium and the SOC of the auditory brainstem at three developmental stages (E16, P0, P6) to outline the main GRNs that drive the development of cochlea and SOC and to establish potential

regulatory interactions between miRNAs and their target genes. Indeed mir-96 emerged in the list with many target genes involved in inhibitory synapses (Bordeynik-Cohen et al., 2023). Two interesting candidates from this data were *Gabra1* and *Hapln4.* Hyaluronan and Proteoglycan Link Protein 4 (*Hapln4*) is a crucial structural component for synapse associated extracellular matrix known as perineural network. It plays a significant role in in establishing and facilitating the transmission of inhibitory GABAergic synapses (Edamatsu et al., 2018) while *Gabra1* codes for a ligand-gated $Cl^-$ channel which is a crucial component of the $GABA_A$ receptor (GABAARs) responsible for binding to GABA, which is the primary inhibitory neurotransmitter in the brain and in the formation of functional inhibitory GABAergic synapses (Fuchs et al., 2013). These findings prompted us to investigate these markers in the LSO, where inhibition is essential for detecting interaural level differences for sound source localization.

## 1.7 Main questions and aim of thesis

All the above outlined findings establish the miR-183 cluster and specially miR-96 as essential gene regulatory components in both the peripheral and central auditory system. In the auditory hindbrain the findings prior to my thesis can be summarized as follows: Postnatal upregulation of miR-96 expression in brainstem (Rosengauer et al., 2012) is important for proper development of auditory brainstem nuclei (with a specific focus on morphology and function of excitatory synapses in MNTB) (Krohs et al., 2021; Schluter et al., 2018). This raises the question: Does the miR-183 cluster has a role beyond the excitatory neurotransmission in auditory brainstem since it targets many genes relevant to inhibitory neurotransmission? To address this question, I made use of the constitutive *Mir-183/96^dko* previously used to analyse the role of these two miRNAs in development and function of excitatory neurotransmission (Krohs et al., 2021). The inhibitory gene markers will be validated on the protein level by the use of immunohistochemistry in the LSO. We aimed furthermore on a more global picture of the requirement of miR-183/96 in auditory brainstem nuclei on the gene regulatory level. To answer this question, I performed RNA-seq analysis to evaluate gene expression data by focusing on the LSO and MNTB.

# 2 Materials and methods

## 2.1 Materials

*Table 2.1 Primers*

| Primer | Sequence (5´-´3´) | Application |
|---|---|---|
| miR-183-96ko_for | TATTGGGATGTGATGGGAAACTCTG | Genotyping of |
| miR-183-96ko_rev | TAGCAGAAGGCTAGACCCCAAAGAC | *Mir-183/96$^{dko}$* mice |

*Table 2.2 Enzymes*

| Enzymes | Manufacturer / Order number |
|---|---|
| Dream Taq | Thermo Fisher Scientific Cat. No. EP0701 |

*Table 2.3 Antibodies*

| Primary Antibodies | Dilution | Manufacturer / Order number |
|---|---|---|
| anti-GluA1, monoclonal mouse | 1:500 | Synaptic Systems, Cat. No. 182011 |
| anti-Homer1b/c, polyclonal rabbit | 1:500 | Synaptic Systems, Cat. No. 160023 |
| anti-Kcc2, polyclonal rabbit | 1:300 | Millipore Cat. No. 07-432 |
| anti-Gad2/65, monoclonal mouse | 1:500 | Synaptic Systems, Cat. No. 198111 |
| anti-Gphn, monoclonal mouse | 1:500 | Synaptic Systems, Cat. No. 147021 |
| anti-Gabra1, polyclonal guinea pig | 1:500 | Synaptic Systems, Cat. No. 224205 |
| anti-Hapln4, polyclonal goat | 1:500 | R&D Systems, Cat. No.AF4085 |

| Secondary Antibodies | Dilution | Manufacturer / Order number |
|---|---|---|
| Alexa Fluor 488 goat anti mouse | 1:1000 | Invitrogen Cat. No. A-11001 |
| Alexa Fluor 488 goat anti rabbit | 1:1000 | Invitrogen Cat. No. A-11008 |
| Alexa Fluor 488 goat anti guinea pig | 1:1000 | Invitrogen Cat. No. A-21450 |
| Alexa Fluor 647 goat anti rabbit | 1:1000 | Invitrogen Cat. No. A-21244 |
| Alexa Flour 488 donkey anti goat | 1:1000 | Invitrogen Cat. No. A.11055 |

*Table 2.4 Accessories and consumables for RNA-seq*

| Name | Manufacturer / Order number |
|------|----------------------------|
| Steel frame slides with POL membrane (0.9 µm) | Leica Microsystems / Cat. No. 11505191 |
| 0.5-µl adhesive cap | Carl Zeiss B.V./ Cat. No. 415190-9211-000 |
| RNase-Free DNase Set (50) | QIAGEN Cat. No .79254 |
| RNeasy Micro kit (50x) | Qiagen /Cat. No. 74004 |
| Agilent RNA 6000 Pico Kit | Agilent technologies Cat. No. 5067-1513 |

*Table 2.5 Chemical Reagents*

| Reagents | Company |
|----------|---------|
| Bovine Serum Albumin (BSA) | Carl Roth, Cat. No. 8076.2 |
| Chloroform | Fisher Chemical Cat. No. 2106876 |
| Cresyl violet | MERCK Cat. No. K20587835 |
| DEPC | Carl Roth, Cat. No. K028.1 |
| Ethanol | VWR chemicals Cat. No.22J254028 |
| Mowiol + DAPCO + DAPI | Carl Roth Cat. No. 0713.1 |
| Paraformaldehyde (PFA) | ROTH |
| RNase free Water | Qiagen |
| Roti®-Histokitt II | Carl Roth Cat. No. T160.1 |
| Tissue freezing medium | TBS Durham, North Carolina, USA |
| Triton X-100 | Serva Cat. No. 37240 |
| Hydrogen peroxide ($H_2O_2$) | Sigma-Aldrich |

*Table 2.6 Solutions & Buffers*

| Solutions /Buffers | Compounds |
|--------------------|-----------|
| Blocking solution (Immunohistochemistry) | 2% BSA, 0.3% Triton X-100, 10% goat serum in PBS |
| Carrier (Immunohistochemistry) | 1% BSA, 0.3% Triton X-100, 1% goat serum in PBS |

| | |
|---|---|
| Blocking solution (Immunohistochemistry Hapln4) | 2% BSA, 0.3% milk Powder, 0.5% Donkey serum in PBS |
| Ethanol (75%) (RNA-seq) | 75% EtOH in DEPC $H_2O$ |
| Ethanol (90%) (RNA-seq) | 90% EtOH in DEPC $H_2O$ |
| Gelatin-Chromalaun solution | 0.25% Gelatin, 0.025% Chrom (III)-Potassium sulphate in $H_2O$ dest |
| 10X PBS | 1.369 M NaCl, 0.027 M KCl ,0.101 M Na2HPO4*$H_2O$, 0.018 M KH2PO4 in VE-Water, pH 7,4 |
| 3% $H_2O_2$ | 3% $H_2O_2$ in PBS |
| 4% Paraformaldehyde (PFA) | 4% paraformaldehyde in PBS, pH 7.4 |
| Zamboni | 15% picric acid saturated $H_2O$, 2% PFA in PBS |

**Table 2.7 Instrumentation**

| Instrument | Manufacturer |
|---|---|
| Olympus BX63 automated fluorescence microscope | Olympus, Hamburg, Germany |
| Confocal Microscope Leica SP8 | Leica Biosystems, Nußloch, Germany |
| LMD7 Laser capture microdissection microscope | Leica Biosystems, Nußloch, Germany |
| Slide Scanning Microscope AxioScan Z1 | Zeiss, Oberkochen, Germany |
| Cryostat Leica CM1950 | Leica Biosystems, Nußloch, Germany |
| Nanophotometer | Implen GmbH, München, Germany |
| Agilent 2100 Bioanalyzer | Agilent Technologies, Waldbronn, Germany |
| Sliding Microtome Cuttec S | SLEE Medical GmbH, Germany |
| Tabletop Centrifuge Eppendorf 5424R | Eppendorf AG, Hamburg, Germany |
| Thermocycler Biometra Professional | Analytik Jena AG, Jena, Germany |

**Table 2.8 Software**

| Software | Manufacturer / Version |
|---|---|
| GraphPad Prism | GraphPad Software, LLC, Version 10.0.2 |
| ImageJ | Wayne Rasband, NIH, USA Version 1.54f |
| Agilent 2100 expert Software | Agilent Technologies, Version B.02.11.SI811 |
| Cellsens Imaging Software | Olympus soft Imaging solutions, Münster, Version 2.1 |
| LMD6500 software | Leica Biosystems, Nußloch, Germany, Version 7.0 |

## 2.2 Methods

### 2.2.1 Animals

#### Ethical approval

The local animal care and use committee (LAVES, Oldenburg) approved all procedures related to the care and use of animals, and all experiments adhered to the regulations outlined by the German federal law and the guidelines provided by the EU Directive 2010/63/EU for animal experimentation.

#### Mouse line

The mouse line investigated in this study is a double knockout of both *Mir183* and *Mir96* referred to as *Mir-183/96$^{dko}$* maintained on a C57BL/6N background (Prosser et al., 2011). *Mir-183/96$^{dko}$* mice were compared to their wt littermates of both sexes at P25-27 in all experiments except for volume analysis at postnatal stages, P0 mice were analysed.

This inbred strain is known to develop age related hearing loss (AHL) (Noben-Trauth et al., 2003) where after four weeks of age, higher frequencies are affected while lower frequencies remain unaffected for up to six months (Li & Borg, 1991). A similar pattern was observed in wt mice from *Mir-183/96$^{dko}$* line which exhibited mild progressive hearing loss at 24-42 kHz from 8 weeks of age but retained good hearing sensitivity at frequencies between 3-12 kHz up to 6 months of age. *Mir-183/96$^{dko}$* mice were also found to be profoundly deaf, with most showing no response at the highest sound level tested (95 dB sound pressure level ) at any of the ages tested (14 days to 6 months old) (Lewis et al., 2020). Therefore, AHL in the C57BL/N

background would not impact my results since my study do not involve any functional analyses and all my experiments were performed prior to onset of hearing loss. Figure 2.1 shows the mouse lines used in current study along with their genetic attributes.
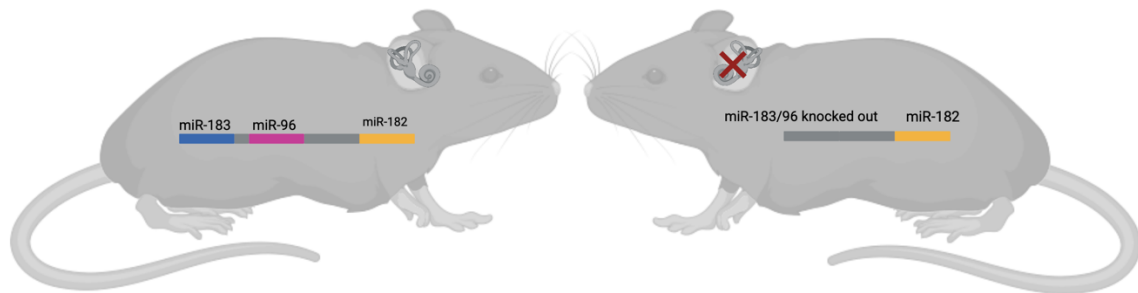


**Figure 2.1 Schematic depiction of mouse models**
*miRNAs of the miR-183 cluster are intact and colour-coded in the wildtype form; miR-183 in blue, miR-96 in pink, and miR-182 in yellow. In the Mir-183/96$^{dko}$ mouse, miRs 183 and 96 are missing and mice are deaf. Figure created with BioRender.com*

## 2.2.2  Genotyping

Genotyping of mice is a crucial molecular technique used in genetics and research to determine the genetic makeup of individual mice. For this purpose, the isolation of genomic DNA followed by stable genotyping PCRs are required.

### Genomic DNA Isolation from mouse toe biopsies

Each animal is number-coded by toe biopsies at P7-9 and tissue from these biopsies is further used for the DNA extraction. Animals are re-genotyped after it was sacrificed for validation. To extract genomic (g)DNA from the toe biopsies, 700 µl of Tail Buffer and 50 µl of 10 mg/ml Proteinase K were added and mixed thoroughly. The mixture was then incubated overnight at 56°C, followed by a 10-minute centrifugation step at 13,000 rpm to separate the supernatant. Isopropanol (500 µl) was added to the supernatant, and the mixture is inverted and incubated at room temperature for 2 minutes. After a second centrifugation step (5 minutes at 13,000 rpm), the supernatant was discarded, and 500 µl of 70% ethanol was added to the DNA pellet. The reaction tubes were inverted to wash the pellet, followed by another 5-minute centrifugation step at 13,000 rpm. The supernatant was discarded, and the remaining ethanol was removed with a pipette. The pellets were air-dried at 37°C for

approximately 10 minutes and then dissolved in 50 µl of nuclease-free water before being stored at 4°C until the genotyping PCR could be performed.

*Genotyping PCR of miR-183/96 mice*

Table 2.9 summarizes the reaction mixture and PCR programme for genotyping. Afterwards, samples were analysed on a 2% TBE-agarose gel for 60 min at 100 V. Wildtype animals only show the wt band (841 bp), knockouts only the ko band (645 bp) while heterozygous animals show both wt and ko bands.

*Table 2.9 Genotyping PCR reaction details*

| Master mix for 1 PCR reaction (25 µl) | PCR Program |
|---|---|
| 2.5 µl 10× Dream Taq Buffer | Initial denaturation: 95°C ➡ 5 min |
| 0.5 µl dNTPs (10 mM each) | |
| 0.5 µl 20 pmol/µl miR-183-96ko_for Primer | Cyclic denaturation: 95°C ➡ 30 s |
| 0.5 µl 20 pmol/µl miR-183-96ko_rev primer | Primer annealing: 62°C ➡ 30 s — 30 cycles |
| 0.1 µl Dream Taq | DNA polymerization: 72°C ➡ 30 s |
| 19.9 µl nuclease free $H_2O$ | |
| 1 µl extracted mouse gDNA | Final DNA polymerization: 72°C ➡ 5 min<br>Hold: 4°C ➡ ∞ |

## 2.2.3  Volume measurements of auditory brainstem nuclei

Volume estimation is one of the methods to detect morphological changes in brain areas. Previously (Krohs et al., 2021) carried out anatomical analysis to detect any changes in volume, cell number or cell size in auditory brainstem nuclei of *Mir-183/96$^{dko}$* mice compared to their wt littermates. In the initial manuscript, volume analysis only covered age P60 but the measurements from P0 and P25-P27 were still required to complete the analysis. Therefore, I performed morphometric analysis of DCN, VCN, LSO and MNTB at P25-P27 and only MNTB at P0 as part of revision for the paper. Figure 2.2 shows an overview about the anatomy of the auditory brainstem nuclei quantified in the revision analysis.
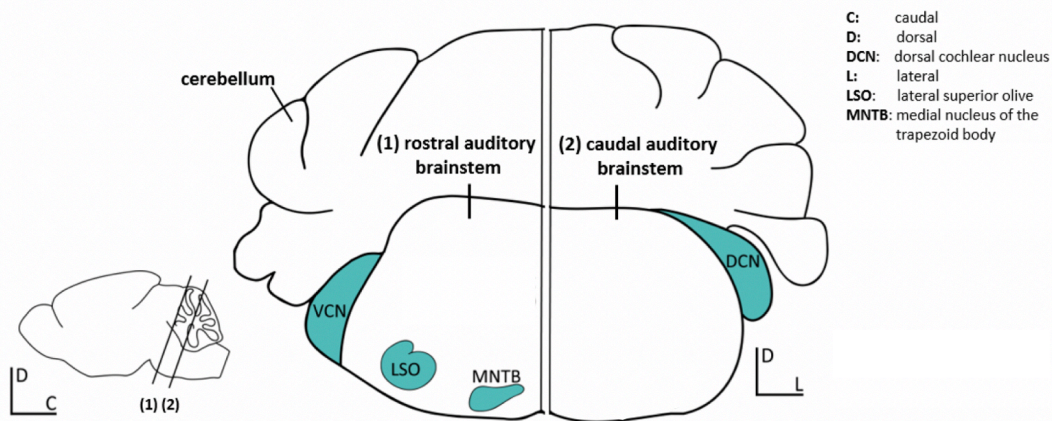
**Figure 2.2 Anatomical organization of auditory brainstem nuclei**
*Schematic illustration of auditory structures and their location in the auditory brainstem of mice. There are two section planes indicated, the more rostral one (1) harbouring the VCN, LSO, MNTB, and the more caudal one (2) harbouring the DCN. Modified from (Krohs, 2020)*

## Tissue preparation

Postnatal day 25-27 *Mir-183/96^{dko}* mice and their wt littermates were injected intraperitoneally with a lethal dose of pentobarbital (Narkodorm ,182,3 mg/kg bodyweight) and perfused transcardially with phosphate buffered saline (PBS) followed by 4% paraformaldehyde (PFA). For P0 mice, chloroform was used instead of pentobarbital while rest of the procedure remains the same. Brains were removed, postfixed for 1-4 hours and incubated in 30% sucrose in PBS overnight at -4°C. Brains were embedded in tissue freezing medium for an hour at -19°C inside cryostat before sectioning. A complete series of auditory brainstem sections of 30 μm starting from the DCN to the end of the MNTB were collected on gelatin-chromalaun coated slides. The stored slides were subsequently subjected to Nissl staining.

## Nissl staining

The histological Nissl staining method is often used to stain the nuclei and accumulations of material around the nuclei in neurons, making the neurons visible. The staining of the tissue was performed using thionin which interacts with negatively charged nucleic acids in DNA and RNA. This stains the DNA in the nucleus, the RNA in the nucleoli, and the ribosomal RNA in the rough endoplasmic reticulum.

To prepare for Nissl staining, the slide series were air-dried and incubated overnight in Chloroform/Ethanol (1:1). The next day they were incubated in 100% EtOH for 60 minutes. The tissue was slowly hydrated by dipping the slides for 3 minutes each in 96% I, 96% II, 90%, 70%, 50% EtOH, and distilled water. The slides were incubated for 1-2 minutes in thionin solution. After staining, the sections were dipped briefly in distilled water and then in an ascending order for 3 minutes per liquid Ethanol series (50%, 70%, 90%, 96% EtOH with acidic acid, and 96% EtOH) dehydrated. The purpose of acetic acid is to adjust staining to wash any unbound basic thionin stain. After the ethanol series, the sections were incubated for 3 minutes each in terpineol-xylene (1:1 ratio), in xylene I and in xylene II. All steps of Nissl staining were performed under a fume hood. Finally, the sections were covered with Roti-Histokitt II mounting medium and coversliped. The Zeiss AxioScan Z1, an automated slide scanning microscope, was used for imaging.

### *Morphometry of auditory brainstem nuclei*

Three specimens were selected from each genotype (*Mir-183/96$^{dko}$* & wt) for morphometric analysis.  The AxioScan microscope was used to scan every section of the left and right DCN, LSO, MNTB and VCN and then saved as a single photograph. Using ImageJ, the area of each auditory nucleus in the sections was calculated by surrounding the nucleus with a selection and measuring the area according to the known image dimensions. In the case of a missing section, the mean was calculated from the sections analysed before and after. The volume of each nucleus was then calculated by multiplying its area in each section by 30 µm (the thickness of the cryosections) and summing up the volume of each section of the nucleus. The averaged values (3 per genotype) from the left and right nucleus were compared statistically using multivariate analysis of variance (MANOVA) to detect any significant differences in volume between *Mir-183/96$^{dko}$* mice and their wt littermates. Cell counting for P0 MNTB was also done in ImageJ, and the total number of cells in each MNTB was calculated by adding the counted cells together. Only cells that were in the area circled beforehand were counted. Missing sections were assumed to have the cell number of the average of the previous and the following sections. The averaged values (3 per genotype) from the left and right nucleus were compared statistically with a Student's t-test or a Mann-Whitney U test after checking for normal distribution.

### 2.2.4 Immunohistochemistry

This method is used to detect and locate proteins within tissue sections by utilizing the specific binding between an antigen and an antibody. The technique involves using a fluorophore-conjugated secondary antibody that binds to the primary antibody-antigen complex allowing for visualization of the target protein through fluorescence microscopy. It is a commonly used technique to assess protein expression levels and spatial distribution in various cell types. The protocol is divided into following steps:

#### *Tissue preparation*

*Mir-183/96$^{dko}$* mice and their wt littermates were deeply anesthetized at P25-27 with Narkodorm (Pentobarbital,182,3 mg/kg bodyweight) and perfused transcardially with PBS followed by Zamboni solution. Brains were removed, postfixed for 1-4h and cryoprotected in 30% sucrose in PBS overnight at -4°C. The brain was embedded in 30 % sucrose (in PBS) and frozen at -30°C for an hour on cooling unit of microtome. Coronal auditory brainstem sections of 30 µm thickness were first collected in 15% sucrose (in PBS) and later stored in PBS at 4°C using a 24 well plate.

#### *Primary antibody incubation*

First the sections of interest were selected using a microscope and transferred to fine meshes in a 6 well plate containing PBS. All subsequent washing and incubation steps were carried out on a shaker. The sections were washed in PBS (3×5 min) and blocked with a blocking solution for an hour. After the primary antibody was diluted in the carrier solution (for dilutions see Table 2.4), the brain sections were transferred to the primary antibody solution in a 24 well plate and incubated overnight at 4°C to allow for specific binding between the primary antibody and the antigen of interest.

#### *Secondary antibody incubation*

The next day sections were transferred back onto the fine meshes and washed (3×5min) in PBS. After dilution of the secondary antibody in 3 ml of carrier solution (1:1,000), the subsequent steps were performed in the dark to avoid any interference caused by the fluorescence of the secondary antibody. The fine meshes containing the washed sections

were then transferred to the secondary antibody solution in a 6-well plate and left to incubate at room temperature for 1.5-2 hours. The sections were again washed in PBS (3×5min) following the incubation period. The free-floating sections were gently transferred onto a gelatin-chromalaun coated slide using a fine brush and air-dried. The sections were then mounted using Mowiol + DABCO + DAPI, cover slipped and left overnight to dry before microscopy.

### *Microscopy and image analysis*

The immunohistochemical staining was evaluated on two kinds of microscopes. For the revision of paper (Krohs et al., 2021) , TCS SP8 confocal laser scanning microscope with HC PL APO 63x/1.4 oil objective was used for imaging. The images were analysed using ImageJ. The quantifications were made on stacks of biggest cell circumference plus the two surrounding scans and then merged via z-project. These images were converted to binary images and thresholded before applying respective ImageJ plugins. The colocalization analysis (homer1/GluA1) was performed by using "*binary feature extractor"* and overlay was set to 1%. For Homer1 area analysis, the area corresponding to Homer1 was marked using "*free hand selection*s" and "*Analyse measure"* feature was employed to give the value. Statistical analysis was performed using two-tailed Student's t- test to assess differences between *Mir-183/96$^{dko}$* mice and their wt littermates.

For Gray value analysis Olympus BX63 automated fluoresce microscope was used. The images were taken with UPLXAPO20X objective. Quantification was performed using ImageJ. Three regions of interest of $100 \times 100$ μm were selected within the LSO as well as outside the SOC or negative control for background subtraction. Mean gray values were calculated, and statistical analysis was performed using two-tailed Student's t test to assess differences between *Mir-183/96$^{dko}$* mice and their wt littermates.


## 2.2.5  RNA-seq analysis of LSO and MNTB

This technique was employed to detect differences in gene expression between *Mir-183/96$^{dko}$* mice and their wt littermates at mRNA level. RNA was isolated from laser micro dissected LSO & MNTB and sent for sequencing. The RNA-seq services were provided by TAmiRNA GmbH, (Vienna, Austria).  The details of the protocol are described below:

### Upstream preparations

1% cresyl violet solution in 100% ethanol was prepared one week prior to use. The falcon tube was covered with aluminium foil as cresyl-violet is sensitive to light, kept in fridge and shaken gently every day. The POL slides were UV treated for 15 min before collection of tissue. A separate RNAse free cryostat blade was used for tissue sectioning.

### Preparation of brains

*Mir-183/96$^{dko}$* mice and their wt littermates were killed with $CO^2$ and decapitated at P25-P27. The brain was immediately prepared out of the skull, embedded in Tissue Tek OCT and frozen in liquid nitrogen. The brains were stored at -80°C.

### Cryo-sectioning

Frozen brains were taken out of -80°C and equilibrated for 20min in the cryostat set at -19°C. Coronal sections of 20µm thickness were cut on cryostat and collected on RNase-free POL membrane slides. The tissue collection on POL slides was done when LSO & MNTB became visible. First section was directly collected in 350 µl RLT buffer (content of Qiagen RNA isolation kit) to serve as cryostat control for overall RNA quality control throughout the protocol. After collection of tissue sections, the slides were stored inside the cryochamber till the whole LSO & MNTB was collected. The cutting and mounting steps were performed as quickly as possible to reduce any chances of RNA degradation. The slides were subjected to a quick cresyl violet staining afterwards.

### Quick Cresyl violet staining

The slides were briefly fixed in 75% (-20°C) ethanol for 2 min. Afterwards they were stained with 1% cresyl violet solution through the sterile filter followed by dehydration in 75% EtOH, 95% and 100% EtOH (30s each). A final fixation of 1 minute in fresh 100% EtOH was done afterwards. Slides were briefly air-dried and stored in 50ml falcon tubes with silica bags to keep them dry. The stained slides were then stored at -80°C.

## *Laser capture microdissection*

The slides were taken out of -80°C and subjected to laser capture microdissection without thawing. The microscope was cleaned with RNAse free solution before each use. Following settings were used during the process: Power 45-50; aperture 15; speed 8; specimen balance 25; line spacing for draw and scan 19. Tissue regions of interest (LSO & MNTB) were selected using LMD6500 software and total areas varying from approx. $4.6 \times 10^6$ to $7.2 \times 10^6$ µm² were micro-dissected using the LMD6500 system. Laser micro-dissected material was collected in a dry adhesive cap. After the completion of LMD session, a tissue section was collected separately to serve as LMD control, and all samples were stored at -80°C until further processing.

## *RNA extraction*

The miRNeasy Micro kit was used for RNA extraction. All samples were removed from -80°C storage and transferred to ice. The cryostat control collected in 350 µl RLT buffer was thawed on ice, while 30 µl RLT buffer was added to the adhesive caps containing dissected material. The caps were allowed to stand for 10-15 minutes before vortex mixing and short centrifugation. The resulting 30 µl RLT buffer with lysed tissue was transferred to a 1.5 ml Eppendorf tube containing 320 µl RLT buffer to reach the required 350 µl total volume as per Qiagen protocol. Then, 70% EtOH was added, mixed with a pipette, and transferred to columns supplied with the kit. The MinElut spin columns were centrifuged for 30 s at 10,000×g, and this step was repeated to ensure that all liquid had passed the filter and the flow-through was discarded. At this stage, RNA was bound to the column.

For the washing step, 350 µl buffer RW1 was added to the column, followed by centrifugation at 10,000×g for 30 s, and the flow-through was discarded. Next, a dilution of 10 µl DNase1 to 70 µl Buffer RDD per sample was made, and 80 µl DNase mix was added per column. Samples were then incubated at room temperature for 15 min, followed by centrifugation with 350 µl of buffer RW1 at 10,000×g for 30 s. The collector tube was replaced with a fresh one before the next step. 500 µl RPE buffer was added to the column, centrifuged at 10,000×g for 30 s, and the flow-through was discarded. Final washing was done by adding 500 µl of 80% EtOH and centrifuging at 10,000×g for 2 min. The collector tube was again replaced with a fresh

one after this step. To remove all traces of EtOH, the columns were centrifuged at maximum speed with their lids removed at 15,000×g for 5 min. For elution, the column was placed into an RNase-free 1.5 ml Eppendorf tube and 14 µl of RNase-free water was added to the centre of the column followed by centrifugation at 15,000×g for 1 min. The flow-through was pipetted back into the column and centrifuged 2-3 times to maximize the yield of RNA. Afterwards, the RNA was stored at -80°C.

## RNA quality control

Total RNA yields were evaluated using the Agilent Bioanalyzer 2100 together with the RNA 6000 Pico kit. A software algorithm is used by the bioanalyzer for assessing multiple features of the micro-capillary electrophoretogram of each RNA sample to calculate RNA Integrity Number (RIN) ranging from 1 to 10. RNA of a RIN higher than 7 is generally considered ideal for downstream applications. The company required at least 20 µl volume for downstream analysis with stable quantities and RIN number. Since the Qiagen kit allows an elution volume of 14 µl only; pooling of RNA samples was required to meet the desired volume. For this purpose, 10 µL of eluted RNA each from two mice per genotype were combined to make a 20 µl volume per sample. A total of 3 $MiR-183/96^{wt}$ samples were analysed in comparison to 3 $MiR-183/96^{dko}$ samples for both nuclei. Table 2.10 gives an overview of all samples pooled along with their quality control.

**Table 2.10 RNA-seq sample pooling**

| Genotype | Tissue | Two RNA Samples combined(20ul) RNA concentration-RIN | |
|---|---|---|---|
| $MiR-183/96^{wt}$ | LSO | 3324 pg/µl- 7.80 | 216 pg/µl- 8.10 |
| $MiR-183/96^{wt}$ | LSO | 1512 pg/µl- 8.20 | 339 pg/µl- 7.80 |
| $MiR-183/96^{wt}$ | LSO | 1187 pg/µl- 8.40 | 1660 pg/µl- 8.40 |
| $MiR-183/96^{dko}$ | LSO | 770 pg/µl- 8.30 | 730 pg/µl- 8.10 |
| $MiR-183/96^{dko}$ | LSO | 668 pg/µl- 8.50 | 949 pg/µl- 8.40 |
| $MiR-183/96^{dko}$ | LSO | 931 pg/µl- 7.90 | 660 pg/µl- 8.00 |
| $MiR-183/96^{wt}$ | MNTB | 697 pg/µl- 8.30 | 1087 pg/µl- 7.80 |
| $MiR-183/96^{wt}$ | MNTB | 2094 pg/µl- 7.80 | 98 pg/µl- 7.80 |
| $MiR-183/96^{wt}$ | MNTB | 1563 pg/µl- 7.80 | 440 pg/µl- 8.20 |

| MiR-183/96$^{dko}$ | MNTB | 107 pg/µl- 7.90 | 262 pg/µl- 7.70 |
|---|---|---|---|
| MiR-183/96$^{dko}$ | MNTB | 557 pg/µl- 81.0 | 156 pg/µl- 7.30 |
| MiR-183/96$^{dko}$ | MNTB | 985 pg/µl- 7.50 | 557 pg/µl- 7.10 |

### *RNA sequencing*

RNA samples were sent to TAmiRNA, Austria for sequencing and bioinformatic analysis. The company used following tools to analyse the data. Overall quality of the next-generation sequencing data was evaluated both automatically and manually with fastQC v0.11.8 (Andrews, 2010) and multiQC v1.7 (Ewels et al., 2016). Reads from all passing samples were adapter trimmed and quality filtered using bbduk from the bbmap package v38.69 (Bushnell, 2015) and filtered for a minimum length of 17nt and Phred quality of 30. Alignment steps were performed with STAR v2.7 (Dobin et al., 2013) using samtools v1.9 (Li et al., 2009) for indexing, whereas reads were mapped against the genomic reference GRCm38.p6 provided by Ensembl (Zerbino et al., 2018). Assignment of features to the mapped reads was done with htseq-count v0.13 (Anders et al., 2015). Differential expression analysis with EdgeR v3.30 (Robinson et al., 2010) used the quasi-likelihood negative binomial generalized log-linear model functions provided by the package. The independent filtering method of DESeq2 (Love et al., 2014) was adapted for use with EdgeR to remove low abundant genes and thus optimize the false discovery rate (FDR) correction. Figure 2.3 summarizes the overall process of RNA-seq analysis.

From the analyses provided by the company, I made use of the Principal component analysis (PCA) and differential gene expression analysis (DGE). PCA is a statistical technique employed to reduce the dimensionality of a dataset, while preserving as much variability as possible. The primary utility of this method lies in presenting a multivariate data table into a more concise set of variables which facilitates the observation of trends, jumps, clusters, and outliers within the data (Jolliffe & Cadima, 2016). While DGE uses statistical tests to find mRNA that are over or under expressed in a group. Annotations in these result by company are standardized, as that for a contrast of LSO ko vs. LSO wt, a positive logFC indicates that the mRNA is upregulated in LSO ko.

Apart from these, I also used Sylamer analysis to examine the broad effects of *Mir-183/96$^{dko}$* on the transcriptomes of the LSO and MNTB (Van Dongen et al., 2008). The tool is freely

available to use but the site is under construction for upgrading. Due to this, Dr Enright,s team performed the analysis for me. Sylamer is a tool which examines all potential heptamers (microRNA seed region sequences) within the 3'UTR of genes robustly detected in the RNA-seq data organized by expression values;  from most upregulated to most downregulated irrespective of the significance. The output is a landscape enrichment plot that shows show significance profiles for each microRNA seed sequences studied across the sorted gene list. The analysis was performed on the list of genes that survived the filtering and were analysed by EdgeR for DGE by the company.
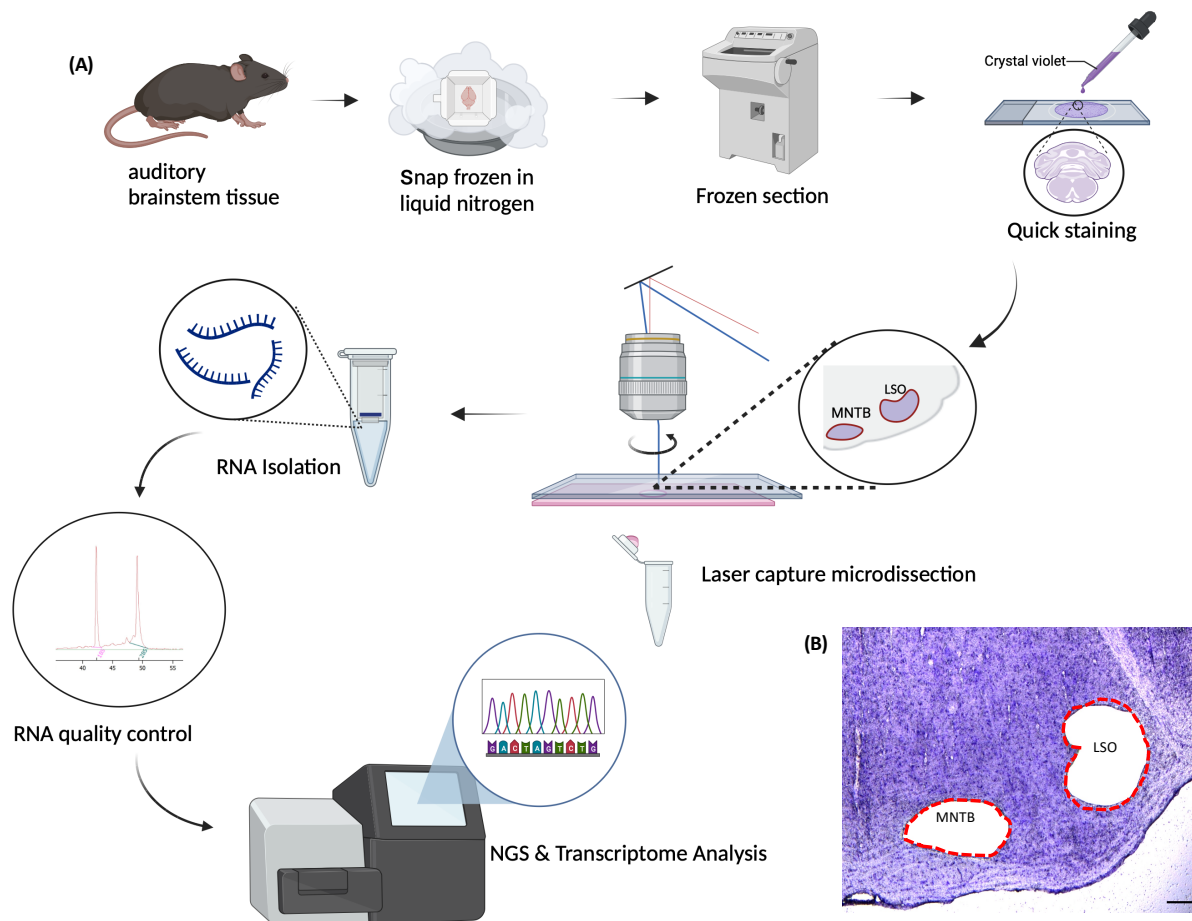


**Figure 2.3  Laser microdissection coupled RNA-seq workflow**
*A, The workflow includes preparation of CV stained cryosections from auditory brainstem tissue, LMD into adhesive caps, RNA extraction and quality control followed by sample sequencing and analysis. Figure was created with BioRender.com. B, Stained coronal brainstem slice section after being subjected to laser capture microdissection for collection of LSO & MNTB. Scale bar 100um*

# 3 Results

## 3.1 Own contribution to the publication "Loss of miR-183/96 Alters Synaptic Strength via Presynaptic and Postsynaptic Mechanisms at a Central Synapse „

The following results are part of a publication (Krohs et al., 2021) where I performed additional experiments during the revision of the manuscript. In this study, the central auditory system of the *Mir-183/96$^{dko}$* mouse was characterized for further elaborating the role of the miR-183 cluster for development and function of the auditory hindbrain. The focus was set on overall auditory brainstem morphology and, particularly, the calyx of Held to identify the genetic factors that drive its morphological and functional maturation. Notably, the two miRNAs emerged as a significant regulator of auditory brainstem development and synaptic strength. Krohs and colleagues observed significant reduction in volume, specifically in auditory hindbrain nuclei. Whereas the detailed analysis of the calyx of Held synapse revealed that presynaptically, these calyces exhibited an increase in release-ready SVs, quantal content, and the presence of the proteins Bassoon and Piccolo. Postsynaptically, there was an increase in quantal size, as well as the number and size of GluA1 puncta. These results confirmed a critical contribution of this miRNA cluster to auditory brainstem development and function.

### 3.1.1 Reduced volume of auditory brainstem nuclei in *Mir-183/96$^{dko}$* mice at P25-P27

In the initial manuscript the anatomy of the auditory hindbrain nuclei of *Mir-183/96$^{dko}$* mice was investigated at age P60 to assess the impact of miR-183/96 loss on integrity of these structures. The analysis revealed three out of four CNC nuclei (VCN, LSO & MNTB except DCN) having significantly reduced volumes in *Mir-183/96$^{dko}$* mice. However, to match the results with subsequent electrophysiology and immunohistology analysis, assessment at P25-P27 was required. Furthermore, to frame the timeline of volume and cell loss in the hindbrain of *Mir-183/96$^{dko}$* mice, additional analysis at P0 was also essential. Therefore, I conducted the morphological analysis of auditory hindbrain at both P0 and P25-P27. The quantitative analysis of Nissl-stained sections at age P25-P27 showed significantly reduced volumes of all

four CNC nuclei (DCN, VCN, LSO and MNTB) in *Mir-183/96*<sup>dko</sup> mice (Fig. 3.2). The DCN volume was reduced by 28.6% (wt: $0.164 \pm 0.0094$ mm$^3$; ko: $0.117 \pm 0.052$ mm$^3$; p = 0.0263) whereas the volume of VCN was reduced by 30.6% (wt: $0.186 \pm 0.0122$ mm$^3$; ko: $0.129 \pm 0.0203$ mm$^3$; p = 0.0263). The LSO displayed a volume loss of 94.4% in *Mir-183/96*<sup>dko</sup> animals (wt: $0.061 \pm 0.0013$ mm$^3$; ko: $0.0034 \pm 0.0030$ mm$^3$; p = 0.013) and the MNTB showed a volume reduction by 34.2% (wt: $0.038 \pm 0.0022$ mm$^3$; ko: $0.025 \pm 0.0019$ mm$^3$; p = 0.0239). To analyse the timeline of these changes, I further focused on the MNTB in P0 mice, as only this nucleus is clearly identifiable at this early postnatal stages. The MNTB already at birth (P0), displayed a drastic volume loss of 28.9% (wt: $0.119 \pm 0.0006$ mm$^3$; ko: $0.0085 \pm 0.0008$ mm$^3$; p = 0.028) whereas cell number was not significantly altered (wt: $3274 \pm 217.4$ ; ko: $2738 \pm 225.1$; p = 0.162) (Fig. 3.1). These additional findings together with studies at P60 strengthened the claim that miR-183 and miR-96 are essential for proper development of auditory hindbrain.
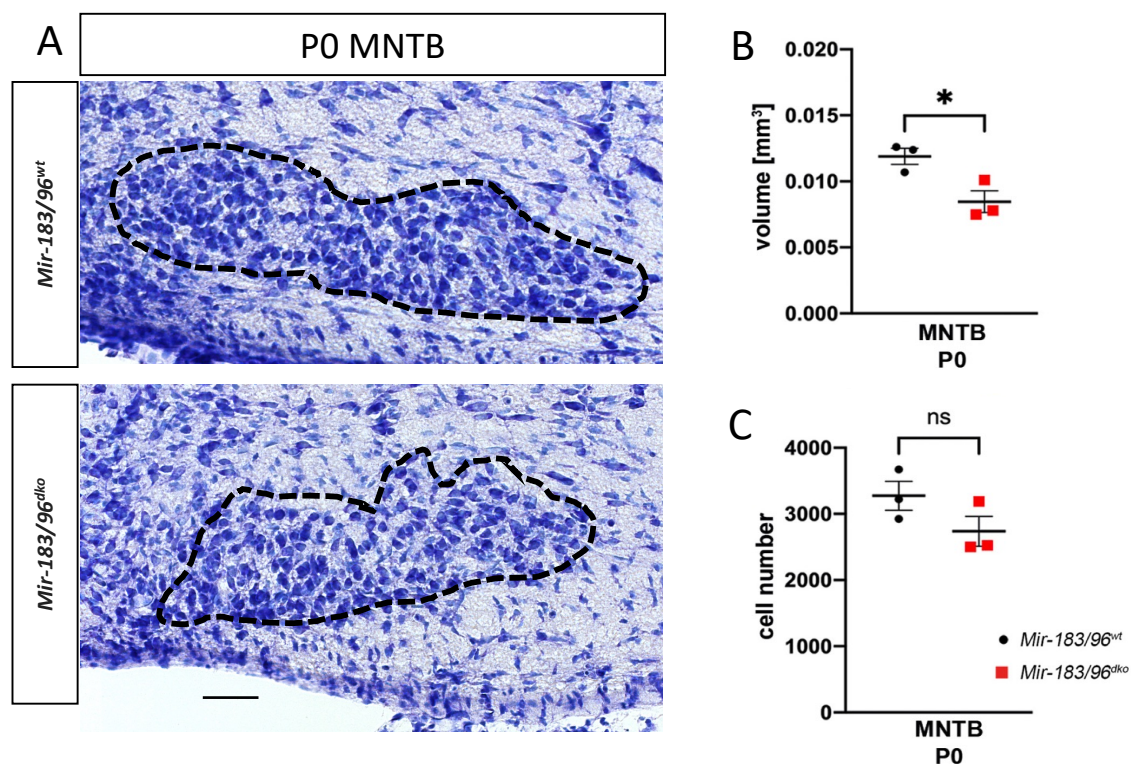


***Figure 3.1 Morphometric analysis of MNTB at P0***
*A; Representative images of MNTB on Nissl-stained coronal sections of Mir-183/96*<sup>dko</sup> *and wt mice at comparable section planes. The nuclei are outlined with a black dashed line. The images indicate clear reduction of MNTB size in Mir-183/96*<sup>dko</sup> *mice. Scale bar: 100um. B,C; Quantification of the volume and cell in Mir-183/96*<sup>dko</sup> *mice and wt littermates at P0.*
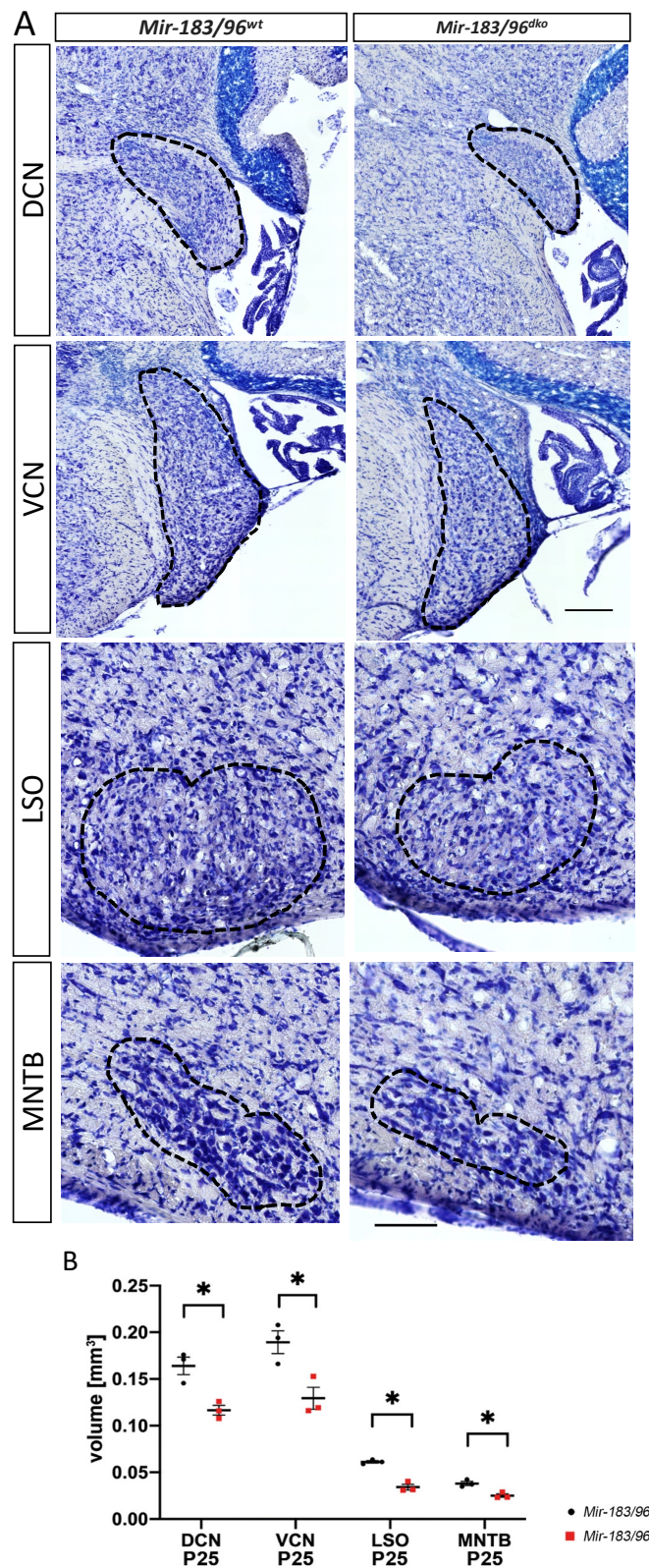
**A**

### 3.1.2 Increased area of Homer1 puncta and co-localization of Homer1 with GluA1 in *Mir-183/96$^{dko}$* mice

In the initially submitted manuscript of Krohs and colleagues, electrophysiological analysis of the calyx of Held synapse revealed an increase in spontaneous excitatory postsynaptic currents (sEPSCs) and thus synaptic strength at *Mir-183/96$^{dko}$* calyces. To explain this increase in amplitude, the post-synaptic density was analysed since sEPSC amplitudes are a postsynaptic component. The α-amino-3-hydroxy-5-methyl-4-isoxazolepropionic acid receptor (AMPAR) subunit GluA1; which is a validated target of miR-96 (Dambal et al., 2015; Jensen & Covault, 2011) was analysed by means of immunohistochemistry to quantify the abundance of GluA1 in the MNTB principal cell and its synaptic localization. GluA1 formed larger clusters in the cell interior in *Mir-183/96$^{dko}$* mice as compared with wt littermates. To explain this increase in number and size of GluA1 puncta which led to a stronger incorporation of GluA1 subunits into the postsynaptic receptor complexes further experiments were required. Therefore, I performed experiments to examine co-localization of GluA1 with Homer1. Homer1 is a post synaptic density marker protein which acts as a scaffold that clusters and colocalizes with NMDA (N-methyl-D-aspartate) and mGluR receptors (Tu et al., 1999). The puncta where at least 1% overlap was observed were defined as co-localized in small confocal image stacks. The number of GluA1 puncta colocalized with Homer1 was increased in *Mir-183/96$^{dko}$* synapses (wt: 0.439 ± 0.053; ko: 0.939 ± 0.131; p = 0.0009) (Fig. 3.2A, B). *Homer1* is a validated target of miR-96 (Dambal et al., 2015; Jensen & Covault, 2011) and in agreement with this, I observed a 53% increase in total area of Homer1 puncta in *Mir-183/96$^{dko}$* synapses as compared with wt synapses (wt: 31.11 ± 3.03 ; ko: 47.67 ± 2.71; p = 0.0001) (Fig. 3.2A,C). Due to the enlarged Homer1 area in *Mir-183/96$^{dko}$* synapses, I employed a normalization approach by dividing the number of colocalized GluA1 puncta by the total Homer1 area. This was done to address the potential issue of overestimating co-localized Homer1 and GluA1 puncta. After this normalization, I still observed a higher number of GluA1 puncta that co-localized with Homer1 in the data (Fig. 3.2 B). This result suggests an increased incorporation of postsynaptic GluA1 proteins into the AMPAR complexes in the PSD of *Mir-183/96$^{dko}$* MNTB neurons. This might provide a molecular explanation for the higher sEPSCs observed in *Mir-183/96$^{dko}$* animals.
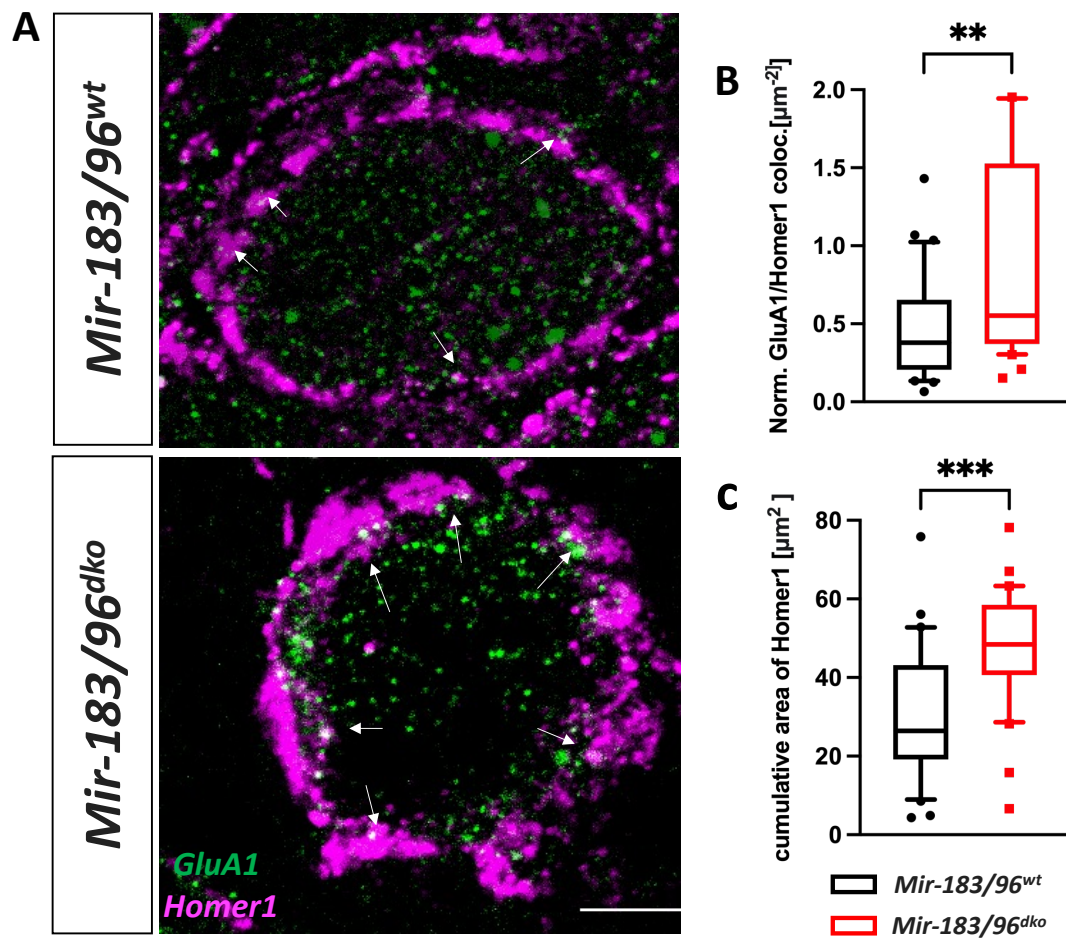
**Figure 3.3 Increased Homer1 area and colocalization with GluA1**
*A; Representative MNTB principal cells after immunolabeling of GluA1(green) and the PSD protein Homer1 (magenta) in Mir-183/96<sup>dko</sup> and corresponding wt animals. Arrows indicate areas of co-localization (white). Images represent maximal intensity projections of small confocal image stacks, Scale bar: 5 µm. B; Co-localization analysis of Homer1 and GluA1 puncta showing at least 1% overlap. The number of co-localized puncta was normalized to the cumulative Homer1 area, which was enlarged in Mir-183/96<sup>dko</sup> mice. C: Quantification of the cumulative Homer1 area at the PSD of the calyx of Held. N = 30 cells from three animals per genotype at the age of P25-27. Statistics: Student's t test. \*\*p < 0.01, \*\*\*p < 0.001.*

## 3.2 Loss of miR-183/96 Impacts inhibitory neurotransmission proteins and the transcriptomes of LSO and MNTB

The following results are part of my investigation on inhibitory synapse related gene targets of miR-96 in the LSO and transcriptome analysis of LSO, MNTB nuclei in *Mir-183/96<sup>dko</sup>* mice as compared to their wt littermates.

### 3.2.1 Immunoreactivity of inhibitory proteins in LSO of *Mir-183/96^{dko}* mice

A technique often used to identify experimentally miRNA targets is comparative quantitative immunohistochemistry between wildtype and genetically altered mice. Schlüter et al. (2018) had successfully shown that the miR-96 *Dmdo* mutation leads to decreased expression of the potassium channel subunits Kv1.6 and BKβ2 in the LSO and MNTB whose genes *Kcna6* and *Kcnmb2* are predicted targets for the mutated miR-96 (Schluter et al., 2018). Similarly, (Krohs et al., 2021) ) employed immunohistochemistry to study the effects of miR-96/183 ko on putative targets and revealed increased expression of GluA1 and Homer1 in MNTB of *Mir-183/96^{dko}* mice. Studies by (Lewis et al., 2016; Lewis et al., 2020; Lewis et al., 2009) also showed strong downregulation of oncomodulin (Ocm) in both miR-96 *Dmdo* and *Mir-183/96^{dko}* hair cells in mice via immunohistochemical analysis. I therefore chose the same approach to investigate whether loss of miR-183/96 altered the expression of genes (validated or predicted targets of miR-96/miR-183) involved in inhibitory transmission.

For identifying gene targets of miR-96 that are critical for inhibitory neurotransmission, I first performed a literature search. This resulted in various validated gene targets of miR-96 (Jensen & Covault, 2011).  Apart from that, a recent RNA-seq project of Neurogenetics division (Bordeynik-Cohen et al., 2023) predicted several gene targets of the miR-183 cluster. From both data sets, genes relevant to inhibitory neurotransmission were selected (*Kcc2, Gad2/65, Gphn, Gabra1, Hapln4*) and the effect of miR-96/miR-183 loss on their expression was quantified using immunohistochemistry in *Mir-183/96^{dko}* mice and their wt littermates. Gphn is the main post-synaptic scaffold protein that forms sub-membranous cytoplasmic lattices at the post-synaptic complex of GABAergic and glycinergic synapses (Luscher & Keller, 2004). Immunoblot analysis had validated it as a target of miR-96 (Jensen & Covault, 2011). Immunoreactivity of Gphn in the LSO revealed a significant 52% increase in gray values of Gphn in ko as compared to wt (wt: 26.9 ± 3.78; ko: 41.0 ± 4.12; p = 0.0196) (Fig. 3.4A,B). I then investigated Gad65 and Kcc2, both of which are also targets of miR-96  (Jensen & Covault, 2011). Gad65 is an enzyme involved in the synthesis of GABA, the main inhibitory neurotransmitter in mammalian brain. It is membrane-associated in GABA vesicles and creates GABA for quick synaptic release in response to neural activation and  affects GABA levels throughout postnatal maturity (Kaufman et al., 1991). Gray value analysis of Gad2

revealed no significant differences between *Mir-183/96^{dko}* and their wildtype littermates (wt: 0.237 ± 3.35; ko: -9.40 ± 3.30; p = 0.0687) (Fig. 3.4A,B). Next, I quantified Kcc2, encoded by *Slc12a5*. Kcc2 is located in the postsynaptic membrane of neurons, particularly near symmetrical inhibitory synapses in the brainstem. Its primary role is to facilitate the co-transport of potassium and chloride ions which is crucial for establishing the electrochemical gradient of chloride ions within neurons. Consequently, Kcc2 significantly influences the effectiveness and the polarity of synaptic transmissions mediated by GABA and glycine, both of which rely on chloride ion fluxes for their signalling (Blaesse et al., 2009; Blaesse et al., 2006). Quantification of immunoreactivity signals for Kcc2 also showed no differences between wildtype and ko mice in LSO (wt: 65.4± 15.7; ko: 55.7 ± 24; p = 0.375) (Fig. 3.4A,B). Third I analysed the two proteins Gabra1 and Hapln4. Both appeared as potential targets of miR-96 in the RNA-seq data (Bordeynik-Cohen et al., 2023) generated by the Neurogenetics division. Hapln4 plays a significant role in establishing and facilitating transmission of inhibitory GABAergic synapses by organizing the perineural networks in synaptic cleft (Edamatsu et al., 2018). Our quantification of Hapln4 immunoreactivity showed no significant differences between *Mir-183/96^{dko}* and their wildtype littermates (wt: 32.2 ± 18.0; ko: 29.2 ± 17.3; p = 0.605; Fig. 3.4A,B). Lastly, I quantified Gabra1 immunoreactivity. This protein is ligand-gated chloride channel protein which is a  crucial component of GABAARs responsible for binding to GABA, which is the primary inhibitory neurotransmitter in the brain (Fuchs et al., 2013). My analysis revealed a 57% decrease in Gabra1 immunoreactivity in *Mir-183/96^{dko}* mice in comparison to the wildtype (wt: 127 ± 29.9; ko: 54.9 ± 32.6; p < 0.001) (Fig. 3.4A,B). Since miRs downregulate gene expression, the possible outcome in their absence would be an upregulation of their target genes. However, I observed varied effects on gene expression in the knockout mouse model. This suggests that microRNA mediated gene regulation is not governed by a straightforward mechanism; rather they contribute to a complex gene regulatory network, where numerous factors come into play to ensure precise post-transcriptional gene expression.
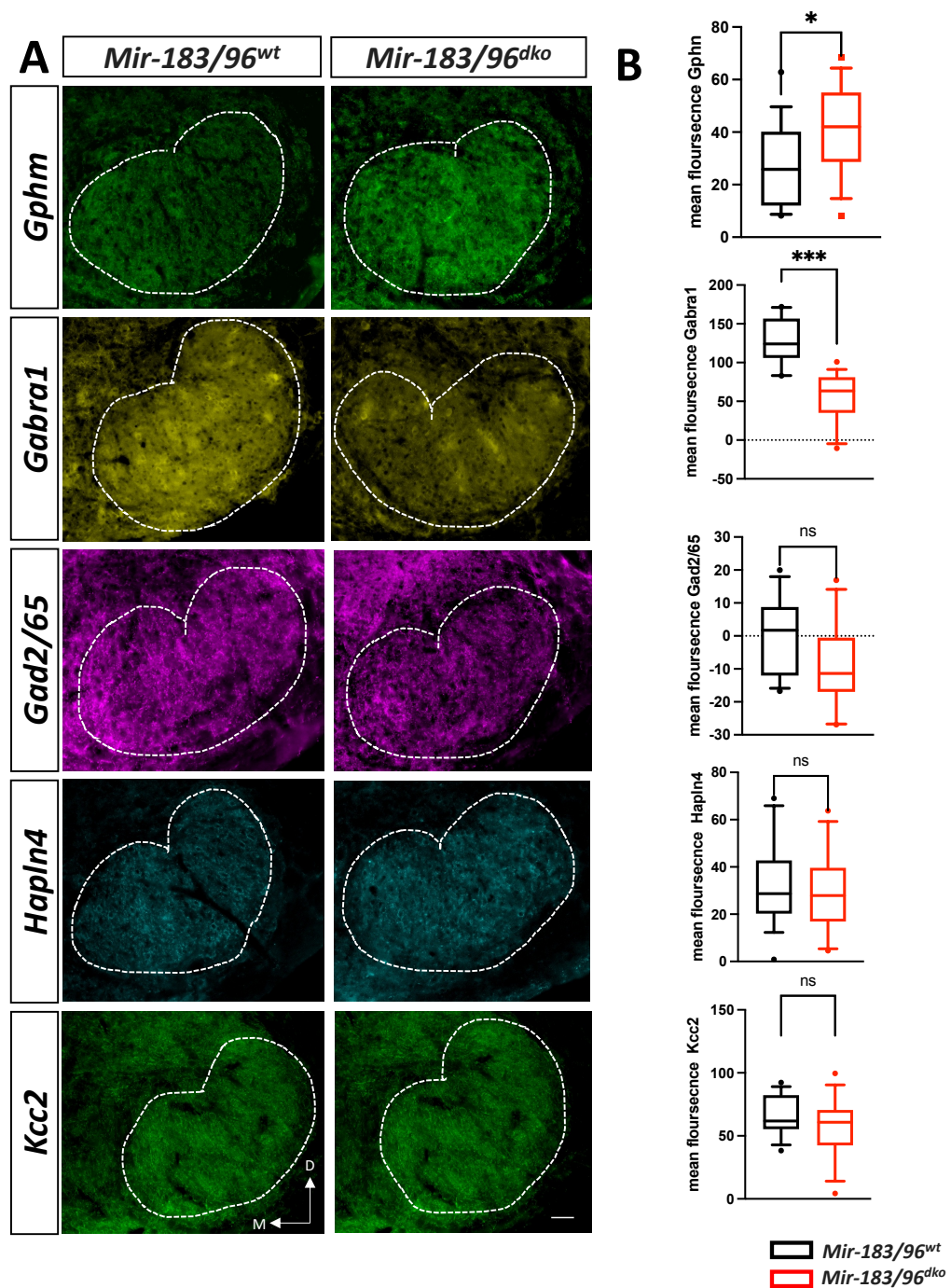
**Figure 3.4 Immunohistochemical analysis of inhibitory neurotransmission proteins in LSO**
*A, Immunohistochemistry for Gphn, Gabra1, Gad2/65, Hapln4 and Kcc2 in the LSO of Mir-183/96$^{dko}$ and their wt littermate controls at P25-P27. Scale bar: 50µm. B, Quantification of Gphn, Gabra1, Gad2/65, Hapln4 and Kcc22 signal in the LSO relative to fluorescence outside the SOC area (mean ± SEM., 12–18 LSO slices from three animals for each genotype). In the Mir-183/96$^{dko}$, the relative intensity of Gphn was higher, whereas Gabra1 displayed decreased relative intensity compared to the wildtype controls. No difference in relative intensities of Gad2/65, Hapln4 and Kcc2 was observed between the two genotypes. Student's t test was used as a test for statistical significance. Black, Mir-183/96$^{wt}$ control; red, Mir-183/96$^{dko}$ mice.*

### 3.2.2 RNA-seq analysis reveals misregulation of gene expression both in LSO and MNTB in *Mir-183/96^{dko}* mice

To investigate the impact of *Mir-183/96^{dko}* mutation on overall gene expression in LSO and MNTB, I carried out RNA-seq of laser micro-dissected LSO and MNTB tissue from P25-27 *Mir-183/96^{dko}* mice and their littermate wt controls. Around, 10,000 genes were identified per sample robustly (data not shown).

PCA was employed to assess the factors influencing the overall gene expression data from both nuclei (Fig. 3.5). It revealed a clear separation between LSO and MNTB tissues as expected since they are distinct auditory brainstem nuclei having specialized structures and functions . I also observed moderate clustering of samples by their genotype (wt and ko) which points towards differential gene expression between wildtype and knockout samples. Only one wt MNTB sample stands out as a clear outlier in the analysis. This sample had the lowest amount of RNA in comparison to other samples revealed by the RNA quality control done by the company (data not shown), which might explain it. Overall, we can see a minimal effect of *Mir-183/96^{dko}* on the transcriptome.
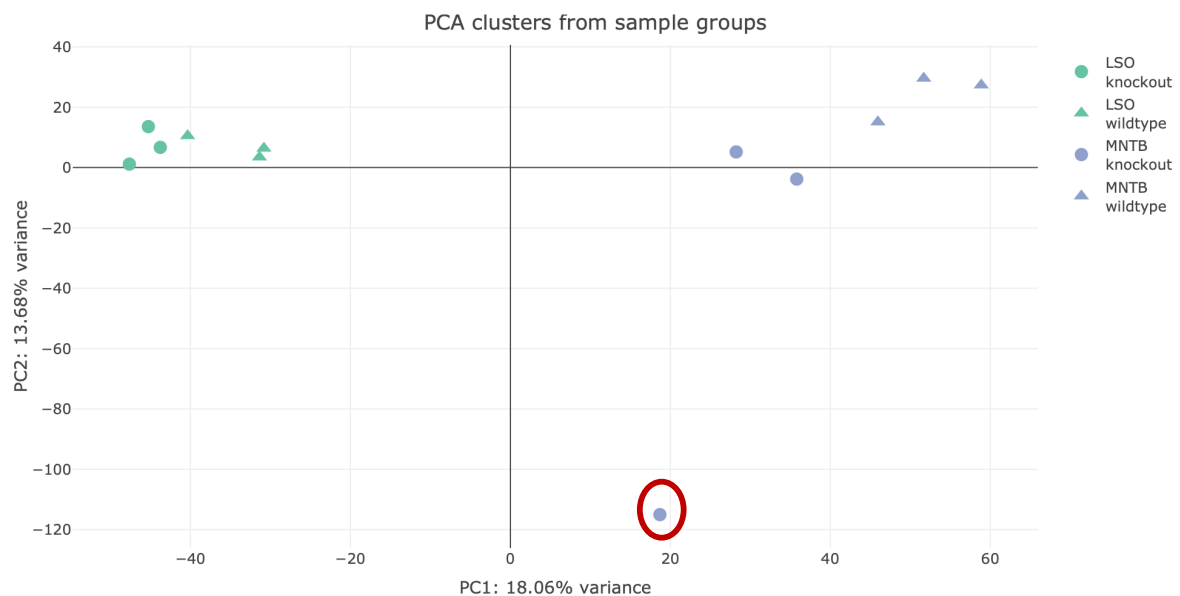


**Figure 3.5 Principal component analysis**
*PCA plot illustrates the transcriptional pattern of LSO (green) and MNTB (blue) tissues by the profiles of gene expression in wt (triangles) and Mir-183/96^{dko} (circles) mice. Samples clustered based on a PCA of differentially expressed genes between wildtype and knockout samples. The MNTB ko outlier sample is marked in red circle. The axes: the principal components PC1 and PC2 with the proportion of explained variance of the data for each principal component.*

In agreement with this first impression, DGE analysis in the LSO resulted in only 34 significantly misregulated genes (false discovery rate (FDR) < 0.05) in *Mir-183/96$^{dko}$* as compared to wildtype. Out of these, 15 were upregulated (green) and 19 were downregulated (red) compared with their wt littermates (Fig. 3.5, Table 3.1).
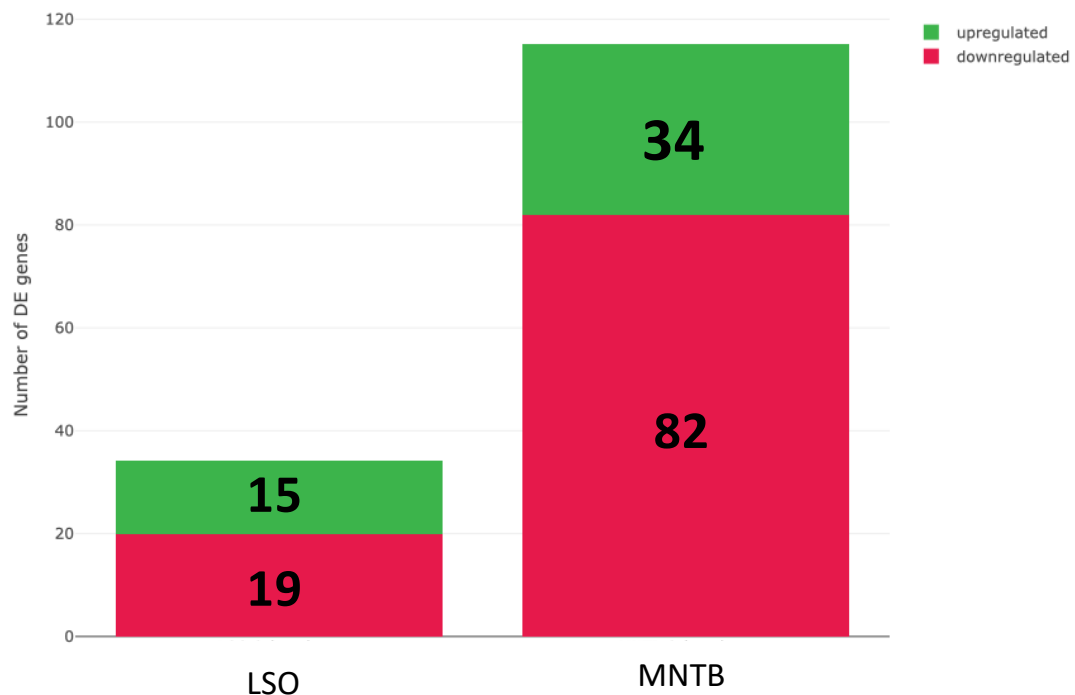


***Figure 3.6 Differential Gene Expression***
*The graph shows the summary of differently expressed genes in Mir-183/96$^{dko}$ compared to wt controls in LSO and MNTB tissues. Green areas correspond to upregulated genes while red areas correspond to downregulated genes in the respective tissue. Numbers represent up- or down-regulated genes in the respective tissue.*

To assess a direct effect of the two microRNAs on the expression of these genes, I used target prediction databases TargetScan (Lewis et al., 2005) and miRDB (Chen & Wang, 2020) to check whether the 3'UTRs of misregulated genes in our data show complementarity with the seed region of miR-96 and miR-183. I found only 4 genes (*Myt1l, Rgs17,Sv2c* and *Nrp2*) that show complementarity to either the miR-96 or miR-183 seed region in their 3'UTRs (Table 3.1). Next, I checked if these direct targets have any relevance to the auditory system. Only *Rgs17* and *Sv2c* were found related to auditory system. *Rgs17* (regulator of G-protein signalling 17), upregulated in our data, is a target of miR-96 (Table 3.1). It is a novel mediator of cisplatin induced ototoxicity and a potential therapeutic target for treating hearing loss. The increased expression of Rgs17 was associated with cisplatin-induced hearing loss while Rgs17

knockdown could suppress this hearing loss (Dhukhwa et al., 2021). *SV2c* (synaptic vesicle glycoprotein 2) was downregulated and has target sites for both miR-96 and miR-183 (Table 3.1). It is a glycoprotein localized on the surface of neuronal synaptic vesicles (Janz & Südhof, 1999), associated with deafness in a study exploring gene expression changes in the inferior colliculus after single-sided deafness (Kil et al., 2021). Next, I explored other misregulated genes in this list which are not targets of miR-96/183 but could be of importance in the auditory system. Of the upregulated genes, 3 are of particular interest: *Ednrb*, *Vgf* and *Sparcl1*. *Ednrb* (endothelin receptor type B) is a very important gene for enteric nervous system development. Mutations in *Ednrb* gene are known to cause congenital sensorineural deafness in rats (Dang et al., 2011) and humans (AitRaise et al., 2022; Stanchina et al., 2006). *Vgf* (VGF nerve growth factor inducible) is a secreted neuronal protein, that is expressed in neurons throughout the brain (Levi et al., 2004). A study exploring the rapid onset antidepressant-like actions of ketamine identified Vgf as important to regulate the TrkB/mTOR/BICC1 signalling pathway and AMPA receptor GluA1 phosphorylation in mice (Shen et al., 2018). The mTOR signalling pathway is also linked to hearing loss (Cortada et al., 2021) while GluA1 was implicated in synaptic strength studies (Krohs et al., 2021). *Sparcl1* (SPARC like protein 1) expression was detected in human brainstem neurons where it functions to relay and regulate motor and sensory signals in the brainstem (Hashimoto et al., 2016). From the downregulated genes list, *Lamp5* (Lysosome-associated membrane protein 5) is highly expressed in auditory brainstem nuclei where it is exclusively localized to inhibitory synaptic terminals and plays an essential role in sensorimotor processing (Koebis et al., 2019). Interestingly, the miR-96 gene targets (*Kcc2, Gad2/65, Gphn, Gabra1, Hapln4*), that were analysed by immunohistochemistry are not significantly misregulated in the LSO DGE analysis. Although , both Gphn and Gabra1 are differentially expressed at protein levels, the complex mechanisms involved between transcription and translation are not yet sufficiently well-defined to able to compute protein concentrations from mRNA levels (Greenbaum et al., 2003). Apart from that, noise and error in both mRNA and protein experiments could also limit the ability to get a clear picture (Baldi & Long, 2001).

*Table 3.1 Significantly misregulated genes (FDR< 0.05) in LSO of Mir-183/96$^{dko}$ RNA-seq*

| Gene symbol | Gene ID | logFC | FDR | Seed region matches in 3'UTRs | | |
|---|---|---|---|---|---|---|
| | | | | miR-96 | miR-182 | miR-183 |
| Ucn | ENSMUSG00000038676 | 3.113898 | 1.54E-07 | | | |
| Zcchc12 | ENSMUSG00000036699 | 2.737133 | 0.000858 | | | |
| Calca | ENSMUSG00000030669 | 2.405585 | 2.95E-51 | | | |
| Hs3st2 | ENSMUSG00000046321 | 2.1227 | 0.04904 | | | |
| Vgf | ENSMUSG00000037428 | 2.026894 | 1.54E-07 | | | |
| Slc15a2 | ENSMUSG00000022899 | 1.81812 | 0.029989 | | | |
| Cacna2d3 | ENSMUSG00000021991 | 1.582306 | 0.025624 | | | |
| Myt1l | ENSMUSG00000061911 | 1.471998 | 0.00181 | | | yes |
| Ednrb | ENSMUSG00000022122 | 1.049528 | 0.034081 | | yes | |
| Agt | ENSMUSG00000031980 | 0.994437 | 0.034081 | | | |
| Nsg2 | ENSMUSG00000020297 | 0.859391 | 0.014224 | | | |
| Rgs17 | ENSMUSG00000019775 | 0.818436 | 0.023815 | yes | yes | |
| Ap1s2 | ENSMUSG00000031367 | 0.795875 | 0.029989 | | | |
| Sparcl1 | ENSMUSG00000029309 | 0.252397 | 0.001035 | | | |
| Plp1 | ENSMUSG00000031425 | -0.20447 | 1.12E-09 | | | |
| mt-Nd5 | ENSMUSG00000064367 | -0.21777 | 0.044091 | | | |
| Cox7c | ENSMUSG00000017778 | -0.29701 | 0.036903 | | | |
| Cox8a | ENSMUSG00000035885 | -0.39457 | 0.005665 | | | |
| Atp5md | ENSMUSG00000071528 | -0.44549 | 0.000712 | | | |
| Apod | ENSMUSG00000022548 | -0.46145 | 0.04904 | | | |
| mt-Co1 | ENSMUSG00000064351 | -0.46963 | 1.59E-16 | | | |
| Lamp5 | ENSMUSG00000027270 | -0.49544 | 0.014159 | | | |
| Cox6a1 | ENSMUSG00000041697 | -0.54377 | 1.18E-06 | | | |
| Cox6b1 | ENSMUSG00000036751 | -0.54594 | 2.47E-05 | | | |
| Slc38a2 | ENSMUSG00000022462 | -0.70371 | 0.000112 | | | |
| Rgs5 | ENSMUSG00000026678 | -0.87905 | 0.00103 | | | |
| Olig2 | ENSMUSG00000039830 | -0.9177 | 0.041859 | | | |
| Kcnab1 | ENSMUSG00000027827 | -1.03592 | 0.04904 | | | |
| Cacng4 | ENSMUSG00000020723 | -1.19843 | 0.034081 | | | |

| | | | | | | |
|---|---|---|---|---|---|---|
| *Sv2c* | ENSMUSG00000051111 | -1.28586 | 5.04E-05 | yes | | yes |
| *Mcf2l* | ENSMUSG00000031442 | -1.48564 | 0.01867 | | | |
| *Cox8b* | ENSMUSG00000025488 | -1.60871 | 0.04904 | | | |
| *Igfbp2* | ENSMUSG00000039323 | -1.98316 | 6.06E-06 | | | |
| *Nrp2* | ENSMUSG00000025969 | -2.99634 | 0.000239 | | | yes |

In the MNTB, 116 genes were significantly misregulated (FDR < 0.05). Thirty-four of these genes were upregulated (green) while 82 of them were downregulated (red) in the knockout (Fig 3.5). This data set was analysed in a similar manner to the LSO data. We found 7 genes (*Cygb, Rplp0, Slc12a5, Gpm6b, Map1b, Rap1gap2 ,Rgs2*) whose sequences showed complementarity to either the miR-96 or miR-183 seed region in their 3'UTRs (Table 3.2). From these genes, only *Cygb* and *Slc12a5 (Kcc2)* are relevant to auditory system. *Cygb* (cytoglobin) plays a vital role in maintaining oxygen homeostasis within both the peripheral and central auditory nervous system on physiological level (Reuss et al., 2023) and has target site for miR-96 (Table 3.2). Furthermore, it is upregulated in a specific subset of oxidative stress related genes that are linked to age related hearing loss in rats (Tanaka et al., 2012). *Slc12a5* coding potassium chloride co-transporter Kcc2 is important for an intracellularly directed Cl⁻ gradient and hence for maturation of postsynaptic GABAergic inhibitory neurons (Blaesse et al., 2006; Rivera et al., 1999). Several other non-target genes relevant to the auditory system popped up in this data set as well. Of the upregulated genes, 2 are of particular interest: *Camk2g* and *Cldn11. Camk2g* (gamma subunit of calcium/calmodulin-dependent protein kinase 2) is expressed throughout the brain and is associated with neurodevelopmental disorders (Rigter et al., 2023). Reduced normal auditory input upsets the excitation-inhibition balance in the IC, so a study utilized Affymetrix GeneChip arrays to examine gene expression changes in the rat IC, 3 and 21 days post-bilateral deafening, with a specific focusing on neurotransmission-related genes. *Camk2g* which modulates glycine receptor function showed decreased expression in this study (Holt et al., 2005). It also thus appeared in a list of genes termed important for hearing in a review paper related to targeting of hearing related genes in mice (Gao et al., 2004). *Cldn11* plays an important in the central nervous system since its absence alters properties of myelin. *Cldn11⁻/⁻* mice exhibit severe deafness along with glutamate imbalance in the brainstem (Gow et al., 2004; Maheras et al., 2018). From the downregulated genes list, I identified *Mt-nd1, Snap25* and *Lamp5* as

interesting genes. *Mt-nd1* (mitochondrially encoded NADH Dehydrogenase 1) is a mitochondrial gene which plays a pivotal role in the electron transport chain of oxidative phosphorylation. A novel heteroplasmic mutation in the gene caused profound sensorineural hearing loss and neurodevelopmental delay in humans (Ammar et al., 2016). *Snap25* (Synaptosomal-Associated Protein, 25) is a key component of the neuronal SNARE complex responsible for sustained and fast calcium-dependent synaptic vesicle fusion at the ribbon synapses of IHCs (Safieddine & Wenthold, 1999). Studies in a knockout mouse model of targeted deleted *Snap25* in IHCs, causes deafness both when occurring at neonatal and at mature stages due to defective IHCs exocytosis leading to ribbon degeneration and IHCs loss (Calvet et al., 2022). Apart from that Snap25 also facilitates GABA release during development since it is present at the presynaptic terminals of mature GABAergic neurons (Tafoya et al., 2006). *Calb1* (Calbindin1), a small cytoplasmic calcium binding protein and a classic marker for MNTB and other nuclei of SOC was also found to be downregulated in our data (Friauf, 1993; Rosengauer et al., 2012). Finally, similar to the LSO, *Lamp5* (Lysosome-associated membrane protein 5) was downregulated in the MNTB as well.

**Table 3.2 Significantly misregulated genes (FDR< 0.05) in MNTB of Mir-183/96<sup>dko</sup> RNA-seq**

| Gene symbol | Gene ID | logFC | FDR | Seed region matches in 3'UTR | | |
|---|---|---|---|---|---|---|
| | | | | miR96 | miR182 | miR183 |
| *Pcp4* | ENSMUSG00000090223 | 2.181712 | 6.2E-07 | | | |
| *mt-Tv* | ENSMUSG00000064338 | 1.289448 | 0.001774 | | | |
| *Edil3* | ENSMUSG00000034488 | 1.268862 | 0.014802 | | | |
| *Id4* | ENSMUSG00000021379 | 1.254712 | 0.047662 | | | |
| *Camk2b* | ENSMUSG00000057897 | 1.253807 | 0.047662 | | | |
| *Plpp3* | ENSMUSG00000028517 | 1.237137 | 0.024214 | | | |
| *Ptn* | ENSMUSG00000029838 | 1.123377 | 0.049217 | | | |
| *Lypd1* | ENSMUSG00000026344 | 1.097379 | 0.024214 | | | |
| *Tagln3* | ENSMUSG00000022658 | 1.011511 | 0.000753 | | yes | |
| *Eif3f* | ENSMUSG00000031029 | 0.969631 | 0.033615 | | | |
| *Tmem106b* | ENSMUSG00000029571 | 0.967628 | 0.043182 | | | |
| *Cygb* | ENSMUSG00000020810 | 0.879325 | 0.018409 | yes | yes | |
| *Rps14* | ENSMUSG00000024608 | 0.781861 | 0.002135 | | | |

| | | | | | | |
|---|---|---|---|---|---|---|
| *Naa38* | ENSMUSG00000059278 | 0.780986 | 0.036807 | | | |
| *Ptgds* | ENSMUSG00000015090 | 0.773335 | 0.001224 | | | |
| *Rplp0* | ENSMUSG00000067274 | 0.762066 | 0.040877 | | | yes |
| *Hba-a1* | ENSMUSG00000069919 | 0.747941 | 0.001645 | | | |
| *Camk2g* | ENSMUSG00000021820 | 0.696963 | 0.043182 | | | |
| *Hbb-bs* | ENSMUSG00000052305 | 0.67928 | 8.09E-05 | | | |
| *Mal* | ENSMUSG00000027375 | 0.677763 | 0.001859 | | | |
| *Slc12a5* | ENSMUSG00000017740 | 0.669888 | 0.032276 | yes | yes | |
| *Eef1a1* | ENSMUSG00000037742 | 0.665993 | 0.017198 | | | |
| *Mbp* | ENSMUSG00000041607 | 0.645134 | 1.52E-40 | | | |
| *Mobp* | ENSMUSG00000032517 | 0.598769 | 1.77E-06 | | | |
| *Cldn11* | ENSMUSG00000037625 | 0.590153 | 0.000495 | | | |
| *Gpm6b* | ENSMUSG00000031342 | 0.578282 | 0.003241 | yes | yes | |
| *Bc1* | ENSMUSG00000115783 | 0.563973 | 0.016421 | | | |
| *Tmsb4x* | ENSMUSG00000049775 | 0.550923 | 0.000162 | | yes | |
| *Dbi* | ENSMUSG00000026385 | 0.436492 | 0.049504 | | | |
| *Cst3* | ENSMUSG00000027447 | 0.424304 | 0.003513 | | | |
| *Fth1* | ENSMUSG00000024661 | 0.306686 | 0.001645 | | | |
| *Calm1* | ENSMUSG00000001175 | 0.232235 | 0.044212 | | | |
| *Plp1* | ENSMUSG00000031425 | 0.19712 | 0.000106 | | | |
| *mt-Nd1* | ENSMUSG00000064341 | -0.11761 | 0.021831 | | | |
| *mt-Cytb* | ENSMUSG00000064370 | -0.16701 | 0.000536 | | | |
| *Atp5g3* | ENSMUSG00000018770 | -0.25322 | 0.013891 | | | |
| *Snap25* | ENSMUSG00000027273 | -0.27026 | 0.030204 | | | |
| *Atp1b1* | ENSMUSG00000026576 | -0.28856 | 0.000228 | | | |
| *mt-Co1* | ENSMUSG00000064351 | -0.30219 | 0.009421 | | | |
| *Atp5b* | ENSMUSG00000025393 | -0.32599 | 0.047484 | | | |
| *Map1b* | ENSMUSG00000052727 | -0.33401 | 0.027311 | | | yes |
| *mt-Nd2* | ENSMUSG00000064345 | -0.33586 | 0.009351 | | | |
| *Slc25a4* | ENSMUSG00000031633 | -0.3695 | 0.003961 | | | |
| *Cox6a1* | ENSMUSG00000041697 | -0.37495 | 0.016077 | | | |
| *Atp5md* | ENSMUSG00000071528 | -0.41142 | 0.003961 | | | |
| *Atp1a3* | ENSMUSG00000040907 | -0.43812 | 0.020167 | | | |

| | | | | | | |
|---|---|---|---|---|---|---|
| *Nap1l5* | ENSMUSG00000055430 | -0.44358 | 0.049314 | | | |
| *Nefl* | ENSMUSG00000022055 | -0.44392 | 0.003566 | | | |
| *Cox6b1* | ENSMUSG00000036751 | -0.45153 | 0.00222 | | | |
| *Slc25a3* | ENSMUSG00000061904 | -0.45539 | 0.001774 | | | |
| *Atp2a2* | ENSMUSG00000029467 | -0.47722 | 0.043182 | | | |
| *Map1lc3b* | ENSMUSG00000031812 | -0.48433 | 0.023926 | | | |
| *Calb1* | ENSMUSG00000028222 | -0.5043 | 0.002283 | | | |
| *Slc32a1* | ENSMUSG00000037771 | -0.51351 | 0.032276 | | | |
| *Stxbp1* | ENSMUSG00000026797 | -0.52755 | 0.00769 | | | |
| *Mdh1* | ENSMUSG00000020321 | -0.53539 | 6.2E-07 | | | |
| *Eif4g3* | ENSMUSG00000028760 | -0.54584 | 0.049217 | | | |
| *Nefh* | ENSMUSG00000020396 | -0.55265 | 0.000188 | | | |
| *Ndrg4* | ENSMUSG00000036564 | -0.5808 | 5.37E-12 | | | |
| *Kif5c* | ENSMUSG00000026764 | -0.60399 | 0.034494 | | | |
| *Rgs7bp* | ENSMUSG00000021719 | -0.61589 | 0.001085 | | | |
| *Mif* | ENSMUSG00000033307 | -0.62767 | 0.004685 | | | |
| *Kcnc1* | ENSMUSG00000058975 | -0.63289 | 0.005368 | | | |
| *Lrrc49* | ENSMUSG00000047766 | -0.66601 | 0.038182 | | | |
| *Rcan2* | ENSMUSG00000039601 | -0.68012 | 0.006618 | | | |
| *Pitpnc1* | ENSMUSG00000040430 | -0.68113 | 0.03273 | | | |
| *Lamp5* | ENSMUSG00000027270 | -0.68245 | 6.2E-07 | | | |
| *Hspa4l* | ENSMUSG00000025757 | -0.68696 | 0.022714 | | | |
| *Rab6b* | ENSMUSG00000032549 | -0.692 | 0.001034 | | yes | |
| *Ogdh* | ENSMUSG00000020456 | -0.7275 | 0.003175 | | | |
| *Sgpp2* | ENSMUSG00000032908 | -0.75085 | 0.009351 | | | |
| *Enah* | ENSMUSG00000022995 | -0.75474 | 0.013591 | | yes | |
| *Syt7* | ENSMUSG00000024743 | -0.77512 | 0.012659 | | | |
| *Ina* | ENSMUSG00000034336 | -0.78669 | 2.96E-09 | | yes | |
| *Glg1* | ENSMUSG00000003316 | -0.79502 | 0.049504 | | | |
| *Anxa5* | ENSMUSG00000027712 | -0.80776 | 0.040877 | | | |
| *Efr3a* | ENSMUSG00000015002 | -0.82427 | 0.000228 | | | |
| *Spp1* | ENSMUSG00000029304 | -0.82951 | 1.51E-08 | | | |
| *Arl3* | ENSMUSG00000025035 | -0.83081 | 0.022123 | | | |

| | | | | | | |
|---|---|---|---|---|---|---|
| **Hspa5** | ENSMUSG00000026864 | -0.83891 | 0.000135 | | | |
| **Dnajc5** | ENSMUSG00000000826 | -0.85374 | 0.009319 | | | |
| **Nos1** | ENSMUSG00000029361 | -0.89746 | 0.032276 | | | |
| **Zfp365** | ENSMUSG00000037855 | -0.96922 | 0.021574 | | | |
| **Fabp3** | ENSMUSG00000028773 | -0.99933 | 0.034328 | | | |
| **Pdgfa** | ENSMUSG00000025856 | -1.00018 | 0.022926 | | | |
| **Dner** | ENSMUSG00000036766 | -1.02589 | 1.57E-05 | | | |
| **Odr4** | ENSMUSG00000006010 | -1.03485 | 0.018409 | | | |
| **Rap1gap2** | ENSMUSG00000038807 | -1.04662 | 0.009351 | yes | | |
| **Nefm** | ENSMUSG00000022054 | -1.05922 | 2.31E-23 | | | |
| **Rbms1** | ENSMUSG00000026970 | -1.1205 | 0.004438 | | yes | |
| **Pbx3** | ENSMUSG00000038718 | -1.14675 | 0.032276 | | | |
| **Fryl** | ENSMUSG00000070733 | -1.15351 | 0.045982 | | | |
| **Elovl5** | ENSMUSG00000032349 | -1.16093 | 6.12E-09 | | | |
| **Gm13889** | ENSMUSG00000087006 | -1.18877 | 0.000135 | | | |
| **Slc38a1** | ENSMUSG00000023169 | -1.22119 | 6.2E-07 | | | |
| **Rab15** | ENSMUSG00000021062 | -1.23314 | 0.017126 | | | |
| **Zswim6** | ENSMUSG00000032846 | -1.25757 | 0.049504 | | | |
| **Grm1** | ENSMUSG00000019828 | -1.27052 | 0.000712 | | | |
| **Homer1** | ENSMUSG00000007617 | -1.28345 | 0.037034 | | | |
| **Ctsa** | ENSMUSG00000017760 | -1.29699 | 0.014802 | | | |
| **Rgs2** | ENSMUSG00000026360 | -1.31525 | 0.017126 | yes | yes | yes |
| **Glra1** | ENSMUSG00000000263 | -1.32826 | 3.68E-10 | | | |
| **Ank1** | ENSMUSG00000031543 | -1.3351 | 4.31E-05 | | | |
| **Hcn4** | ENSMUSG00000032338 | -1.47032 | 0.016015 | | | |
| **Nexn** | ENSMUSG00000039103 | -1.49157 | 5.82E-07 | | | |
| **Nrip3** | ENSMUSG00000034825 | -1.53337 | 0.000102 | | | |
| **Lgi2** | ENSMUSG00000039252 | -1.53711 | 1.29E-12 | | | |
| **Cntnap5a** | ENSMUSG00000070695 | -1.58336 | 0.000135 | | | |
| **Timm10** | ENSMUSG00000027076 | -1.61302 | 0.002283 | | | |
| **Pianp** | ENSMUSG00000030329 | -1.66442 | 0.002188 | | | |
| **Cox8b** | ENSMUSG00000025488 | -1.8915 | 1.94E-09 | | | |
| **Inhbb** | ENSMUSG00000037035 | -1.96369 | 0.00029 | | | |

| | | | | | | |
|---|---|---|---|---|---|---|
| *Mafa* | ENSMUSG00000047591 | -2.03833 | 1.87E-05 | | | |
| *Stk24* | ENSMUSG00000063410 | -2.3206 | 1.01E-05 | | | |
| *Doc2g* | ENSMUSG00000024871 | -2.88758 | 1.45E-14 | | | |

Since I didn't find miR-96 or miR-183 targeting many significantly differentially regulated genes, Sylamer analysis was used to examine the broad effects of *Mir-183/96$^{dko}$* on the transcriptome of the LSO and MNTB (Van Dongen et al., 2008). The goal was to identify 3'UTRs of all genes robustly detected in our data for enrichment of seed regions (6-mers, 7-mers or 8-mers) corresponding to miR-96 and -183. In case of enrichment in upregulated or downregulated genes, part of the expression changes can be attributed to direct effects of these miRs. After filtering 4,121 genes in LSO and 2,005 genes in MNTB were analysed by EdgeR for DGE (list not shown here). I used the same lists for Sylamer analysis. We did not see any seeds corresponding to miR-96 or 183 in the top 6 hits (top 3 under- and over-represented), when examining 6-mers, 7-mers or 8-mers (plots not shown here). There were also no other miRNA seed region -mers enriched in the gene list of *Mir-183/96$^{dko}$* for both LSO and MNTB. The enrichment analysis plot combines all the seeds for each microRNA to show overall enrichment peaks for both LSO and MNTB data sets (Fig 3.5). As per Dr. Enright,s team, the Sylamer analysis usually deals with large datasets with more than 10,000 genes while our gene lists are comparatively smaller due to independent filtering , which might explain why we did not observe any enrichment in our data.
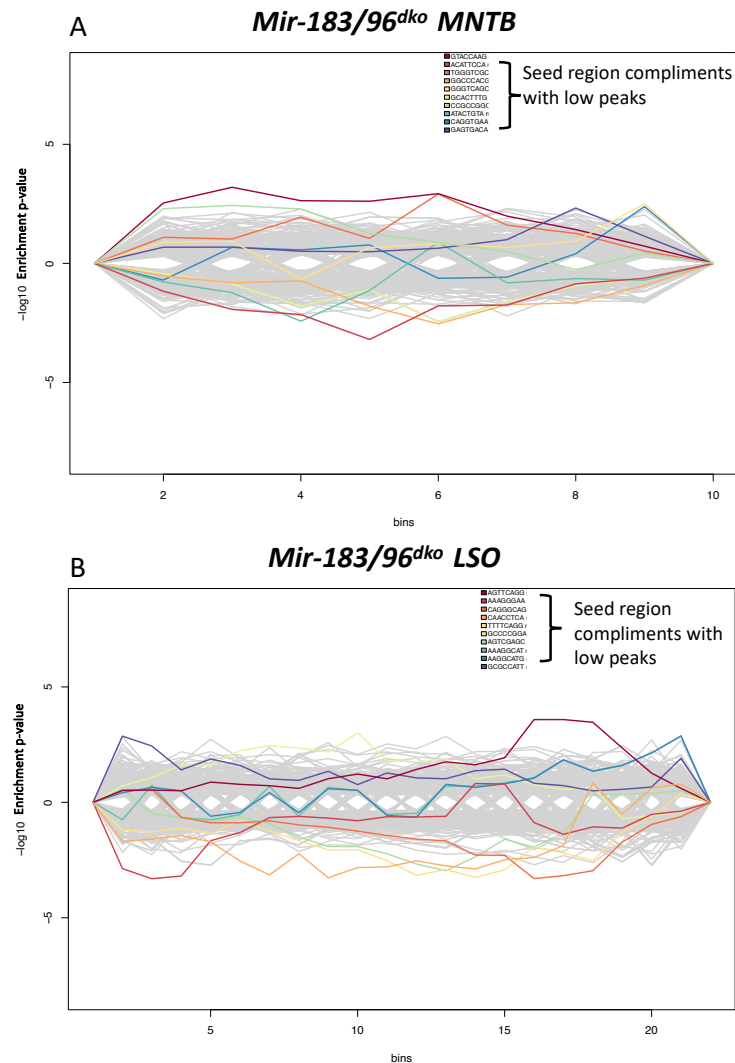
**Figure 3.7 Sylamer analysis showing overall enrichment and depletion of seed regions (6, 7 and 8-mers) in the 3'UTRs in RNA-seq data of LSO and MNTB from Mir-183/96$^{dko}$ mice**
*(A) Mir-183/96$^{dko}$ MNTB. (B) Mir-183/96$^{dko}$ LSO. The x-axis represents the sorted gene list from most upregulated on the left to most downregulated on the right. The y-axis shows the hypergeometric significance for enrichment or depletion of seed regions in 3'UTRs. UTRs are organized in bins (200 genes/bin), starting with the most upregulated genes until all genes have been considered. Coloured lines indicate the enrichment of each seed region; positive values indicate enrichment and negative values indicate depletion. A peak above +/- 5 would be considered as significant which is not seen here for any seed regions.*

Taken together, the loss of both miRs seem to have mild effects on transcriptome, however the expression of direct targets is changed on protein levels. Thus, validation at protein levels is important as it gives a substantial evidence of microRNA effects which can be further strengthened by functional studies for an overall conclusion.

# 4 Discussion

In this thesis, the role of miR-96 and miR-183 in the auditory brainstem was investigated using a *Mir-183/96^{dko}* mouse model. My first project dealt with additional morphometric and molecular analyses for a manuscript elaborating the role of miR-96 for proper development and function of the auditory hindbrain (Krohs et al., 2021). The second project addressed the impact of miR-183/96 loss on expression of inhibitory protein markers in LSO and overall gene expression in both the LSO and MNTB of *Mir-183/96^{dko}* mice. I will discuss these two projects in the following.

## 4.1 On site effect of miR-96/183 on auditory brainstem nuclei: volume reduction

The volume of auditory brainstem nuclei of *Mir-183/96^{dko}* was analysed at both P0 and P25-P27. At P25-P27 reduced volumes were observed in VCN, DCN, and two SOC nuclei, namely the MNTB and LSO. The result is consistent with the initial findings at P60 where three (VCN, MNTB & LSO) out of four nuclei were found to be significantly reduced in volume. These anatomical changes suggest that proper auditory brainstem development depend on on-site expression of miR-183/96 in the auditory brainstem (Krohs et al., 2021). In principle, these changes can also be attributed to lack of neuronal input caused by peripheral deafness. Various studies revealed that cochlear removal causes widespread cell death in second-order auditory hindbrain nuclei (DCN,VCN), however the survival of the third-order SOC nuclei (MNTB, LSO) seems be less dependent on peripheral activity (Nothwang et al., 2015). In a congenitally deaf dn/dn mouse model (Steel & Bock, 1980), a mutation in the *Tmc-1* gene results in the absence of spontaneous activity in the auditory nerve (Walmsley et al., 2006; Youssoufian et al., 2005), leading to volume reduction of the VCN (Webster, 1985). Peripheral deafness in a mouse line lacking the vesicular glutamate transporter 3 (VGlut3) in the IHCs also results in significant reduction of the CNC volume but the SOC volume remained unaffected (Seal et al., 2008). So, at least the observed anatomical changes in the third-order nuclei of the SOC can be attributed to an on-site effect of *Mir-183/96^{dko}*. In line with this are the results of a *Cldn14^{ko}* mouse line that was analysed to control for the effects of peripheral deafness alongside the *Mir-183/96^{dko}* mouse line. The cochlear hair cells of this peripherally

deaf mouse line are absent at P10-13 and their ABRs demonstrate deafness at P15-P17 (Ben-Yosef et al., 2003), similar to the *Mir-183/96*$^{dko}$ mouse. Yet, our analysis revealed unchanged volumes of auditory hindbrain structures in this mouse model, supporting the idea of an on-site effect of *Mir-183/96*$^{dko}$ during auditory brainstem development. Furthermore, peripheral deafness genes *Cacna1c* and *Cacna1d* encoding L-type calcium channels Cav1.2 and Cav1.3 respectively were also shown to be auditory specific since their conditional absence resulted in reduced volumes of auditory hindbrain nuclei but the rest of brainstem nuclei which also expresses these channels, remained unchanged. These anatomical changes were not due to loss of cochlea-driven neuronal input, since the mice showed normal inner ear function (Ebbers et al., 2015; Satheesh et al., 2012). Another striking factor is the timeline of these changes, as in *Mir-183/96*$^{dko}$ animals, volume was already reduced in the P0 MNTB, which points to a critical role of both miRs in proper embryonic development. This is in line with the loss of the entire SOC in mice lacking the miRNA processing enzyme Dicer pointing towards embryonic requirement of miRNAs (Rosengauer et al., 2012). Overall, it is likely that auditory brainstem development is dependent on miRNAs-183 and -96.

## 4.2 *Mir-183/96*$^{dko}$ synapses show elevated GluA1-homer1 co-localization along with enlarged homer1 area suggesting enhanced incorporation of GluA1 into postsynaptic receptor complexes

In the study (Krohs et al., 2021), the calyx of Held was investigated in detail on functional and molecular level. An increase in the quantal amplitude of sEPSCs in *Mir-183/96*$^{dko}$ calyces was observed on the postsynaptic level which was explained by increased synaptic co-localization of the AMPAR subunit GluA1 with postsynaptic density scaffold protein Homer1. In the following, I will focus the discussion on my co-localization analysis. I not only observed an increased co-localization of GluA1 with Homer1 but also an abundance in GluA1 subunits along with enlarged areas of Homer1 in *Mir-183/96*$^{dko}$ mice. As both GluA1 and Homer1 are validated targets of miR-96 (Jensen & Covault, 2011), the observed increase in their expression likely reflects the lack of downregulation in the absence of miR-96. The importance of this downregulation is seen around the onset of hearing at P10-11 when GluA1

predominantly switches to another AMPAR subunit, GluA4 (Caicedo & Eybalin, 1999; Koike-Tani et al., 2005; Lesperance et al., 2020). This is necessary since GluA1 has slower kinetics than GluA4 (Mosbacher et al., 1994) that normally dominate the calyx of Held synapse (Yang et al., 2011) and is best suited for the ultrafast synaptic transmission at the calyx of held (Borst & Soria van Hoeve, 2012). The unaltered, fast EPSC decay kinetics in *Mir-183/96^{dko}* calyces suggests that most likely they are still carried mainly by GluA4 containing AMPARs (Krohs et al., 2021). Thus, the increased incorporation of GluA1 could either take place as homomeric GluA1 receptors or heteromeric GluA1/4 AMPARs, both of which differ in their biophysical properties and regulation. Since GluA1 is much more sensitive for glutamate than GluA4 (Traynelis et al., 2010), its incorporation into these heteromeric GluA1/4 AMPARs could result in more AMPARs opening in response to SV fusion and glutamate release which partially explains the electrophysiological phenotype observed in *Mir-183/96^{dko}* mice (Krohs et al., 2021).

## 4.3  Post-transcriptional regulation of inhibitory genes by microRNA 96 & 183 proposes complex mechanisms

In this section I switch to my analysis of inhibitory gene targets in the LSO of *Mir-183/96^{dko}* mice. I first analysed three validated and two predicted gene targets of miR-96 at the protein level using immunohistochemistry. The goal was to evaluate whether the absence of miR-96/183 would impact their expression and to understand the potential impact on inhibitory neurotransmission in knockout mice. In this particular study I observed different effects of the lack of the two miRNAs on these gene targets at protein level. Gphn, a validated miR-96 target (Jensen & Covault, 2011) was upregulated in the knockout mice possibly due to the absence of posttranscriptional regulation which is required for proper clustering of Gphn at inhibitory synapses (Kirsch & Betz, 1998). In contrast, *Mir-183/96^{dko}* mice did not show altered immunoreactivity of Kcc2, Hapln4, and Gad2/65 in the LSO. A possible explanation lies in the different mechanisms of  miRNA regulation; where instead of complete repression, they buffer transcriptional noise leading to expression being maintained at a consistent, intermediate level (Hornstein & Shomron, 2006). The loss of this buffering could result in variable effects on gene expression which sometimes is not evident on both mRNA and protein levels. This  effect is evident on the transcriptome analysis in the inner ear of *MiR-*

*183/96^(dko)* mice (Lewis et al., 2020) where variable expression of genes was observed in hair cells and several targets such as *Zeb1, Foxo1 and Nr3c1* were not significantly misregulated. Although the transcriptional noise is less likely to be consistent between mice but nonetheless it contributed to the degraded functionality of the hair cell in those mice (Lewis et al., 2020). Unexpectedly, immunohistochemistry demonstrated downregulation of Gabra1 in the LSO of knockout mice. Again, another mechanism of  miRNA regulation could have resulted in observed downregulation. This could be attributed to microRNAs and their associated protein complexes that can elicit alternate functions that enable the stimulation of gene expression, in addition to their assigned repressive roles (Lee & Vasudevan, 2012; Vasudevan, 2012). Toll-like receptor 4 (TLR4) is upregulated by miR-511 in monocyte-derived cells under quiescent conditions (Tserel et al., 2011). In serum-starved cells, AGO2 and Fragile-X-mental retardation-related protein 1 (FXR1), a protein associated with the miRNA-protein complex, are linked to AU-rich elements (AREs) in the 3' UTR, leading to the activation of translation. During cell cycle arrest, several miRNAs, including let-7, associate with AGO2 and FXR1, facilitating translation activation (Vasudevan & Steitz, 2007).

Of note, none of these proteins were significantly misregulated in our RNA-seq data. MicroRNA targets can undergo translational repression without a significant decline in mRNA levels, or exhibit a substantial decrease in mRNA levels with minimal alterations in protein levels at a specific time point (Selbach et al., 2008). Also the complex mechanisms involved between transcription and translation are not yet sufficiently well-defined to able to compute protein concentrations from mRNA levels (Greenbaum et al., 2003). Apart from that, noise and error in both mRNA and protein experiments could also limit the ability to get a clear overall picture (Baldi & Long, 2001). Therefore, validation of targets at protein level is necessary to comprehend the effect on gene expression and subsequent functional analyses in case of misregulation. Taken together, miRNAs effectively suppress some genes while finely tuning others, overall allowing a customized expression of respective proteins. This microRNA-mediated control layer, integrated with transcriptional and other regulatory processes, enhances the complexity of gene expression in metazoans.

## 4.4 *Mir-183/96*[dko] inhibitory synapses : possible consequences of misregulated Inhibitory Proteins

The question arises as to the effect of misregulated Gphn and Gabra1 on inhibitory synapses? GABA and glycine neurotransmitters operate in fast synaptic inhibition by activating GABAA and glycine receptors (Bowery & Smart, 2006). Both receptor types are postsynaptically anchored by Gphn, a master organizer protein for nearly all inhibitory synapses, forming a self-assembling scaffold that interacts with the cytoskeleton (Choii & Ko, 2015; Fritschy et al., 2008). Posttranslational modifications of Gphn play a crucial role in regulating the formation and plasticity of these inhibitory synapses. Various studies report that any changes in the structure or stability of its clustering can change the density of inhibitory receptors and, therefore, alter inhibitory neurotransmission (Tyagarajan & Fritschy, 2014). Gphn is important for regulation of synaptic strength at glycinergic inhibitory synapses (Alvarez, 2017). Furthermore, abrogated Gphn clustering has the potential to disturb GABAergic transmission during critical periods of brain development (Chattopadhyaya et al., 2004). GABAARs are the essential functional postsynaptic components of GABAergic synapses (Fuchs et al., 2013). Importantly, Gabra1 is the predominant subtype accounting for approximately 60% of all GABAA receptors. Numerous studies demonstrated that mutations in the *Gabra1* gene induce structural and functional implications in GABAA receptors. These consequences, which are closely associated with the channel-gating process, may lead to impaired inhibitory synaptic transmission (Hernandez et al., 2019; Samarut et al., 2018). A recent study implicated microRNA mediated regulation of GABAergic synapse function. Gabra1 levels were reduced due to overexpression of miR-502-3p and the electrophysiology analysis revealed reduced GABA receptor functions (Kumar, 2022). Of note, there is an interesting connection between Gphn and Gabra1, as Gphn itself relies on the presence of GABAARs to establish postsynaptic clusters in GABAergic synapses in a cell-specific manner. Targeted deletion of *Gabra1* resulted in disruption of Gphn clustering in cerebellar purkinje cells and thalamic relay neurons without influencing the distribution of extrasynaptic, α4-containing GABAARs in the latter cells (Kralic et al., 2006). Similarly, mutant neurons lacking postsynaptic α1-containing GABAARs show larger Gphn aggregates in the soma and dendrites and electrophysiology couldn't detect any GABAergic synaptic currents in these cells (Peden et al., 2008). Taken together, these findings clearly indicate that misexpression of Gphn and Gabra1 leads to

impaired inhibitory synapse structure and function. However, since we only quantified the immunoreactivity of these proteins in LSO synapses, functional analysis is required to fully comprehend the effect of their misregulation on inhibitory neurotransmission in the LSO of *MiR-183/96dko* mice. Using whole-cell patch-clamp recordings of LSO neurons in acute brain stem slices, the physiological changes of inhibitory postsynaptic currents (IPSCs), could be analysed in *MiR-183/96dko* mice. Since IPSCs could be both GABAergic and glycinergic, the relative glycine versus GABA contributions to IPSCs could be determined by addition of the pharmacological antagonists such as strychnine as glycine receptor antagonist, and bicucullin as GABAA receptor antagonist (Fischer et al., 2019; Lim et al., 2000). These experiments together with immunohistological findings will provide a concrete evidence of *MiR-183/96dko* loss on inhibitory neurotransmission in LSO.

## 4.5 Loss of miR-183/96 has a mild impact on the transcriptome of LSO and MNTB

MicroRNAs can have subtle effects on the expression levels of numerous genes, which may not be readily apparent through immunohistochemical analysis. Consequently, we opted for a genome-wide approach to thoroughly examine the impact of miR-183 and 96 loss on gene expression in LSO and MNTB of *MiR-183/96dko* mice. The RNA-seq analysis revealed only 34 genes being differentially expressed in the LSO and 116 in MNTB knockout mice compared to wt. Furthermore, few genes from both these data sets showed complementarity to the seed regions of miR-96 and -183. Our transcriptomic data thus closely resembles a previous *MiR-183/96dko* transcriptome analysis of the organ of Corti (Lewis et al., 2020). There, the differentially expressed gene set was also small with few genes having complementarity to the seed regions of miR-183 cluster members (Lewis et al., 2020). But we were able to identify several genes such as *Rgs17*, *Vgf* and *Sparcl1* in the LSO and *Cygb, Camk2g* and *Cldn11* in the MNTB which were upregulated in the knockout and are associated with the auditory system. We also found downregulated genes like *Sv2c* and *Snap25* relevant to the auditory system. Most of these genes have reported roles in peripheral auditory system (see 3.2.2). *Lamp5* is downregulated in the LSO and presents a potential candidate for further validation in inhibitory synapses since it is highly expressed in auditory brainstem nuclei where it is exclusively localized to inhibitory synaptic terminals (Koebis et al., 2019). Although it is not a

target of either miR-96 or -183, the observed downregulation could be a downstream effect as was observed for Ocm in IHC transcriptome data. This gene was neither target of the mutated or wildtype miR-96 or other members but was downregulated in both *dmdo* and *MiR-183/96$^{dko}$* data sets and this change was attributed as a downstream effect as a result of loss of both miRs (Lewis et al., 2016; Lewis et al., 2020).

Of these mis-regulated genes only *Myt1l, Rgs17,Sv2c* and *Nrp2* in LSO and *Cygb, Rplp0, Slc12a5, Gpm6b, Map1b, Rap1gap2 ,Rgs2)* in MNTB are predicted targets of miR-96 and -183 while the rest of genes in both data sets don`t have a target site for these miRs in their 3'UTRs. Numerous studies have unveiled the complex nature of gene regulation mediated by miRNAs. MiRNAs can bind to specific sequences located in the 3'-UTR of target mRNAs, leading to translational repression alongside mRNA deadenylation and decapping processes (Huntzinger & Izaurralde, 2011). This is in line with the upregulation of gene targets we observed in the absence of miR-96 and -183 in the knockout mouse model. Additionally, miRNA-binding sites have been identified in diverse mRNA regions, including the 5' UTR and coding sequence, as well as within promoter regions (Xu et al., 2014). The miRNA binding to the 5' UTR and coding regions tends to repress gene expression (Forman et al., 2008; Zhang et al., 2018). Since the majority of target recognition databases have a biased focus on seed-region matched sites within the 3'UTRs of targeted mRNAs (Xu et al., 2014), this could limit the prediction of possible microRNAs gene targets in other regions in a transcriptome data. This might explain the upregulated genes in our data set that have no target sites for the miR-183 cluster in these databases. Lewis and colleagues also created a network analysis to identify regulatory interactions connecting miR-96 to as many of the misregulated genes as possible and identified several transcription factors and regulators that likely contribute to the observed differential gene expression. They hypothesized that ectopic expression of theses intermediate targets in the absence of regulation by microRNAs could lead to variable expression of many genes. Even after extensive bioinformatic analysis , the links between the direct targets of miR-96 and the consistently misregulated downstream genes have yet to be discovered (Lewis et al., 2020) and this likely holds true for my dataset as well.

Despite the predominant focus on the down-regulatory role of miRNAs in gene expression, some studies have documented instances in which miRNAs upregulate gene expression. For example miRNA interactions with promoter regions have been documented to stimulate transcription (Dharap et al., 2013). MiRNA-mediated upregulation of gene expression has also

been observed in quiescent cells such as oocytes (Bukhari et al., 2016; Truesdell et al., 2012). Additionally, instances of gene activation by miRNAs include their binding to the 5' UTR of mRNAs that encode ribosomal proteins during amino acid starvation (Ørom et al., 2008). A recent review also discussed several studies on transcriptional upregulation by microRNAs challenging the conventional view that microRNAs solely repress gene expression (Vasudevan, 2012). Thus, multiple evidence recently mounted that miRNAs can also post-transcriptionally stimulate gene expression through selective, context-dependent mechanisms influenced by RNA sequence, various RNA related factors, and cellular conditions. These findings underscore the diverse and intricate ways in which miRNAs control gene expression, emphasizing the importance of both cis and trans regulatory elements (Vasudevan, 2012).

Taken together, the complexity of miRNA-mediated gene regulation results in a dynamic nature of miRNA actions. Despite the significant phenotypic effects observed in knockout studies of miRNA biogenesis pathway components, most predicted miRNA targets show subtle changes at the mRNA and protein levels when miRNA expression is altered.

## 4.6 Outlook

Our results demonstrate the importance of miR-183/96 for development and function of the auditory brainstem. The findings point towards an essential role of the miR-183 cluster in the shared gene regulatory network between peripheral and central auditory system. Molecular characterization of inhibitory synapse related proteins in *MiR-183/96*[dko] mice revealed mis-regulation of proteins important for inhibitory neurotransmission. Further investigation of the functional consequences could contribute to a better understanding of the regulation of key synaptic properties at inhibitory synapses. Furthermore, the transcriptome analysis provided valuable insights into miRNA driven gene regulation and validation of such phenomenon in a knockout mouse model. This brings me to the double knockout mouse model which lacked both miR-183 and miR-96 from the polycistronic miR-183 cluster investigated in this study. When the mouse line was generated through embryonic stem cell (ESC) targeting, deleting miR-96 alone was technically challenging because the intergenic region between miR-183 and -96 consists of only 117 nucleotides (Prosser et al., 2011). As discussed in section 1.6, both miRs share high sequence homology, but with small differences

within their sequences, resulting in regulation of common and unique target genes. Therefore, the observed phenotypes cannot be exclusively assigned to either miR-183 or -96 since both are expressed in the brainstem (Rosengauer et al., 2012). Studies by Lewis and colleagues in the peripheral auditory system employed miR-183/96 ko and miR-182 ko mice in comparison to the *Dmdo* mouse line but the individual role of miR-183 still remains unclear in hearing (Lewis et al., 2020). A validation of these results in regard to specific microRNA is only possible in mice with targeted deletion of the individual microRNAs which are now available (Sun et al., 2021; Zhang et al., 2020). These studies used clustered regulatory interspaced short palindromic repeats with associated protein9 (CRISPR/Cas9) technology with single-guide RNAs specifically targeting biogenesis processing sites of selected microRNAs in the same family or with highly conserved sequences (Chang et al., 2016). Future studies in these mouse lines will enable us to resolve the individual function of the microRNAs of the miR-183 family in the auditory system. Both Gphn and Gabra1 have important physiological roles for precise inhibitory neurotransmission. Their misregulation at molecular level in *MiR-183/96*[dko] mice, points towards the importance of miR-183 cluster in inhibitory neurotransmission. However, subsequent electrophysiological analysis is required to functionally characterize the impact of this misregulation and precise role of miR-96 and -183 on inhibitory neurotransmission in auditory brainstem.

## 4.7 Summary

MicroRNAs are small non-coding RNAs that post-transcriptionally regulate gene expression. They repress translation of mRNAs into proteins via complementary base pairing to their target mRNAs. The microRNA 183 cluster, comprising of miRs-183, -96 and -182, plays an important role in the development and function of sensory systems. In the central auditory system, miR-183 and miR-96 play a key role in the proper development of auditory brainstem structures and synaptic transmission in a central excitatory synapse in the auditory brainstem, the calyx of Held. In order to gain insight into the function of the inhibitory synapses of the central auditory system, I analysed a *MiR-183/96*[dko] mouse model in which miR-183 and miR-96 were deleted. Using immunohistochemistry, the expression of proteins important for inhibitory neurotransmission in the *MiR-183/96*[dko] mice have been quantified. The data showed significant differences in the expression of the proteins Gphn and Gabra1, both of

which are critical organizers of inhibitory postsynaptic density, suggesting that changes in inhibitory neurotransmission may occur. No changes were found in the expression of other proteins such as Kcc2, Hapln4 and Gad2/65. Another aim of this work was to investigate the role of the miR-183 cluster on the transcriptome of the two core SOC regions LSO and MNTB. In *MiR-183/96*<sup>dko</sup>, 34 differentially expressed genes were identified in the LSO and 116 differentially expressed genes in the MNTB compared to wild type. These lists revealed genes in both LSO and MNTB, important for synaptic transmission and hearing loss. Figure 4.1 shows a summary of all results in a schematic illustration.

## 4.8 Zusammenfassung

MicroRNAs sind kurze nicht-codierende RNAs, welche die Genexpression posttranskriptionell regulieren. Sie unterdrücken die Translation von mRNAs in Proteine durch komplementäre Basenpaarung mit ihren Ziel-mRNAs. Das microRNA 183-Cluster, bestehend aus miR-183, -96 und -182, spielt eine wichtige Rolle bei der Entwicklung und Funktion sensorischer Systeme. Im Zentralen Auditorischen System spielen miR-183 und miR-96 eine Schlüsselrolle für die korrekte Entwicklung der Strukturen des auditorischen Hirnstamms und der synaptischen Übertragung in einer zentralen erregenden Synapse im auditorischen Hirnstamm, der Calyx von Held. Um auch Einblicke in die Funktion inhibitorischer Synapsen des zentralen auditorischen Systems zu gewinnen, wurde ein *MiR-183/96*<sup>dko</sup> -Mausmodell, in welchem miR-183 und miR-96 deletiert wurden analysiert. Mittels Immunhistochemie wurde die Expression von Proteinen, die für die inhibitorische Neurotransmission wichtig sind, in den MiR-183/96dko-Mäusen quantifiziert. Die Daten zeigten signifikante Unterschiede in der Expression von Gphn und Gabra1, die beide kritische Organisatoren der inhibitorischen postsynaptischen Dichte sind, was darauf schließen lässt, dass es zu Veränderungen in der inhibitorischen Neurotransmission kommen könnte. Es konnten keine Veränderungen in der Expression weiterer Proteine wie Kcc2, Hapln4 und Gad2/65 festgestellt werden. Ein weiteres Ziel dieser Arbeit war es, die Rolle des miR-183-Clusters auf das Transkriptom der beiden SOC Kerngebiete LSO und MNTB zu untersuchen. Es konnten in Gewebe von *MiR-183/96*<sup>dko</sup> Mäusen, im Vergleich zum Wildtyp, 34 differenziell exprimierte Gene in der LSO und 116 differenziell exprimierte Gene im MNTB identifiziert werden. Die so entstandenen Listen enthüllten in beiden Kernen Gene, die sowohl für die synaptische Übertragung als auch für

Discussion

Hörverlust wichtig sind. Abbildung 4.1 zeigt eine Zusammenfassung aller Ergebnisse in einer schematischen Darstellung.
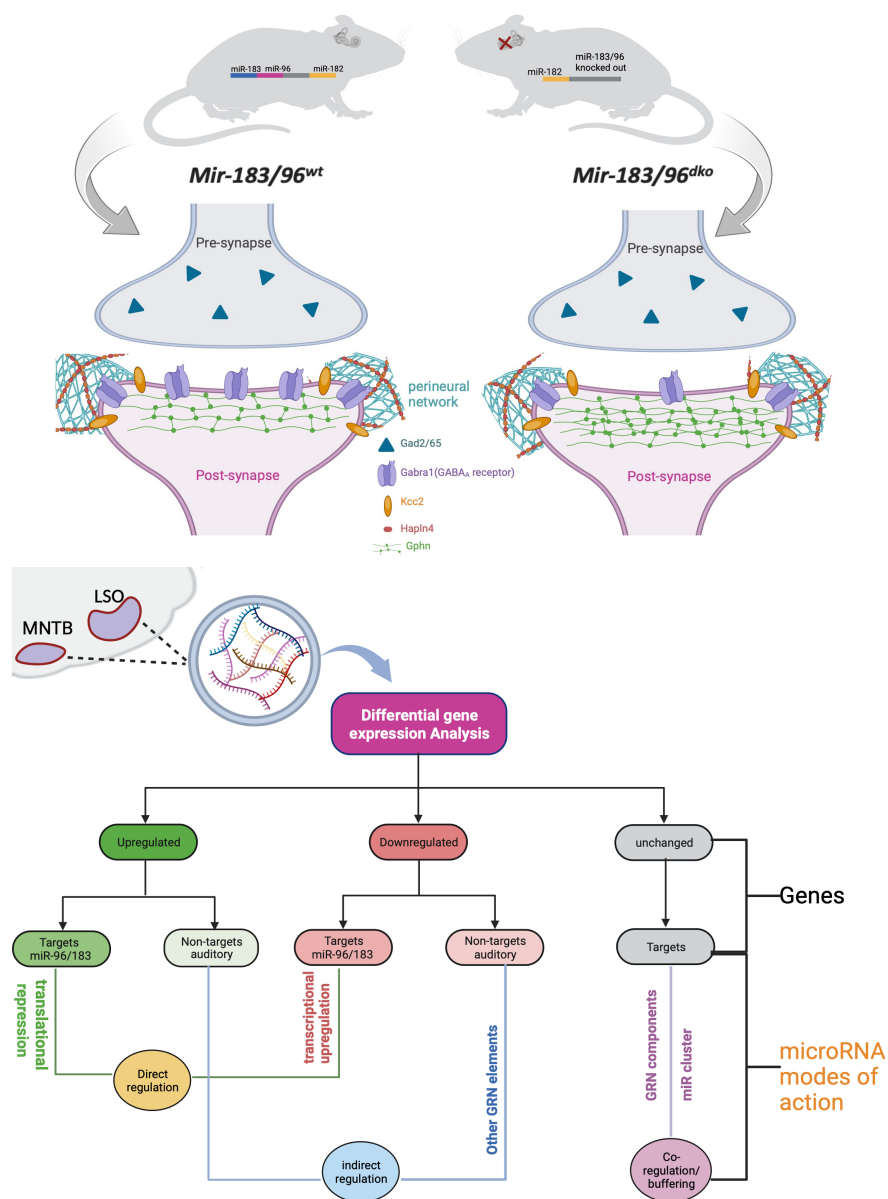


**Figure 4.1 Summary of current findings**

*The figure presents overall schematic presentation of results in this thesis. The upper part shows difference of protein expression between miR183/96 wt and ko inhibitory synapses of LSO. The lower part presents the RNA-seq results and proposed mode of microRNA regulation effects on gene expression.*

61

# 5 References

AitRaise, I., Amalou, G., Bousfiha, A., Charoute, H., Rouba, H., Abdelghaffar, H., Bonnet, C., Petit, C., & Barakat, A. (2022). Genetic heterogeneity in GJB2, COL4A3, ATP6V1B1 and EDNRB variants detected among hearing impaired families in Morocco. *Molecular Biology Reports*, *49*(5), 3949-3954.

Alarcon, C. R., Lee, H., Goodarzi, H., Halberg, N., & Tavazoie, S. F. (2015). N6-methyladenosine marks primary microRNAs for processing. *Nature*, *519*(7544), 482-485. https://doi.org/10.1038/nature14281

Altieri, S. C., Zhao, T., Jalabi, W., & Maricich, S. M. (2014). Development of glycinergic innervation to the murine LSO and SPN in the presence and absence of the MNTB. *Front Neural Circuits*, *8*, 109. https://doi.org/10.3389/fncir.2014.00109

Alvarez, F. J. (2017). Gephyrin and the regulation of synaptic strength and dynamics at glycinergic inhibitory synapses. *Brain research bulletin*, *129*, 50-65.

Ammar, M., Tabebi, M., Sfaihi, L., Alila-Fersi, O., Maalej, M., Felhi, R., Chabchoub, I., Keskes, L., Hachicha, M., Fakhfakh, F., & Mkaouar-Rebai, E. (2016). Mutational screening in patients with profound sensorineural hearing loss and neurodevelopmental delay: Description of a novel m.3861A > C mitochondrial mutation in the MT-ND1 gene. *Biochem Biophys Res Commun*, *474*(4), 702-708. https://doi.org/10.1016/j.bbrc.2016.05.014

Anders, S., Pyl, P. T., & Huber, W. (2015). HTSeq--a Python framework to work with high-throughput sequencing data. *Bioinformatics*, *31*(2), 166-169. https://doi.org/10.1093/bioinformatics/btu638

Andrews, S. (2010). FastQC: a quality control tool for high throughput sequence data. In: Babraham Bioinformatics, Babraham Institute, Cambridge, United Kingdom.

Babiarz, J. E., Ruby, J. G., Wang, Y., Bartel, D. P., & Blelloch, R. (2008). Mouse ES cells express endogenous shRNAs, siRNAs, and other Microprocessor-independent, Dicer-dependent small RNAs. *Genes Dev*, *22*(20), 2773-2785. https://doi.org/10.1101/gad.1705308

Bak, M., Silahtaroglu, A., Moller, M., Christensen, M., Rath, M. F., Skryabin, B., Tommerup, N., & Kauppinen, S. (2008). MicroRNA expression in the adult mouse central nervous system. *Rna*, *14*(3), 432-444. https://doi.org/10.1261/rna.783108

Baldi, P., & Long, A. D. (2001). A Bayesian framework for the analysis of microarray expression data: regularized t-test and statistical inferences of gene changes. *Bioinformatics*, *17*(6), 509-519.

Bartel, D. P. (2009). MicroRNAs: target recognition and regulatory functions. *Cell*, *136*(2), 215-233.

Bartel, D. P. (2018). Metazoan MicroRNAs. *Cell*, *173*(1), 20-51. https://doi.org/10.1016/j.cell.2018.03.006

Bartel, D. P., & Chen, C. Z. (2004). Micromanagers of gene expression: the potentially widespread influence of metazoan microRNAs. *Nat Rev Genet*, *5*(5), 396-400. https://doi.org/10.1038/nrg1328

Ben-Yosef, T., Belyantseva, I. A., Saunders, T. L., Hughes, E. D., Kawamoto, K., Van Itallie, C. M., Beyer, L. A., Halsey, K., Gardner, D. J., & Wilcox, E. R. (2003). Claudin 14 knockout mice, a model for autosomal recessive deafness DFNB29, are deaf due to cochlear hair cell degeneration. *Human molecular genetics*, *12*(16), 2049-2061.

Benson, D. A., Karsch-Mizrachi, I., Lipman, D. J., Ostell, J., & Sayers, E. W. (2009). GenBank. *Nucleic acids research*, *37*(suppl_1), D26-D31.

Bernstein, E., Kim, S. Y., Carmell, M. A., Murchison, E. P., Alcorn, H., Li, M. Z., Mills, A. A., Elledge, S. J., Anderson, K. V., & Hannon, G. J. (2003). Dicer is essential for mouse development. *Nature Genetics*, *35*(3), 215-217.

Blaesse, P., Airaksinen, M. S., Rivera, C., & Kaila, K. (2009). Cation-chloride cotransporters and neuronal function. *Neuron*, *61*(6), 820-838. https://doi.org/10.1016/j.neuron.2009.03.003

Blaesse, P., Guillemin, I., Schindler, J., Schweizer, M., Delpire, E., Khiroug, L., Friauf, E., & Nothwang, H. G. (2006). Oligomerization of KCC2 correlates with development of inhibitory neurotransmission. *J Neurosci*, *26*(41), 10407-10419. https://doi.org/10.1523/JNEUROSCI.3257-06.2006

Bordeynik-Cohen, M., Sperber, M., Ebbers, L., Messika-Gold, N., Krohs, C., Koffler-Brill, T., Noy, Y., Elkon, R., Nothwang, H. G., & Avraham, K. B. (2023). Shared and organ-specific gene-expression programs during the development of the cochlea and the superior olivary complex. *RNA Biol*, *20*(1), 629-640. https://doi.org/10.1080/15476286.2023.2247628

Borst, J. G., & Soria van Hoeve, J. (2012). The calyx of Held synapse: from model synapse to auditory relay. *Annu Rev Physiol*, *74*, 199-224. https://doi.org/10.1146/annurev-physiol-020911-153236

Bowery, N., & Smart, T. (2006). GABA and glycine as neurotransmitters: a brief history. *British journal of pharmacology*, *147*(S1), S109-S119.

Bukhari, S. I., Truesdell, S. S., Lee, S., Kollu, S., Classon, A., Boukhali, M., Jain, E., Mortensen, R. D., Yanagiya, A., & Sadreyev, R. I. (2016). A specialized mechanism of translation mediated by FXR1a-associated microRNP in cellular quiescence. *Molecular cell*, *61*(5), 760-773.

Bushnell, B. (2015). BBMap short-read aligner, and other bioinformatics tools. *Berkeley: University of California*.

Caicedo, A., & Eybalin, M. (1999). Glutamate receptor phenotypes in the auditory brainstem and mid-brain of the developing rat. *Eur J Neurosci*, *11*(1), 51-74. https://doi.org/10.1046/j.1460-9568.1999.00410.x

Calvet, C., Peineau, T., Benamer, N., Cornille, M., Lelli, A., Plion, B., Lahlou, G., Fanchette, J., Nouaille, S., & de Monvel, J. B. (2022). The SNARE protein SNAP-25 is required for normal exocytosis at auditory hair cell ribbon synapses. *Iscience*, *25*(12).

Cant, N. B. (1992). The cochlear nucleus: neuronal types and their synaptic organization. In *The mammalian auditory pathway: Neuroanatomy* (pp. 66-116). Springer.

Chang, H., Yi, B., Ma, R., Zhang, X., Zhao, H., & Xi, Y. (2016). CRISPR/cas9, a novel genomic tool to knock down microRNA in vitro and in vivo. *Sci Rep*, *6*, 22312. https://doi.org/10.1038/srep22312

Chatterjee, S., & Ahituv, N. (2017). Gene regulatory elements, major drivers of human disease. *Annual review of genomics and human genetics*, *18*, 45-63.

Chattopadhyaya, B., Di Cristo, G., Higashiyama, H., Knott, G. W., Kuhlman, S. J., Welker, E., & Huang, Z. J. (2004). Experience and activity-dependent maturation of perisomatic GABAergic innervation in primary visual cortex during a postnatal critical period. *J Neurosci*, *24*(43), 9598-9611. https://doi.org/10.1523/JNEUROSCI.1851-04.2004

Chen, Y., & Wang, X. (2020). miRDB: an online database for prediction of functional microRNA targets. *Nucleic acids research*, *48*(D1), D127-D131.

Choii, G., & Ko, J. (2015). Gephyrin: a central GABAergic synapse organizer. *Exp Mol Med*, *47*, e158. https://doi.org/10.1038/emm.2015.5

Collaborators, G. B. D. H. L. (2021). Hearing loss prevalence and years lived with disability, 1990-2019: findings from the Global Burden of Disease Study 2019. *Lancet*, *397*(10278), 996-1009. https://doi.org/10.1016/S0140-6736(21)00516-X

Cortada, M., Levano, S., & Bodmer, D. (2021). mTOR signaling in the inner ear as potential target to treat hearing loss. *International Journal of Molecular Sciences*, *22*(12), 6368.

Costa, M. C., Leitão, A. L., & Enguita, F. J. (2012). Biogenesis and mechanism of action of small non-coding RNAs: insights from the point of view of structural biology. *International Journal of Molecular Sciences*, *13*(8), 10268-10295.

Dambal, S., Shah, M., Mihelich, B., & Nonn, L. (2015). The microRNA-183 cluster: the family that plays together stays together. *Nucleic acids research*, *43*(15), 7173-7188.

Dang, R., Torigoe, D., Suzuki, S., Kikkawa, Y., Moritoh, K., Sasaki, N., & Agui, T. (2011). Genetic background strongly modifies the severity of symptoms of Hirschsprung disease, but not hearing loss in rats carrying Ednrb(sl) mutations. *PLoS One*, *6*(9), e24086. https://doi.org/10.1371/journal.pone.0024086

Davidson, E. H., & Erwin, D. H. (2006). Gene regulatory networks and the evolution of animal body plans. *Science*, *311*(5762), 796-800. https://doi.org/10.1126/science.1113832

De Rie, D., Abugessaisa, I., Alam, T., Arner, E., Arner, P., Ashoor, H., Åström, G., Babina, M., Bertin, N., & Burroughs, A. M. (2017). An integrated expression atlas of miRNAs and their promoters in human and mouse. *Nature biotechnology*, *35*(9), 872-878.

Denli, A. M., Tops, B. B., Plasterk, R. H., Ketting, R. F., & Hannon, G. J. (2004). Processing of primary microRNAs by the Microprocessor complex. *Nature*, *432*(7014), 231-235. https://doi.org/10.1038/nature03049

Dharap, A., Pokrzywa, C., Murali, S., Pandi, G., & Vemuganti, R. (2013). MicroRNA miR-324-3p induces promoter-mediated expression of RelA gene. *PLoS One*, *8*(11), e79467.

Dhukhwa, A., Al Aameri, R. F. H., Sheth, S., Mukherjea, D., Rybak, L., & Ramkumar, V. (2021). Regulator of G protein signaling 17 represents a novel target for treating cisplatin induced hearing loss. *Sci Rep*, *11*(1), 8116. https://doi.org/10.1038/s41598-021-87387-5

Dobin, A., Davis, C. A., Schlesinger, F., Drenkow, J., Zaleski, C., Jha, S., Batut, P., Chaisson, M., & Gingeras, T. R. (2013). STAR: ultrafast universal RNA-seq aligner. *Bioinformatics*, *29*(1), 15-21. https://doi.org/10.1093/bioinformatics/bts635

Ebbers, L., Altaf, F., & Nothwang, H. G. (2022). MicroRNAs in the auditory system: tiny molecules with big impact. *Neuroforum*, *28*(4), 211-221.

Ebbers, L., Satheesh, S. V., Janz, K., Ruttiger, L., Blosa, M., Hofmann, F., Morawski, M., Griesemer, D., Knipper, M., Friauf, E., & Nothwang, H. G. (2015). L-type Calcium Channel Cav1.2 Is Required for Maintenance of Auditory Brainstem Nuclei. *J Biol Chem*, *290*(39), 23692-23710. https://doi.org/10.1074/jbc.M115.672675

Edamatsu, M., Miyano, R., Fujikawa, A., Fujii, F., Hori, T., Sakaba, T., & Oohashi, T. (2018). Hapln4/Bral2 is a selective regulator for formation and transmission of GABA ergic synapses between Purkinje and deep cerebellar nuclei neurons. *Journal of neurochemistry*, *147*(6), 748-763.

Ehmann, H., Hartwich, H., Salzig, C., Hartmann, N., Clément-Ziza, M., Ushakov, K., Avraham, K. B., Bininda-Emonds, O. R., Hartmann, A. K., & Lang, P. (2013). Time-dependent gene expression analysis of the developing superior olivary complex. *Journal of Biological Chemistry*, *288*(36), 25865-25879.

Ewels, P., Magnusson, M., Lundin, S., & Kaller, M. (2016). MultiQC: summarize analysis results for multiple tools and samples in a single report. *Bioinformatics*, *32*(19), 3047-3048. https://doi.org/10.1093/bioinformatics/btw354

Fan, J., Jia, L., Li, Y., Ebrahim, S., May-Simera, H., Wood, A., Morell, R. J., Liu, P., Lei, J., Kachar, B., Belluscio, L., Qian, H., Li, T., Li, W., Wistow, G., & Dong, L. (2017). Maturation arrest in early postnatal sensory receptors by deletion of the miR-183/96/182 cluster in mouse. *Proc Natl Acad Sci U S A*, *114*(21), E4271-E4280. https://doi.org/10.1073/pnas.1619442114

Fischer, A. U., Muller, N. I. C., Deller, T., Del Turco, D., Fisch, J. O., Griesemer, D., Kattler, K., Maraslioglu, A., Roemer, V., Xu-Friedman, M. A., Walter, J., & Friauf, E. (2019). GABA is a modulator, rather than a classical transmitter, in the medial nucleus of the trapezoid body-lateral superior olive sound localization circuit. *J Physiol*, *597*(8), 2269-2295. https://doi.org/10.1113/JP277566

Forman, J. J., Legesse-Miller, A., & Coller, H. A. (2008). A search for conserved sequences in coding regions reveals that the let-7 microRNA targets Dicer within its coding sequence. *Proceedings of the National Academy of Sciences*, *105*(39), 14879-14884.

Friauf, E. (1993). Transient appearance of calbindin-D28k-positive neurons in the superior olivary complex of developing rats. *Journal of Comparative Neurology*, *334*(1), 59-74.

Friauf, E., Krächan, E. G., & Müller, N. I. (2018). Lateral superior olive: organization, development, and plasticity.

Friedman, L. M., Dror, A. A., Mor, E., Tenne, T., Toren, G., Satoh, T., Biesemeier, D. J., Shomron, N., Fekete, D. M., Hornstein, E., & Avraham, K. B. (2009). MicroRNAs are essential for development and function of inner ear hair cells in vertebrates. *Proc Natl Acad Sci U S A*, *106*(19), 7915-7920. https://doi.org/10.1073/pnas.0812446106

Friedman, R. C., Farh, K. K.-H., Burge, C. B., & Bartel, D. P. (2009). Most mammalian mRNAs are conserved targets of microRNAs. *Genome research*, *19*(1), 92-105.

Fritschy, J.-M., Harvey, R. J., & Schwarz, G. (2008). Gephyrin: where do we stand, where do we go? *Trends in neurosciences*, *31*(5), 257-264.

Fuchs, C., Abitbol, K., Burden, J. J., Mercer, A., Brown, L., Iball, J., Anne Stephenson, F., Thomson, A. M., & Jovanovic, J. N. (2013). GABAA receptors can initiate the formation of functional inhibitory GABA ergic synapses. *European Journal of Neuroscience*, *38*(8), 3146-3158.

Fukao, A., Mishima, Y., Takizawa, N., Oka, S., Imataka, H., Pelletier, J., Sonenberg, N., Thoma, C., & Fujiwara, T. (2014). MicroRNAs trigger dissociation of eIF4AI and eIF4AII from target mRNAs in humans. *Molecular cell*, *56*(1), 79-89.

Gao, J., Wu, X., & Zuo, J. (2004). Targeting hearing genes in mice. *Molecular brain research*, *132*(2), 192-207.

Gebert, L. F., & MacRae, I. J. (2019). Regulation of microRNA function in animals. *Nature reviews Molecular cell biology*, *20*(1), 21-37.

Geng, R., Furness, D. N., Muraleedharan, C. K., Zhang, J., Dabdoub, A., Lin, V., & Xu, S. (2018). The microRNA-183/96/182 Cluster is Essential for Stereociliary Bundle Formation and Function of Cochlear Sensory Hair Cells. *Scientific Reports*, *8*(1), 18022. https://doi.org/10.1038/s41598-018-36894-z

Glendenning, K. K., & Masterton, R. B. (1998). Comparative morphometry of mammalian central auditory systems: variation in nuclei and form of the ascending system. *Brain Behav Evol*, *51*(2), 59-89. https://doi.org/10.1159/000006530

Gow, A., Davies, C., Southwood, C. M., Frolenkov, G., Chrustowski, M., Ng, L., Yamauchi, D., Marcus, D. C., & Kachar, B. (2004). Deafness in Claudin 11-null mice reveals the critical contribution of basal cell tight junctions to stria vascularis function. *J Neurosci*, *24*(32), 7051-7062. https://doi.org/10.1523/JNEUROSCI.1640-04.2004

Greenbaum, D., Colangelo, C., Williams, K., & Gerstein, M. (2003). Comparing protein abundance and mRNA expression levels on a genomic scale. *Genome Biol*, *4*(9), 117. https://doi.org/10.1186/gb-2003-4-9-117

Grothe, B., & Pecka, M. (2014). The natural history of sound localization in mammals--a story of neuronal inhibition. *Front Neural Circuits*, *8*, 116. https://doi.org/10.3389/fncir.2014.00116

Grothe, B., Pecka, M., & McAlpine, D. (2010). Mechanisms of sound localization in mammals. *Physiol Rev*, *90*(3), 983-1012. https://doi.org/10.1152/physrev.00026.2009

Ha, M., & Kim, V. N. (2014). Regulation of microRNA biogenesis. *Nat Rev Mol Cell Biol*, *15*(8), 509-524. https://doi.org/10.1038/nrm3838

Han, J., Lee, Y., Yeom, K. H., Kim, Y. K., Jin, H., & Kim, V. N. (2004). The Drosha-DGCR8 complex in primary microRNA processing. *Genes Dev*, *18*(24), 3016-3027. https://doi.org/10.1101/gad.1262504

Harrison, J., & Irving, R. (1966). Visual and Nonvisual Auditory Systems in Mammals: Anatomical evidence indicates two kinds of auditory pathways and suggests two kinds of hearing in mammals. *Science*, *154*(3750), 738-743.

Hashimoto, N., Sato, T., Yajima, T., Fujita, M., Sato, A., Shimizu, Y., Shimada, Y., Shoji, N., Sasano, T., & Ichikawa, H. (2016). SPARCL1-containing neurons in the human brainstem and sensory ganglion. *Somatosens Mot Res*, *33*(2), 112-117. https://doi.org/10.1080/08990220.2016.1197115

Heffner, H. E., & Heffner, R. S. (2007). Hearing ranges of laboratory animals. *Journal of the American Association for Laboratory Animal Science*, *46*(1), 20-22.

Helfert, R. H., & Schwartz, I. R. (1987). Morphological features of five neuronal classes in the gerbil lateral superior olive. *American journal of anatomy*, *179*(1), 55-69.

Hernandez, C. C., XiangWei, W., Hu, N., Shen, D., Shen, W., Lagrange, A. H., Zhang, Y., Dai, L., Ding, C., Sun, Z., Hu, J., Zhu, H., Jiang, Y., & Macdonald, R. L. (2019). Altered inhibitory synapses in de novo GABRA5 and GABRA1 mutations associated with early onset epileptic encephalopathies. *Brain*, *142*(7), 1938-1954. https://doi.org/10.1093/brain/awz123

Hilgers, V., Bushati, N., & Cohen, S. M. (2010). Drosophila microRNAs 263a/b confer robustness during development by protecting nascent sense organs from apoptosis. *PLoS biology*, *8*(6), e1000396.

Hirtz, J. J., Boesen, M., Braun, N., Deitmer, J. W., Kramer, F., Lohr, C., Muller, B., Nothwang, H. G., Striessnig, J., Lohrke, S., & Friauf, E. (2011). Cav1.3 calcium channels are required for normal development of the auditory brainstem. *J Neurosci*, *31*(22), 8280-8294. https://doi.org/10.1523/JNEUROSCI.5098-10.2011

Holt, A. G., Asako, M., Lomax, C. A., MacDonald, J. W., Tong, L., Lomax, M. I., & Altschuler, R. A. (2005). Deafness-related plasticity in the inferior colliculus: gene expression profiling following removal of peripheral activity. *J Neurochem*, *93*(5), 1069-1086. https://doi.org/10.1111/j.1471-4159.2005.03090.x

Hornstein, E., & Shomron, N. (2006). Canalization of development by microRNAs. *Nat Genet*, *38 Suppl*, S20-24. https://doi.org/10.1038/ng1803

Huntzinger, E., & Izaurralde, E. (2011). Gene silencing by microRNAs: contributions of translational repression and mRNA decay. *Nat Rev Genet*, *12*(2), 99-110. https://doi.org/10.1038/nrg2936

Janz, R., & Südhof, T. (1999). SV2C is a synaptic vesicle protein with an unusually restricted localization: anatomy of a synaptic vesicle protein family. *Neuroscience*, *94*(4), 1279-1290.

Jensen, K. P., & Covault, J. (2011). Human miR-1271 is a miR-96 paralog with distinct non-conserved brain expression pattern. *Nucleic acids research*, *39*(2), 701-711.

Jo, M. H., Shin, S., Jung, S.-R., Kim, E., Song, J.-J., & Hohng, S. (2015). Human Argonaute 2 has diverse reaction pathways on target RNAs. *Molecular cell*, *59*(1), 117-124.

Jolliffe, I. T., & Cadima, J. (2016). Principal component analysis: a review and recent developments. *Philosophical transactions of the royal society A: Mathematical, Physical and Engineering Sciences*, *374*(2065), 20150202.

Kaufman, D. L., Houser, C. R., & Tobin, A. J. (1991). Two forms of the γ-aminobutyric acid synthetic enzyme glutamate decarboxylase have distinct intraneuronal distributions and cofactor interactions. *Journal of neurochemistry*, *56*(2), 720-723.

Kil, H. K., Kim, K. W., Lee, D. H., Lee, S. M., Lee, C. H., & Kim, S. Y. (2021). Changes in the Gene Expression Profiles of the Inferior Colliculus Following Unilateral Cochlear Ablation in Adult Rats. *Biochem Genet*, *59*(3), 731-750. https://doi.org/10.1007/s10528-021-10034-1

Kim, Y. K., & Kim, V. N. (2007). Processing of intronic microRNAs. *The EMBO journal*, *26*(3), 775-783.

Kirsch, J., & Betz, H. (1998). Glycine-receptor activation is required for receptor clustering in spinal neurons. *Nature*, *392*(6677), 717-720.

Koebis, M., Urata, S., Shinoda, Y., Okabe, S., Yamasoba, T., Nakao, K., Aiba, A., & Furuichi, T. (2019). LAMP5 in presynaptic inhibitory terminals in the hindbrain and spinal cord: a role in startle response and auditory processing. *Mol Brain*, *12*(1), 20. https://doi.org/10.1186/s13041-019-0437-4

Koike-Tani, M., Saitoh, N., & Takahashi, T. (2005). Mechanisms underlying developmental speeding in AMPA-EPSC decay time at the calyx of Held. *Journal of Neuroscience*, *25*(1), 199-207.

Kopp-Scheinpflug, C., Tozer, A. J., Robinson, S. W., Tempel, B. L., Hennig, M. H., & Forsythe, I. D. (2011). The sound of silence: ionic mechanisms encoding sound termination. *Neuron*, *71*(5), 911-925. https://doi.org/10.1016/j.neuron.2011.06.028

Korada, S., & Schwartz, I. R. (1999). Development of GABA, glycine, and their receptors in the auditory brainstem of gerbil: a light and electron microscopic study. *Journal of Comparative Neurology*, *409*(4), 664-681.

Kralic, J. E., Sidler, C., Parpan, F., Homanics, G. E., Morrow, A. L., & Fritschy, J. M. (2006). Compensatory alteration of inhibitory synaptic circuits in cerebellum and thalamus of γ-aminobutyric acid type A receptor α1 subunit knockout mice. *Journal of Comparative Neurology*, *495*(4), 408-421.

Krohs, C. (2020). *Functional characterization of miR-96 in the mouse auditory brainstem and identification of new auditory-related microRNAs* Universität Oldenburg].

Krohs, C., Korber, C., Ebbers, L., Altaf, F., Hollje, G., Hoppe, S., Dorflinger, Y., Prosser, H. M., & Nothwang, H. G. (2021). Loss of miR-183/96 Alters Synaptic Strength via Presynaptic and Postsynaptic Mechanisms at a Central Synapse. *J Neurosci*, *41*(32), 6796-6811. https://doi.org/10.1523/JNEUROSCI.0139-20.2021

Kuhn, S., Johnson, S. L., Furness, D. N., Chen, J., Ingham, N., Hilton, J. M., Steffes, G., Lewis, M. A., Zampini, V., Hackney, C. M., Masetto, S., Holley, M. C., Steel, K. P., & Marcotti, W. (2011). miR-96 regulates the progression of differentiation in mammalian cochlear inner and outer hair cells. *Proc Natl Acad Sci U S A*, *108*(6), 2355-2360. https://doi.org/10.1073/pnas.1016646108

Kumar, S. (2022). MicroRNA-502-3p regulates the GABAergic synapse function in Alzheimer's disease. *Alzheimer's & Dementia*, *18*, e063745.

Lagos-Quintana, M., Rauhut, R., Meyer, J., Borkhardt, A., & Tuschl, T. (2003). New microRNAs from mouse and human. *Rna*, *9*(2), 175-179.

Lee, S., & Vasudevan, S. (2012). Post-transcriptional stimulation of gene expression by microRNAs. *Ten Years of Progress in GW/P Body Research*, 97-126.

Lesperance, L. S., Yang, Y.-M., & Wang, L.-Y. (2020). Delayed expression of activity-dependent gating switch in synaptic AMPARs at a central synapse. *Molecular brain*, *13*, 1-18.

Levi, A., Ferri, G. L., Watson, E., Possenti, R., & Salton, S. R. (2004). Processing, distribution, and function of VGF, a neuronal and endocrine peptide precursor. *Cell Mol Neurobiol*, *24*(4), 517-533. https://doi.org/10.1023/b:cemn.0000023627.79947.22

Lewis, B. P., Burge, C. B., & Bartel, D. P. (2005). Conserved seed pairing, often flanked by adenosines, indicates that thousands of human genes are microRNA targets. *Cell*, *120*(1), 15-20.

Lewis, M. A., Buniello, A., Hilton, J. M., Zhu, F., Zhang, W. I., Evans, S., van Dongen, S., Enright, A. J., & Steel, K. P. (2016). Exploring regulatory networks of miR-96 in the developing inner ear. *Sci Rep*, *6*, 23363. https://doi.org/10.1038/srep23363

Lewis, M. A., Di Domenico, F., Ingham, N. J., Prosser, H. M., & Steel, K. P. (2020). Hearing impairment due to Mir183/96/182 mutations suggests both loss and gain of function effects. *Dis Model Mech*, *14*(2). https://doi.org/10.1242/dmm.047225

Lewis, M. A., Quint, E., Glazier, A. M., Fuchs, H., De Angelis, M. H., Langford, C., van Dongen, S., Abreu-Goodger, C., Piipari, M., Redshaw, N., Dalmay, T., Moreno-Pelayo, M. A., Enright, A. J., & Steel, K. P. (2009). An ENU-induced mutation of miR-96 associated with progressive hearing loss in mice. *Nat Genet*, *41*(5), 614-618. https://doi.org/10.1038/ng.369

Li, H., Handsaker, B., Wysoker, A., Fennell, T., Ruan, J., Homer, N., Marth, G., Abecasis, G., Durbin, R., & Genome Project Data Processing, S. (2009). The Sequence Alignment/Map format and SAMtools. *Bioinformatics*, *25*(16), 2078-2079. https://doi.org/10.1093/bioinformatics/btp352

Li, H. S., & Borg, E. (1991). Age-related loss of auditory sensitivity in two mouse genotypes. *Acta Otolaryngol*, *111*(5), 827-834. https://doi.org/10.3109/00016489109138418

Lim, R., Alvarez, F. J., & Walmsley, B. (2000). GABA mediates presynaptic inhibition at glycinergic synapses in a rat auditory brainstem nucleus. *The Journal of Physiology*, *525*(2), 447-459.

Love, M. I., Huber, W., & Anders, S. (2014). Moderated estimation of fold change and dispersion for RNA-seq data with DESeq2. *Genome Biol*, *15*(12), 550. https://doi.org/10.1186/s13059-014-0550-8

Luscher, B., & Keller, C. A. (2004). Regulation of GABAA receptor trafficking, channel activity, and functional plasticity of inhibitory synapses. *Pharmacol Ther*, *102*(3), 195-221. https://doi.org/10.1016/j.pharmthera.2004.04.003

Maheras, K. J., Peppi, M., Ghoddoussi, F., Galloway, M. P., Perrine, S. A., & Gow, A. (2018). Absence of Claudin 11 in CNS Myelin Perturbs Behavior and Neurotransmitter Levels in Mice. *Sci Rep*, *8*(1), 3798. https://doi.org/10.1038/s41598-018-22047-9

Majorossy, K., & Kiss, A. (1990). Types of neurons and synaptic relations in the lateral superior olive of the cat: normal structure and experimental observations. *Acta Morphologica Hungarica*, *38*(3-4), 207-215.

Meijer, H. A., Smith, E. M., & Bushell, M. (2014). Regulation of miRNA strand selection: follow the leader? *Biochem Soc Trans*, *42*(4), 1135-1140. https://doi.org/10.1042/BST20140142

Mencia, A., Modamio-Hoybjor, S., Redshaw, N., Morin, M., Mayo-Merino, F., Olavarrieta, L., Aguirre, L. A., del Castillo, I., Steel, K. P., Dalmay, T., Moreno, F., & Moreno-Pelayo, M. A. (2009). Mutations in the seed region of human miR-96 are responsible for nonsyndromic progressive hearing loss. *Nat Genet*, *41*(5), 609-613. https://doi.org/10.1038/ng.355

Michalski, N., & Petit, C. (2019). Genes involved in the development and physiology of both the peripheral and central auditory systems. *Annual review of neuroscience*, *42*, 67-86.

Middlebrooks, J. (2015). Auditory system: central pathways.

Moore, D. R. (1991). Anatomy and physiology of binaural hearing. *Audiology*, *30*(3), 125-134.

Morton, C. C., & Nance, W. E. (2006). Newborn hearing screening—a silent revolution. *New England Journal of Medicine*, *354*(20), 2151-2164.

Mosbacher, J., Schoepfer, R., Monyer, H., Burnashev, N., Seeburg, P. H., & Ruppersberg, J. P. (1994). A molecular determinant for submillisecond desensitization in glutamate receptors. *Science*, *266*(5187), 1059-1062. https://doi.org/10.1126/science.7973663

Nance, W. E. (2003). The genetics of deafness. *Ment Retard Dev Disabil Res Rev*, *9*(2), 109-119. https://doi.org/10.1002/mrdd.10067

Noben-Trauth, K., Zheng, Q. Y., & Johnson, K. R. (2003). Association of cadherin 23 with polygenic inheritance and genetic modification of sensorineural hearing loss. *Nat Genet*, *35*(1), 21-23. https://doi.org/10.1038/ng1226

Nothwang, H. G., Ebbers, L., Schluter, T., & Willaredt, M. A. (2015). The emerging framework of mammalian auditory hindbrain development. *Cell Tissue Res*, *361*(1), 33-48. https://doi.org/10.1007/s00441-014-2110-7

O'Brien, J., Hayder, H., Zayed, Y., & Peng, C. (2018). Overview of microRNA biogenesis, mechanisms of actions, and circulation. *Frontiers in endocrinology*, *9*, 402.

Ohlemiller, K. K. (2019). Mouse methods and models for studies in hearing. *J Acoust Soc Am*, *146*(5), 3668. https://doi.org/10.1121/1.5132550

Okada, C., Yamashita, E., Lee, S. J., Shibata, S., Katahira, J., Nakagawa, A., Yoneda, Y., & Tsukihara, T. (2009). A high-resolution structure of the pre-microRNA nuclear export machinery. *Science*, *326*(5957), 1275-1279. https://doi.org/10.1126/science.1178705

Ollo, C., & Schwartz, I. R. (1979). The superior olivary complex in C57BL/6 mice. *American journal of anatomy*, *155*(3), 349-373.

Ørom, U. A., Nielsen, F. C., & Lund, A. H. (2008). MicroRNA-10a binds the 5' UTR of ribosomal protein mRNAs and enhances their translation. *Molecular cell*, *30*(4), 460-471.

Pawlik, B., Schluter, T., Hartwich, H., Breuel, S., Heepmann, L., & Nothwang, H. G. (2016). Comparative Analysis of Gene Regulatory Network Components in the Auditory Hindbrain of Mice and Chicken. *Brain Behav Evol*, *88*(3-4), 161-176. https://doi.org/10.1159/000449447

Pecka, M., Zahn, T. P., Saunier-Rebori, B., Siveke, I., Felmy, F., Wiegrebe, L., Klug, A., Pollak, G. D., & Grothe, B. (2007). Inhibiting the inhibition: a neuronal network for sound localization in reverberant environments. *J Neurosci*, *27*(7), 1782-1790. https://doi.org/10.1523/JNEUROSCI.5335-06.2007

Peden, D. R., Petitjean, C. M., Herd, M. B., Durakoglugil, M. S., Rosahl, T. W., Wafford, K., Homanics, G. E., Belelli, D., Fritschy, J. M., & Lambert, J. J. (2008). Developmental maturation of synaptic and extrasynaptic GABAA receptors in mouse thalamic ventrobasal neurones. *J Physiol*, *586*(4), 965-987. https://doi.org/10.1113/jphysiol.2007.145375

Peng, C., Li, L., Zhang, M. D., Bengtsson Gonzales, C., Parisien, M., Belfer, I., Usoskin, D., Abdo, H., Furlan, A., Haring, M., Lallemend, F., Harkany, T., Diatchenko, L., Hokfelt, T., Hjerling-Leffler, J., & Ernfors, P. (2017). miR-183 cluster scales mechanical pain sensitivity by regulating basal and neuropathic pain genes. *Science*, *356*(6343), 1168-1171. https://doi.org/10.1126/science.aam7671

Pickles, J. O. (2015). Auditory pathways: anatomy and physiology. *Handb Clin Neurol*, *129*, 3-25. https://doi.org/10.1016/B978-0-444-62630-1.00001-9

Pierce, M. L., Weston, M. D., Fritzsch, B., Gabel, H. W., Ruvkun, G., & Soukup, G. A. (2008). MicroRNA-183 family conservation and ciliated neurosensory organ expression. *Evolution & development*, *10*(1), 106-113.

Prochnik, S. E., Rokhsar, D. S., & Aboobaker, A. A. (2007). Evidence for a microRNA expansion in the bilaterian ancestor. *Development genes and evolution*, *217*, 73-77.

Prosser, H. M., Koike-Yusa, H., Cooper, J. D., Law, F. C., & Bradley, A. (2011). A resource of vectors and ES cells for targeted deletion of microRNAs in mice. *Nat Biotechnol*, *29*(9), 840-845. https://doi.org/10.1038/nbt.1929

Quaranta, N., Coppola, F., Casulli, M., Barulli, O., Lanza, F., Tortelli, R., Capozzo, R., Leo, A., Tursi, M., Grasso, A., Solfrizzi, V., Sobba, C., & Logroscino, G. (2014). The prevalence

of peripheral and central hearing impairment and its relation to cognition in older adults. *Audiol Neurootol*, *19 Suppl 1*, 10-14. https://doi.org/10.1159/000371597

Reuss, S., Balmaceda, D., Elgurt, M., & Riemann, R. (2023). Neuronal Cytoglobin in the Auditory Brainstem of Rat and Mouse: Distribution, Cochlear Projection, and Nitric Oxide Production. *Brain Sci*, *13*(1). https://doi.org/10.3390/brainsci13010107

Rietzel, H. J., & Friauf, E. (1998). Neuron types in the rat lateral superior olive and developmental changes in the complexity of their dendritic arbors. *Journal of Comparative Neurology*, *390*(1), 20-40.

Rigter, P. M., de Konink, C., & van Woerden, G. M. (2023). Loss of CAMK2G affects intrinsic and motor behavior but has minimal impact on cognitive behavior. *Frontiers in Neuroscience*, *16*, 1086994.

Rivera, C., Voipio, J., Payne, J. A., Ruusuvuori, E., Lahtinen, H., Lamsa, K., Pirvola, U., Saarma, M., & Kaila, K. (1999). The K+/Cl- co-transporter KCC2 renders GABA hyperpolarizing during neuronal maturation. *Nature*, *397*(6716), 251-255. https://doi.org/10.1038/16697

Robinson, M. D., McCarthy, D. J., & Smyth, G. K. (2010). edgeR: a Bioconductor package for differential expression analysis of digital gene expression data. *Bioinformatics*, *26*(1), 139-140. https://doi.org/10.1093/bioinformatics/btp616

Rosengauer, E., Hartwich, H., Hartmann, A. M., Rudnicki, A., Satheesh, S. V., Avraham, K. B., & Nothwang, H. G. (2012). Egr2::cre mediated conditional ablation of dicer disrupts histogenesis of mammalian central auditory nuclei. *PLoS One*, *7*(11), e49503. https://doi.org/10.1371/journal.pone.0049503

Ruby, J. G., Jan, C. H., & Bartel, D. P. (2007). Intronic microRNA precursors that bypass Drosha processing. *Nature*, *448*(7149), 83-86.

Rudnicki, A., & Avraham, K. B. (2012). microRNAs: the art of silencing in the ear. *EMBO Mol Med*, *4*(9), 849-859. https://doi.org/10.1002/emmm.201100922

Sacheli, R., Nguyen, L., Borgs, L., Vandenbosch, R., Bodson, M., Lefebvre, P., & Malgrange, B. (2009). Expression patterns of miR-96, miR-182 and miR-183 in the developing inner ear. *Gene expression patterns*, *9*(5), 364-370.

Safieddine, S., & Wenthold, R. J. (1999). SNARE complex at the ribbon synapses of cochlear hair cells: analysis of synaptic vesicle-and synaptic membrane-associated proteins. *European Journal of Neuroscience*, *11*(3), 803-812.

Samarut, E., Swaminathan, A., Riche, R., Liao, M., Hassan-Abdi, R., Renault, S., Allard, M., Dufour, L., Cossette, P., Soussi-Yanicostas, N., & Drapeau, P. (2018). gamma-

Aminobutyric acid receptor alpha 1 subunit loss of function causes genetic generalized epilepsy by impairing inhibitory network neurodevelopment. *Epilepsia*, *59*(11), 2061-2074. https://doi.org/10.1111/epi.14576

Satheesh, S. V., Kunert, K., Ruttiger, L., Zuccotti, A., Schonig, K., Friauf, E., Knipper, M., Bartsch, D., & Nothwang, H. G. (2012). Retrocochlear function of the peripheral deafness gene Cacna1d. *Hum Mol Genet*, *21*(17), 3896-3909. https://doi.org/10.1093/hmg/dds217

Satzler, K., Sohl, L. F., Bollmann, J. H., Borst, J. G., Frotscher, M., Sakmann, B., & Lubke, J. H. (2002). Three-dimensional reconstruction of a calyx of Held and its postsynaptic principal neuron in the medial nucleus of the trapezoid body. *J Neurosci*, *22*(24), 10567-10579. https://doi.org/10.1523/JNEUROSCI.22-24-10567.2002

Schluter, T., Berger, C., Rosengauer, E., Fieth, P., Krohs, C., Ushakov, K., Steel, K. P., Avraham, K. B., Hartmann, A. K., Felmy, F., & Nothwang, H. G. (2018). miR-96 is required for normal development of the auditory hindbrain. *Hum Mol Genet*, *27*(5), 860-874. https://doi.org/10.1093/hmg/ddy007

Schneggenburger, R., & Forsythe, I. D. (2006). The calyx of Held. *Cell Tissue Res*, *326*(2), 311-337. https://doi.org/10.1007/s00441-006-0272-7

Schofield, B. R. (2002). Ascending and descending projections from the superior olivary complex in guinea pigs: different cells project to the cochlear nucleus and the inferior colliculus. *J Comp Neurol*, *453*(3), 217-225. https://doi.org/10.1002/cne.10402

Seal, R. P., Akil, O., Yi, E., Weber, C. M., Grant, L., Yoo, J., Clause, A., Kandler, K., Noebels, J. L., Glowatzki, E., Lustig, L. R., & Edwards, R. H. (2008). Sensorineural deafness and seizures in mice lacking vesicular glutamate transporter 3. *Neuron*, *57*(2), 263-275. https://doi.org/10.1016/j.neuron.2007.11.032

Selbach, M., Schwanhausser, B., Thierfelder, N., Fang, Z., Khanin, R., & Rajewsky, N. (2008). Widespread changes in protein synthesis induced by microRNAs. *Nature*, *455*(7209), 58-63. https://doi.org/10.1038/nature07228

Shen, M., Lv, D., Liu, X., Li, S., Chen, Y., Zhang, Y., Wang, Z., & Wang, C. (2018). Essential roles of neuropeptide VGF regulated TrkB/mTOR/BICC1 signaling and phosphorylation of AMPA receptor subunit GluA1 in the rapid antidepressant-like actions of ketamine in mice. *Brain Res Bull*, *143*, 58-65. https://doi.org/10.1016/j.brainresbull.2018.10.004

Solda, G., Robusto, M., Primignani, P., Castorina, P., Benzoni, E., Cesarani, A., Ambrosetti, U., Asselta, R., & Duga, S. (2012). A novel mutation within the MIR96 gene causes non-

syndromic inherited hearing loss in an Italian family by altering pre-miRNA processing. *Human molecular genetics*, *21*(3), 577-585.

Soukup, G. A., Fritzsch, B., Pierce, M. L., Weston, M. D., Jahan, I., McManus, M. T., & Harfe, B. D. (2009). Residual microRNA expression dictates the extent of inner ear development in conditional Dicer knockout mice. *Dev Biol*, *328*(2), 328-341. https://doi.org/10.1016/j.ydbio.2009.01.037

Stanchina, L., Baral, V., Robert, F., Pingault, V., Lemort, N., Pachnis, V., Goossens, M., & Bondurand, N. (2006). Interactions between Sox10, Edn3 and Ednrb during enteric nervous system and melanocyte development. *Developmental biology*, *295*(1), 232-249.

Steel, K. P., & Bock, G. R. (1980). The nature of inherited deafness in deafness mice. *Nature*, *288*(5787), 159-161. https://doi.org/10.1038/288159a0

Sun, L., Xia, R., Jiang, J., Wen, T., Huang, Z., Qian, R., Zhang, M.-D., Zhou, M., & Peng, C. (2021). MicroRNA-96 is required to prevent allodynia by repressing voltage-gated sodium channels in spinal cord. *Progress in Neurobiology*, *202*, 102024.

Tafoya, L. C., Mameli, M., Miyashita, T., Guzowski, J. F., Valenzuela, C. F., & Wilson, M. C. (2006). Expression and function of SNAP-25 as a universal SNARE component in GABAergic neurons. *Journal of Neuroscience*, *26*(30), 7826-7838.

Tanaka, C., Coling, D. E., Manohar, S., Chen, G. D., Hu, B. H., Salvi, R., & Henderson, D. (2012). Expression pattern of oxidative stress and antioxidant defense-related genes in the aging Fischer 344/NHsd rat cochlea. *Neurobiol Aging*, *33*(8), 1842 e1841-1814. https://doi.org/10.1016/j.neurobiolaging.2011.12.027

Taschenberger, H., Leao, R. M., Rowland, K. C., Spirou, G. A., & von Gersdorff, H. (2002). Optimizing synaptic architecture and efficiency for high-frequency transmission. *Neuron*, *36*(6), 1127-1143. https://doi.org/10.1016/s0896-6273(02)01137-6

Traynelis, S. F., Wollmuth, L. P., McBain, C. J., Menniti, F. S., Vance, K. M., Ogden, K. K., Hansen, K. B., Yuan, H., Myers, S. J., & Dingledine, R. (2010). Glutamate receptor ion channels: structure, regulation, and function. *Pharmacol Rev*, *62*(3), 405-496. https://doi.org/10.1124/pr.109.002451

Truesdell, S., Mortensen, R., Seo, M., Schroeder, J., Lee, J., LeTonqueze, O., & Vasudevan, S. (2012). MicroRNA-mediated mRNA translation activation in quiescent cells and oocytes involves recruitment of a nuclear microRNP. *Scientific Reports*, *2*(1), 842.

Tserel, L., Runnel, T., Kisand, K., Pihlap, M., Bakhoff, L., Kolde, R., Peterson, H., Vilo, J., Peterson, P., & Rebane, A. (2011). MicroRNA expression profiles of human blood monocyte-derived dendritic cells and macrophages reveal miR-511 as putative

positive regulator of Toll-like receptor 4. *Journal of Biological Chemistry*, *286*(30), 26487-26495.

Tu, J. C., Xiao, B., Naisbitt, S., Yuan, J. P., Petralia, R. S., Brakeman, P., Doan, A., Aakalu, V. K., Lanahan, A. A., & Sheng, M. (1999). Coupling of mGluR/Homer and PSD-95 complexes by the Shank family of postsynaptic density proteins. *Neuron*, *23*(3), 583-592.

Tyagarajan, S. K., & Fritschy, J.-M. (2014). Gephyrin: a master regulator of neuronal function? *Nature Reviews Neuroscience*, *15*(3), 141-156.

Van Dongen, S., Abreu-Goodger, C., & Enright, A. J. (2008). Detecting microRNA binding and siRNA off-target effects from expression data. *Nature methods*, *5*(12), 1023-1025.

Van Eyken, E., Van Camp, G., & Van Laer, L. (2007). The complexity of age-related hearing impairment: contributing environmental and genetic factors. *Audiol Neurootol*, *12*(6), 345-358. https://doi.org/10.1159/000106478

Varoqueaux, F., Jamain, S., & Brose, N. (2004). Neuroligin 2 is exclusively localized to inhibitory synapses. *Eur J Cell Biol*, *83*(9), 449-456. https://doi.org/10.1078/0171-9335-00410

Vasudevan, S. (2012). Posttranscriptional upregulation by microRNAs. *Wiley Interdisciplinary Reviews: RNA*, *3*(3), 311-330.

Vasudevan, S., & Steitz, J. A. (2007). AU-rich-element-mediated upregulation of translation by FXR1 and Argonaute 2. *Cell*, *128*(6), 1105-1118. https://doi.org/10.1016/j.cell.2007.01.038

Walmsley, B., Berntson, A., Leao, R. N., & Fyffe, R. E. (2006). Activity-dependent regulation of synaptic strength and neuronal excitability in central auditory pathways. *The Journal of Physiology*, *572*(2), 313-321.

Webster, D. B. (1985). The spiral ganglion and cochlear nuclei of deafness mice. *Hear Res*, *18*(1), 19-27. https://doi.org/10.1016/0378-5955(85)90107-8

Weston, M. D., Pierce, M. L., Rocha-Sanchez, S., Beisel, K. W., & Soukup, G. A. (2006). MicroRNA gene expression in the mouse inner ear. *Brain Res*, *1111*(1), 95-104. https://doi.org/10.1016/j.brainres.2006.07.006

Weston, M. D., Tarang, S., Pierce, M. L., Pyakurel, U., Rocha-Sanchez, S. M., McGee, J., Walsh, E. J., & Soukup, G. A. (2018). A mouse model of miR-96, miR-182 and miR-183 misexpression implicates miRNAs in cochlear cell fate and homeostasis. *Sci Rep*, *8*(1), 3569. https://doi.org/10.1038/s41598-018-21811-1

Whitfield, T. T. (2015). Development of the inner ear. *Curr Opin Genet Dev*, *32*, 112-118. https://doi.org/10.1016/j.gde.2015.02.006

Wienholds, E., Kloosterman, W. P., Miska, E., Alvarez-Saavedra, E., Berezikov, E., De Bruijn, E., Horvitz, H. R., Kauppinen, S., & Plasterk, R. H. (2005). MicroRNA expression in zebrafish embryonic development. *Science*, *309*(5732), 310-311.

Willaredt, M. A., Schluter, T., & Nothwang, H. G. (2015). The gene regulatory networks underlying formation of the auditory hindbrain. *Cell Mol Life Sci*, *72*(3), 519-535. https://doi.org/10.1007/s00018-014-1759-0

Wu, K. C., Chen, X. J., Jin, G. H., Wang, X. Y., Yang, D. D., Li, Y. P., Xiang, L., Zhang, B. W., Zhou, G. H., Zhang, C. J., & Jin, Z. B. (2019). Deletion of miR-182 Leads to Retinal Dysfunction in Mice. *Invest Ophthalmol Vis Sci*, *60*(4), 1265-1274. https://doi.org/10.1167/iovs.18-24166

Xiang, L., Chen, X. J., Wu, K. C., Zhang, C. J., Zhou, G. H., Lv, J. N., Sun, L. F., Cheng, F. F., Cai, X. B., & Jin, Z. B. (2017). miR-183/96 plays a pivotal regulatory role in mouse photoreceptor maturation and maintenance. *Proc Natl Acad Sci U S A*, *114*(24), 6376-6381. https://doi.org/10.1073/pnas.1618757114

Xu, S., Witmer, P. D., Lumayag, S., Kovacs, B., & Valle, D. (2007). MicroRNA (miRNA) transcriptome of mouse retina and identification of a sensory organ-specific miRNA cluster. *Journal of Biological Chemistry*, *282*(34), 25053-25066.

Xu, W., San Lucas, A., Wang, Z., & Liu, Y. (2014). Identifying microRNA targets in different gene regions. *BMC Bioinformatics*, *15 Suppl 7*(Suppl 7), S4. https://doi.org/10.1186/1471-2105-15-S7-S4

Yang, Y. M., Aitoubah, J., Lauer, A. M., Nuriya, M., Takamiya, K., Jia, Z., May, B. J., Huganir, R. L., & Wang, L. Y. (2011). GluA4 is indispensable for driving fast neurotransmission across a high-fidelity central synapse. *The Journal of Physiology*, *589*(17), 4209-4227.

Yoda, M., Kawamata, T., Paroo, Z., Ye, X., Iwasaki, S., Liu, Q., & Tomari, Y. (2010). ATP-dependent human RISC assembly pathways. *Nat Struct Mol Biol*, *17*(1), 17-23. https://doi.org/10.1038/nsmb.1733

Yost, W. A., & Nielsen, D. W. (2000). *Fundamentals of hearing* (Vol. 3). Academic Press New York.

Youssoufian, M., Oleskevich, S., & Walmsley, B. (2005). Development of a robust central auditory synapse in congenital deafness. *J Neurophysiol*, *94*(5), 3168-3180. https://doi.org/10.1152/jn.00342.2005

Zerbino, D. R., Achuthan, P., Akanni, W., Amode, M. R., Barrell, D., Bhai, J., Billis, K., Cummins, C., Gall, A., & Girón, C. G. (2018). Ensembl 2018. *Nucleic acids research*, *46*(D1), D754-D761.

Zhang, C. J., Xiang, L., Chen, X. J., Wang, X. Y., Wu, K. C., Zhang, B. W., Chen, D. F., Jin, G. H., Zhang, H., Chen, Y. C., Liu, W. Q., Li, M. L., Ma, Y., & Jin, Z. B. (2020). Ablation of Mature miR-183 Leads to Retinal Dysfunction in Mice. *Invest Ophthalmol Vis Sci*, *61*(3), 12. https://doi.org/10.1167/iovs.61.3.12

Zhang, H., Kolb, F. A., Jaskiewicz, L., Westhof, E., & Filipowicz, W. (2004). Single processing center models for human Dicer and bacterial RNase III. *Cell*, *118*(1), 57-68. https://doi.org/10.1016/j.cell.2004.06.017

Zhang, J., Zhou, W., Liu, Y., Liu, T., Li, C., & Wang, L. (2018). Oncogenic role of microRNA-532-5p in human colorectal cancer via targeting of the 5'UTR of RUNX3. *Oncology letters*, *15*(5), 7215-7220.

Zine, A., & Fritzsch, B. (2023). Early Steps towards Hearing: Placodes and Sensory Development. *Int J Mol Sci*, *24*(8). https://doi.org/10.3390/ijms24086994

# Acknowledgements

First and foremost, I would like to thank my Ph.D. supervisor, Prof. Dr Hans Gerd Nothwang, for his guidance and mentorship throughout my doctoral journey. His expertise in the field of neuroscience and constructive feedback have been crucial in shaping the course of my research and academic growth.

A special acknowledgment goes to my co-supervisor, Dr. Lena Ebbers for her invaluable contributions to my research. She has been the kindest mentor I have ever worked with, and her insights, patience, and collaborative spirit have significantly improved the quality of my work.

I would like to thank Prof. Dr. Ulrike Janssen-Bienhold for accepting to evaluate my thesis, Prof. Dr. Christine Köppl for accepting to take part as examiner in my disputation and Dr. Christoph Körber for accepting to evaluate my dissertation as an external assessor.

I extend my appreciation to all current and former colleagues in our lab. Thanks to Dr. Papa Ali and Dr. Frut++ for the shared knowledge during our coffee sessions in kitchen. I would like to acknowledge the technical assistance provided by Laura and Martina for their expertise and assistance during my Ph.D.

Since moving to Oldenburg, I have spent time with many people that have made coming to a new city and facing a new challenge bearable; I value the friendship of all of them and their presence in my life has been truly important. Special gratitude for Laura for being a constant support both in and outside of lab. I could not have done this without you! My Ph.D. friends' group , who have been a pillar of support throughout this academic journey. Their encouragement, support and understanding have made life here much more easier and enjoyable.

Financial and organizational support from Molecular basis of sensory Biology (RTG) and Oltech is gratefully acknowledged. Dr. Kristin Tietje for her constant support and organizing productive scientific and networking events  throughout this journey.

Most importantly, my mother, sisters and brother have been supportive of all my decisions and have been continually encouraging amid frustrations; I would not have been able to reach this point without their support.

Alhamdulillah, I praise and thank Allah SWT for His greatness and for giving me the strength and courage to complete this thesis.

# FAIZA ALTAF

## CONTACT

✉ faiza.altaf@uol.de

I am an enthusiastic and dedicated researcher with a strong background in Neurogenetics and a particular focus on investigating the role of microRNAs in auditory brainstem development. My journey as a Ph.D. candidate at AG Neurogenetics, University of Oldenburg, has provided me with valuable insights into the complex genetic mechanisms that underlie auditory processing. I am deeply passionate about understanding the molecular intricacies that govern neural circuitry and sensory perception.

---------------------------------------------

## EDUCATION

**Master of Science (Molecular Genetics)**

2014–2016

COMSATS Institute of Information Technology, Islamabad, Pakistan

GPA: 3.64/4.00

**Bachelors (Hons) of Science in Biotechnology**

2007–2011

Centre of Biotechnology & Microbiology, University of Peshawar, Pakistan

Grade: A+

---------------------------------------------

## LANGUAGES

Urdu    ◆ ◆ ◆ ◆ ◆

English  ◆ ◆ ◆ ◆ ◆

German  ◆ ◇ ◇ ◇ ◇

## WORK EXPERIENCE

**PhD Position/Scientific Colleague, AG Neurogenetics**    Oct 2019-present

Carl-von-Ossietzky-University, Oldenburg

- Member of Research Training Group and OLTECH Graduate School·
- Project: "Functional Analysis of microRNAs 183/96 in auditory brainstem of mice"

**Biology Lecturer**    Oct 2011 - Sept 2019

- Pearl Chenab College, Ali pur Islamabad, Pakistan
- KIPS College for Girls, Rawalpindi
- KIPS Evening Coaching Academy, Rawalpindi
- Al-Hamd Academy, Tramari
- Jinnah Jam-e-School & College Haripur Pakistan

**Senior Technologist**    Jan 2013- Feb 2014

Shifa International Hospital, Islamabad, Pakistan

- Histopathology & Immunohistochemistry Laboratory

**Laboratory Intern**    Oct 2012- Jan 2013

Noor Surgical Hospital, Haripur, Pakistan

- Basic Diagnostics Laboratory

81

# PUBLICATIONS

- Altaf, F., Vesely, C., Sheikh, A. M., Munir, R., Shah, S. T. A., & Tariq, A. (2019). Modulation of ADAR mRNA expression in patients with congenital heart defects. PLoS One, 14(4), e0200968.

- Krohs, C., Körber, C., Ebbers, L., Altaf, F., Hollje, G., Hoppe, S., ... & Nothwang, H. G. (2021). Loss of miR-183/96 alters synaptic strength via presynaptic and postsynaptic mechanisms at a central synapse. Journal of Neuroscience, 41(32), 6796-6811.

- Ebbers, L., Altaf, F., & Nothwang, H. G. (2022). MicroRNAs in the auditory system: tiny molecules with big impact. Neuroforum, 28(4), 211-221.

-------------------------------------------------

# REFERENCES

**Prof. Dr. Hans Gerd Nothwang**

tel:+494417982499

hans.g.nothwang@uol.de


**Dr. Lena Ebbers**

tel:+494417983299

lena.ebbers@uol.de


**Assistant Prof. Dr. Syed Tahir Abbas**

tel:+92 51 90496119

syedtahirabbas@comsats.edu.pk

# QUALIFICATION SKILLS

## Neuroscience

- Familiarity with auditory brainstem anatomy , Use of basic technical appliances in the lab (Cryostat, Microtome, etc.),
- Immunohistochemistal analysis
- Confocal microscopy, Axioscan microscopy, Laser capture dissection microscope
- RNA-seq
- LNA in-situ Hybridization
- Animal Handling course (specialized in Mice/Gerbils)

## Computer/Software

- Office automation (MS Word, MS Excel, MS PowerPoint), Internet & Software Utilities
- ImageJ use and Analysis
- Basic statistical analysis/Graphpad prism
- Basic bioinformatical data analysis

## Other Laboratory Techniques

- Cytology, staining
- Anti-nuclear antibody test, Immunofloursecence Test
- Polymerase chain reaction, Real-time PCR
- RNA/DNA extraction, Gel-Electrophoresis, cDNA synthesis,
- ELISA, FISH.

# SOFT SKILLS

## Project Management/Organization

- Involved in planning and execution of experiments

## Communication and Presentation

- Presented results in Neurogenetics group, in RTG multi-disciplinary seminars, posters in conferences and workshops.

## Laboratory Responsibilities

- Supervised two students, responsible for organizing lab meetings.

## Teamwork / Networking

- Member of grad-school, worked with other scientists using networking and interpersonal skills.

# Publication List

– Ebbers, L., Altaf, F., & Nothwang, H. G. (2022). MicroRNAs in the auditory system: tiny molecules with big impact. *Neuroforum*, *28*(4), 211-221.

– Krohs, C., Körber, C., Ebbers, L., Altaf, F., Hollje, G., Hoppe, S., ... & Nothwang, H. G. (2021). Loss of miR-183/96 alters synaptic strength via presynaptic and postsynaptic mechanisms at a central synapse. *Journal of Neuroscience*, *41*(32), 6796-6811.

– Altaf, F., Vesely, C., Sheikh, A. M., Munir, R., Shah, S. T. A., & Tariq, A. (2019). Modulation of ADAR mRNA expression in patients with congenital heart defects. *PLoS One*, *14*(4), e0200968.

Hiermit erkläre ich, dass ich die vorliegende Arbeit selbstständig verfasst habe und keine als die angegebenen Quellen und Hilfsmittel verwendet habe. Ich versichere, dass diese Arbeit weder in ihrer Gesamtheit noch in Teilen einer anderen Hochschule zur Begutachtung in einem Promotionsverfahren vorliegt oder vorgelegen hat und dass ich die Leitlinien guter wissenschaftlicher Praxis der Carl von Ossietzky Universität Oldenburg befolgt habe. Weiterhin versichere ich, dass im Zusammenhang mit dem Promotionsvorhaben keine kommerziellen Vermittlungs- oder Beratungsdienste (Promotionsberatung) in Anspruch genommen worden sind.

\_\_\_Oldenburg, 23.11.2023_____ (Ort, Datum) _____ (Faiza Altaf)